

# **Modelling potential impacts of sea level rise on Siwash Island**

**by  
Avazeh Dolatshahi**

Master of Science in Natural Resources Engineering, University of Tehran, 2015

Project Submitted in Partial Fulfillment of the  
Requirements for the Degree of  
Master of Science

in the  
Ecological Restoration Program  
Faculty of Environment (SFU)  
and  
School of Construction and the Environment (BCIT)

© Avazeh Dolatshahi 2024  
SIMON FRASER UNIVERSITY  
BRITISH COLUMBIA INSTITUTE OF TECHNOLOGY  
Spring 2024

Copyright in this work is held by the author. Please ensure that any reproduction or re-use is done in accordance with the relevant national copyright legislation.

## Declaration of Committee

**Name:** Avazeh Dolatshahi

**Degree:** Master of Science

**Title:** Modelling potential impacts of sea level rise on Siwash Island

**Committee:** **Chair: Shawn Chartrand**  
Supervisor  
Faculty, SFU

**Ruth Joy**  
Committee Member  
Faculty, SFU

## **Abstract**

Siwash Island is a tidal marsh situated at the southern end of the Widgeon Marsh Regional Park Reserve, Coquitlam, British Columbia (BC). The numerical model MarshMorpho2D was used to depict the evolution of marsh under various scenarios of sea level rise (SLR), suspended sediment concentration (SSC), and tidal range (TR) over the next 80 years. Changes in SLR and TR substantially impact the island's morphology. Higher TR and SLR cause higher inundation and erosion rate, resulting in loss of vegetation, elevation, and habitat across the island. The model projection indicates that Siwash Island is likely to submerge within the next 80 years. The MarshMorpho2D model provides insights for policymakers and conservationists to develop adaptive strategies to mitigate the effect of SLR on coastal ecosystems.

**Keywords:** Tidal marsh; numerical model; MarshMorpho2D; sea level rise; tidal range; suspended sediment concentration

## **Dedication**

I would like to dedicate this research project to my parents, Shohreh Sherafat and Alireza Dolatshahi, and my sister, Golzar Dolatshahi, who have been my constant source of love, support, and inspiration in this journey. I am grateful for the sacrifices you have made to help me pursue my dreams.

## Acknowledgements

I would like to respectfully acknowledge that this study was done on the unceded territory of the Coast Salish people, including the səlilwətał (Tseil-Waututh), kwikwəłəm (Kwikwetlem), Skwxwú7mesh Úxwumixw (Squamish) and xʷməθkʷəy̓əm (Musqueam) Nations.

I express my deep gratitude to my supervisor, Shawn Chartrand, whose invaluable guidance, patience, and encouragement were essential throughout this project. It was a great privilege to have the opportunity to do my thesis under your guidance.

To my dear parents, who have always been loving, caring, and supportive, I am grateful for your unwavering presence and encouragement. Your endless support means the world to me.

I am grateful to all my professors at SFU and BCIT, and my classmates for their support in this amazing journey.

Sincerely,

Avazeh

# Table of Contents

Declaration of Committee .....	ii
Abstract .....	iii
Dedication .....	iv
Acknowledgements .....	v
Table of Contents .....	vi
List of Tables .....	viii
List of Figures .....	ix
List of Acronyms .....	xiv
<b>Chapter 1. Introduction .....</b>	<b>1</b>
<b>Chapter 2. Goals and Objectives .....</b>	<b>5</b>
2.1. Research Questions: .....	5
2.2. Goals: .....	5
2.3. Objectives: .....	5
<b>Chapter 3. Material and Methods .....</b>	<b>7</b>
3.1. Study Area .....	7
3.2. Cross-section Analysis .....	7
3.3. MarshMorpho2D Model .....	9
<b>Chapter 4. Results .....</b>	<b>13</b>
4.1. Scenario 1: .....	13
4.1.1. Elevation .....	13
4.1.2. Relative Elevation .....	17
4.1.3. Suspended Sediment Concentration (SSC) .....	21
4.1.4. Vegetation Cover .....	25
4.1.5. Velocity .....	28
4.1.6. Water Depth .....	31
4.2. Scenario 2: .....	34
4.2.1. Elevation Change .....	34
4.2.2. Relative Elevation .....	38
4.2.3. Suspended Sediment Concentration .....	42
4.2.4. Vegetation Cover .....	45
4.2.5. Velocity .....	48
4.2.6. Water Depth .....	51
4.3. Scenario 3: .....	55
4.3.1. Elevation .....	55
4.3.2. Relative Elevation .....	58
4.3.3. Suspended Sediment Concentration .....	61
4.3.4. Vegetation Cover .....	63
4.3.5. Velocity .....	65
4.3.6. Water Depth .....	67

<b>Chapter 5. Discussion</b> .....	<b>69</b>
5.1. Differences between scenarios.....	69
5.1.1. Scenarios 1 and 2:.....	69
5.1.2. Scenario 1 and 3.....	70
5.2. General Interpretation of Marsh Evolution:.....	72
5.3. Comparison to other studies:.....	73
5.4. Implications and Management Recommendations.....	74
5.5. Limitations.....	75
5.6. Recommendation.....	76
5.7. Conclusion.....	77
<b>References</b> .....	<b>78</b>

## List of Tables

Table 1	List of Parameters utilized in calibration of model MarshMorpho2D v.2.0 by G.Marriotti (2020). Site values are the ones that are used in this research. ....	11
Table 2	List of scenarios that were run using MarshMorpho2D v.2.0 developed by G.Mariotti (2020). ....	12

## List of Figures

Figure 1	Study area map.....	4
Figure 2	Three cross-sections across Siwash Island.....	8
Figure 3	Digital Elevation Model (DEM) of Siwash Island and surrounding area ..	10
Figure 4	Graphic representing open water (inactive cells) and marsh (active cells) used for each simulations. All cells located in black section experience changes throughout the simulations. ....	10
Figure 5	Results from simulating Siwash Island with G.Mariotti's MarshMorpho2D model (2020). The plots highlight patterns of Siwash Island response through time in the model with the simulation of 12.5 mm/yr of SLR, 1.5 m of TR, and 5 g/cm <sup>3</sup> of SSC. ....	14
Figure 6	Results from simulating Siwash Island with G.Mariotti's MarshMorpho2D model (2020). The plots highlight patterns of Siwash Island response through time in the model with the simulation of 12.5 mm/yr of SLR, 1.5 m of TR, and 20 g/cm <sup>3</sup> of SSC. ....	15
Figure 7	Results from simulating Siwash Island with G.Mariotti's MarshMorpho2D model (2020). The plots highlight patterns of Siwash Island response through time in the model with the simulation of 12.5 mm/yr of SLR, 1.5 m of TR, and 30 g/cm <sup>3</sup> of SSC. ....	16
Figure 8	Results from simulating Siwash Island with G.Mariotti's MarshMorpho2D model (2020). These six subplots show elevation relative to average sea level with the simulation of 12.5 mm/yr of SLR, 1.5 m of TR, and 5 g/cm <sup>3</sup> of SSC. ....	18
Figure 9	Results from simulating Siwash Island with G.Mariotti's MarshMorpho2D model (2020). These six subplots show elevation relative to average sea level with the simulation of 12.5 mm/yr of SLR, 1.5 m of TR, and 20 g/cm <sup>3</sup> of SSC. ....	19
Figure 10	Results from simulating Siwash Island with G.Mariotti's MarshMorpho2D model (2020). These six subplots show elevation relative to average sea level with the simulation of 12.5 mm/yr of SLR, 1.5 m of TR, and 30 g/cm <sup>3</sup> of SSC. ....	20
Figure 11	Results from simulating Siwash Island with G.Mariotti's MarshMorpho2D model (2020). These six subplots show the evolution of suspended sediment concentration over time with the simulation of 12.5 mm/yr of SLR, 1.5 m of TR, and 5 g/cm <sup>3</sup> of SSC.....	22
Figure 12	Results from simulating Siwash Island with G.Mariotti's MarshMorpho2D model (2020). These six subplots show the evolution of suspended sediment concentration over time with the simulation of 12.5 mm/yr of SLR, 1.5 m of TR, and 20 g/cm <sup>3</sup> of SSC.....	23
Figure 13	Results from simulating Siwash Island with G.Mariotti's MarshMorpho2D model (2020). These six subplots show the evolution of suspended sediment concentration over time with the simulation of 12.5 mm/yr of SLR, 1.5 m of TR, and 30 g/cm <sup>3</sup> of SSC.....	24
Figure 14	Results from simulating Siwash Island with G.Mariotti's MarshMorpho2D model (2020). This plot shows the evolution of vegetation cover over time	

	with the simulation of 12.5 mm/yr of SLR, 1.5 m of TR, and 5 g/cm <sup>3</sup> of SSC. ....	25
Figure 15	Results from simulating Siwash Island with G.Mariotti's MarshMorpho2D model (2020). This plot shows the evolution of vegetation cover over time with the simulation of 12.5 mm/yr of SLR, 1.5 m of TR, and 20 g/cm <sup>3</sup> of SSC. ....	26
Figure 16	Results from simulating Siwash Island with G.Mariotti's MarshMorpho2D model (2020). This plot shows the evolution of vegetation cover over time with the simulation of 12.5 mm/yr of SLR, 1.5 m of TR, and 30 g/cm <sup>3</sup> of SSC. ....	27
Figure 17	Results from simulating Siwash Island with G.Mariotti's MarshMorpho2D model (2020). These six subplots show the changes in velocity until 2104 with the simulation of 12.5 mm/yr of SLR, 1.5 m of TR, and 5 g/cm <sup>3</sup> of SSC. ....	28
Figure 18	Results from simulating Siwash Island with G.Mariotti's MarshMorpho2D model (2020). These six subplots show the changes in velocity until 2104 with the simulation of 12.5 mm/yr of SLR, 1.5 m of TR, and 20 g/cm <sup>3</sup> of SSC. ....	29
Figure 19	Results from simulating Siwash Island with G.Mariotti's MarshMorpho2D model (2020). These six subplots show the changes in velocity until 2104 with the simulation of 12.5 mm/yr of SLR, 1.5 m of TR, and 30 g/cm <sup>3</sup> of SSC. ....	30
Figure 20	Results from simulating Siwash Island with G.Mariotti's MarshMorpho2D model (2020). These six subplots show the changes in Water depth over time until 2104 with the simulation of 12.5 mm/yr of SLR, 1.5 m of TR, and 5 g/cm <sup>3</sup> of SSC. ....	31
Figure 21	Results from simulating Siwash Island with G.Mariotti's MarshMorpho2D model (2020). These six subplots show the changes in Water depth over time until 2104 with the simulation of 12.5 mm/yr of SLR, 1.5 m of TR, and 20 g/cm <sup>3</sup> of SSC. ....	32
Figure 22	Results from simulating Siwash Island with G.Mariotti's MarshMorpho2D model (2020). These six subplots show the changes in Water depth over time until 2104 with the simulation of 12.5 mm/yr of SLR, 1.5 m of TR, and 30 g/cm <sup>3</sup> of SSC. ....	33
Figure 23	Results from simulating Siwash Island with G.Mariotti's MarshMorpho2D model (2020). The plots highlight patterns of Siwash Island response through time in the model with the simulation of 12.5 mm/yr of SLR, 2 m of TR, and 5 g/cm <sup>3</sup> of SSC. ....	35
Figure 24	Results from simulating Siwash Island with G.Mariotti's MarshMorpho2D model (2020). The plots highlight patterns of Siwash Island response through time in the model with the simulation of 12.5 mm/yr of SLR, 2 m of TR, and 20 g/cm <sup>3</sup> of SSC. ....	36
Figure 25	Results from simulating Siwash Island with G.Mariotti's MarshMorpho2D model (2020). The plots highlight patterns of Siwash Island response through time in the model with the simulation of 12.5 mm/yr of SLR, 2 m of TR, and 30 g/cm <sup>3</sup> of SSC. ....	37

Figure 26	Results from simulating Siwash Island with G.Mariotti’s MarshMorpho2D model (2020). These six subplots show elevation relative to average sea level with the simulation of 12.5 mm/yr of SLR, 2 m of TR, and 5 g/cm <sup>3</sup> of SSC. ....	39
Figure 27	Results from simulating Siwash Island with G.Mariotti’s MarshMorpho2D model (2020). These six subplots show elevation relative to average sea level with the simulation of 12.5 mm/yr of SLR, 2 m of TR, and 20 g/cm <sup>3</sup> of SSC. ....	40
Figure 28	Results from simulating Siwash Island with G.Mariotti’s MarshMorpho2D model (2020). These six subplots show elevation relative to average sea level with the simulation of 12.5 mm/yr of SLR, 2 m of TR, and 30 g/cm <sup>3</sup> of SSC. ....	41
Figure 29	Results from simulating Siwash Island with G.Mariotti’s MarshMorpho2D model (2020). These six subplots show evolution of suspended sediment concentration over time with the simulation of 12.5 mm/yr of SLR, 2 m of TR, and 5 g/cm <sup>3</sup> of SSC. ....	42
Figure 30	Results from simulating Siwash Island with G.Mariotti’s MarshMorpho2D model (2020). These six subplots show evolution of suspended sediment concentration over time with the simulation of 12.5 mm/yr of SLR, 2 m of TR, and 20 g/cm <sup>3</sup> of SSC. ....	43
Figure 31	Results from simulating Siwash Island with G.Mariotti’s MarshMorpho2D model (2020). These six subplots show evolution of suspended sediment concentration over time with the simulation of 12.5 mm/yr of SLR, 2 m of TR, and 30 g/cm <sup>3</sup> of SSC. ....	44
Figure 32	Results from simulating Siwash Island with G.Mariotti’s MarshMorpho2D model (2020). This plot shows evolution of vegetation cover over time with the simulation of 12.5 mm/yr of SLR, 2 m of TR, and 5 g/cm <sup>3</sup> of SSC. ....	45
Figure 33	Results from simulating Siwash Island with G.Mariotti’s MarshMorpho2D model (2020). This plot shows evolution of vegetation cover over time with the simulation of 12.5 mm/yr of SLR, 2 m of TR, and 20 g/cm <sup>3</sup> of SSC. ....	46
Figure 34	Results from simulating Siwash Island with G.Mariotti’s MarshMorpho2D model (2020). This plot shows evolution of vegetation cover over time with the simulation of 12.5 mm/yr of SLR, 2 m of TR, and 30 g/cm <sup>3</sup> of SSC. ....	47
Figure 35	Results from simulating Siwash Island with G.Mariotti’s MarshMorpho2D model (2020). These six subplots show the changes in velocity over time until 2104 with the simulation of 12.5 mm/yr of SLR, 2 m of TR, and 5 g/cm <sup>3</sup> of SSC.....	48
Figure 36	Results from simulating Siwash Island with G.Mariotti’s MarshMorpho2D model (2020). These six subplots show the changes in velocity over time until 2104 with the simulation of 12.5 mm/yr of SLR, 2 m of TR, and 20 g/cm <sup>3</sup> of SSC.....	49
Figure 37	Results from simulating Siwash Island with G.Mariotti’s MarshMorpho2D model (2020). These six subplots show the changes in velocity over time	

	until 2104 with the simulation of 12.5 mm/yr of SLR, 2 m of TR, and 30 g/cm <sup>3</sup> of SSC.....	50
Figure 38	Results from simulating Siwash Island with G.Mariotti's MarshMorpho2D model (2020). These six subplots show the changes in water depth over time until 2104 with the simulation of 12.5 mm/yr of SLR, 2 m of TR, and 5 g/cm <sup>3</sup> of SSC.....	52
Figure 39	Results from simulating Siwash Island with G.Mariotti's MarshMorpho2D model (2020). These six subplots show the changes in water depth over time until 2104 with the simulation of 12.5 mm/yr of SLR, 2 m of TR, and 20 g/cm <sup>3</sup> of SSC.....	53
Figure 40	Results from simulating Siwash Island with G.Mariotti's MarshMorpho2D model (2020). These six subplots show the changes in water depth over time until 2104 with the simulation of 12.5 mm/yr of SLR, 2 m of TR, and 30 g/cm <sup>3</sup> of SSC.....	54
Figure 41	Results from simulating Siwash Island with G.Mariotti's MarshMorpho2D model (2020). The plots highlight patterns of Siwash Island response through time in the model with the simulation of 25 mm/yr of SLR, 1.5 m of TR, and 20 g/cm <sup>3</sup> of SSC. ....	56
Figure 42	Results from simulating Siwash Island with G.Mariotti's MarshMorpho2D model (2020). The plots highlight patterns of Siwash Island response through time in the model with the simulation of 25 mm/yr of SLR, 2 m of TR, and 20 g/cm <sup>3</sup> of SSC. ....	57
Figure 43	Results from simulating Siwash Island with G.Mariotti's MarshMorpho2D model (2020). These six subplots show elevation relative to average sea level with the simulation of 25 mm/yr of SLR, 1.5 m of TR, and 20 g/cm <sup>3</sup> of SSC. ....	59
Figure 44	Results from simulating Siwash Island with G.Mariotti's MarshMorpho2D model (2020). These six subplots show elevation relative to average sea level with the simulation of 25 mm/yr of SLR, 2 m of TR, and 20 g/cm <sup>3</sup> of SSC. ....	60
Figure 45	Results from simulating Siwash Island with G.Mariotti's MarshMorpho2D model (2020). These six subplots show the evolution of suspended sediment concentration over time with the simulation of 25 mm/yr of SLR, 1.5 m of TR, and 20 g/cm <sup>3</sup> of SSC. ....	61
Figure 46	Results from simulating Siwash Island with G.Mariotti's MarshMorpho2D model (2020). These six subplots show the evolution of suspended sediment concentration over time with the simulation of 25 mm/yr of SLR, 2 m of TR, and 20 g/cm <sup>3</sup> of SSC. ....	62
Figure 47	Results from simulating Siwash Island with G.Mariotti's MarshMorpho2D model (2020). This plot shows the evolution of vegetation cover over time with the simulation of 25 mm/yr of SLR, 1.5 m of TR, and 20 g/cm <sup>3</sup> of SSC. ....	63
Figure 48	Results from simulating Siwash Island with G.Mariotti's MarshMorpho2D model (2020). This plot shows the evolution of vegetation cover over time with the simulation of 25 mm/yr of SLR, 2 m of TR, and 20 g/cm <sup>3</sup> of SSC. ....	64

Figure 49	Results from simulating Siwash Island with G.Mariotti’s MarshMorpho2D model (2020). These six subplots show the changes in velocity over time until 2104 with the simulation of 25 mm/yr of SLR, 1.5 m of TR, and 20 g/cm <sup>3</sup> of SSC.....	65
Figure 50	Results from simulating Siwash Island with G.Mariotti’s MarshMorpho2D model (2020). These six subplots show the changes in velocity over time until 2104 with the simulation of 25 mm/yr of SLR, 2 m of TR, and 20 g/cm <sup>3</sup> of SSC.....	66
Figure 51	Results from simulating Siwash Island with G.Mariotti’s MarshMorpho2D model (2020). These six subplots show the changes in water depth over time until 2104 with the simulation of 25 mm/yr of SLR, 1.5 m of TR, and 20 g/cm <sup>3</sup> of SSC.....	67
Figure 52	Results from simulating Siwash Island with G.Mariotti’s MarshMorpho2D model (2020). These six subplots show the changes in water depth over time until 2104 with the simulation of 25 mm/yr of SLR, 2 m of TR, and 20 g/cm <sup>3</sup> of SSC.....	68
Figure 53	Evolution of main tidal channel on Siwash Island .....	73

## List of Acronyms

ArcGIS	Aeronautical Reconnaissance Coverage Geographic Information System
BC	British Columbia
BCIT	British Columbia Institute of Technology
CSDMS	Community Surface Dynamics Modelling Systems
DEM	Digital Elevation Model
GMSL	Global Mean Sea Level
IPCC	International Panel on Climate Change
MSL	Mean Sea Level
SFU	Simon Fraser University
SLR	Sea Level Rise
SSC	Suspended Sediment Concentration
TR	Tidal Range

# Chapter 1.

## Introduction

Tidal wetlands, situated at the boundary between land and sea, stand out as some of the most dynamic areas of the Earth which are temporarily or permanently covered with water (Conner et al, 2014; Mitsch and Gosselink, 2015), and which support numerous interdependent ecological functions by connecting terrestrial and aquatic environments through energy transfer (Ray, 2005; Turner, 2009; Costanza et al, 1997). Tidal marsh known as type of tidal wetlands and important ecosystem services provided by tidal marshes include flood mitigation, nutrient cycling, sediment trapping, and critical habitat for vegetation and wildlife such as crabs, and juvenile fish as well as nesting sites for migratory waterfowl species and other coastal wildlife (Barbier et al, 2011; Fagherazzi et al, 2012, MacKenzie and Moran, 2004); moreover, tidal marshes offer global benefits by capturing and storing atmospheric carbon dioxide, thereby helping to mitigate global warming (Mcleod et al, 2011). In spite all the advantages of tidal marsh, these ecosystems comprise less than 3 percent of coastal habitats of British Columbia (Pacific Birds Habitat Joint Venture, 2021).

Given their vital ecological functions and services, tidal marshes face an imminent threat from global sea level rise, driven by anthropogenic climate change (Mazor et al, 2021; Horton et al, 2020). The anticipated increase in sea levels is expected to bring about significant effects on coastal environments and low-lying regions worldwide on the global, regional, and local scales. Since 1880, there has been a rise in the global mean sea-level (MSL) of approximately 20 to 24 cm, with approximately 8 cm of that increase occurring since 1993 (Hay et al, 2015). According to Saintilan et al 2022, tidal wetlands are among the most threatened ecosystems on the planet due to increased population, and human activities such as agriculture. In addition to these pressures, an accelerated increase in sea levels can harm tidal marsh and stress vegetation (Craft et al, 2009). Along the Pacific coast of Canada and the United States, sea level rise (SLR) projections range from 1.0 to 2.0 m over the next century, potentially resulting in the loss of 83% of tidal wetlands (National Resource Council, 2012; Thorn et al, 2018). This loss would entail a reduction in valuable ecosystem services provided by tidal marshes such as attenuation of storm surge, carbon sequestration and habitat for

diverse fauna (Mariotti and Fagherazzi, 2010; Barbier et al, 2011). Notably, considering the pronounced regional spatio-temporal variations in sea level influenced by different factors such as ocean currents, land subsidence, geological conditions, and human activities (Triana et al, 2020), examination of tidal marsh behaviour at the local scale is essential to grasp comprehensive information regarding the effect of sea level rise on these features.

Not all tidal marshes will be equally affected by accelerated SLR, as projections can differ significantly between regions and come with a degree of uncertainty (W. Day et al, 2008). For instance, in the Pacific Ocean, there are variations in relative sea level and the subsequent rates of sea level rise from east to west (Parris et al, 2012). Even when focusing on the west coast of North America, sea level rise projections differ along a north-to-south gradient. These variations are partly influenced by factors such as El Niño and vertical land movement, which can occur due to processes like tectonic uplift and isostatic adjustment (National Resource Council, 2012). In addition to different responses of tidal marshes in different regions to sea level rise, a tidal marsh may exhibit different responses due to reasons such as topography, vegetation, and hydrodynamics; therefore, in a tidal marsh, at finer scale, gaining insight into the resilience of a particular marsh and examining spatial variability within a marsh can guide identification of priority areas and implementation of appropriate management and restoration actions (Cahoon and Guntenspergen, 2010; Thorne et al, 2015).

Tidal marshes have historically adapted to SLR, but their adaptive capacity is expected to change in the event of accelerated SLR (Cahoon et al, 2006). Tidal marshes located at the interface of land and sea emerge as highly sensitive and vulnerable to the impact of SLR and climate change via human activities, leading to erosion and inundation (Chen et al, 2023; Pang et al, 2023). There are two primary mechanisms of tidal marsh subsidence due to SLR: 1- landward migration to higher elevation (Enwright et al, 2016), and 2- vertical accretion through sediment accumulation (Morris et al, 2002). One of the most important factors in sustaining marsh habitats is sediment deposition (Morris et al, 2002). Since tidal channels serve as conveyors of sediment during high tide events, site functions depend heavily on sediment supply and tidal influence for self-maintenance. The vertical accretion of sediment, the establishment of habitat for flora and fauna, and the storage of carbon are all made possible by the introduction of sediments and organics into tidal marshes via tidal channels that

distribute matter throughout a marsh (Christiansen et al, 2000). When the rate of SLR exceeds the marsh's capacity for vertical growth, the area experiences prolonged inundation or extended hydroperiods, leading to insufficient root mass in vegetation and alteration in species composition (Kirwan and Guntenspergen, 2012). While tidal marsh has historically adapted to rising sea levels and increased sediment accumulation in response to such changes, the accelerated SLR associated with climate change is poised to disrupt these historical norms, posing a long-term threat to the sustainability of tidal ecosystems (Alizad et al, 2016; Cahoon et al, 2006; Fagherrazi et al, 2012). Landward horizontal migration onto adjacent, low-lying lands can be another factor in adjustment of these ecosystems under future sea level rise (Kirwan et al, 2016). Pacific coastal wetlands vertically accrete through the deposition of mineral sediments which are delivered by rivers and the ocean (Callaway et al, 2012).

Sea level rise exhibits a complex pattern rather than a homogenous pattern regionally. Tidal marshes display diverse characteristics based on topography, sediment composition and vegetation type, which all influence the wetland's response to sea level rise; therefore, this ARP investigates the resilience of tidal wetlands in response to sea level rise, with a specific focus on the critical role played by sedimentation processes at a local scale (Triana et al, 2020; D. Philips, 2018). Understanding the dynamics of tidal marsh responses to rising sea levels, with a central focus on sedimentation, is crucial for development of adaptive and resilient strategies to protect these valuable and vulnerable ecosystems. One approach to predict the future of tidal marshes is the development and application of numerical models. Numerical models are widely used in studies of tidal marshes (Fagherazzi et al, 2012), and models have been employed to assess a single marsh or estuary, primarily with the objective of producing detailed spatial predictions for the region of interest, allowing for localized investigation of marsh ecosystems (B. Raposa et al, 2016).

My ARP focuses on a single marsh to better understand how resilient tidal marsh ecosystems are to sea level rise and the function of sedimentation processes locally. The project's location is Siwash Island, situated within the City of Coquitlam and part of the Widgeon Marsh Regional Park Reserve (Fig. 1). It has been chosen for its unique characteristics and its vulnerability to sea level rise and climate change. The Widgeon Marsh serves as habitat for a diverse array of flora and fauna, playing a crucial part in maintaining regional biodiversity. Additionally, it is a buffer for the rest of the Regional

Park Reserve, contributing to its ecological balance and resilience (Evely, 2016). As a result, the goal of this research is to use numerical modelling to research Siwash Island's unique vulnerabilities and responses, as well as extrapolate insight into the broader strategies for the conservation and adaptive management of tidal marsh ecosystems coming up against similar challenges.

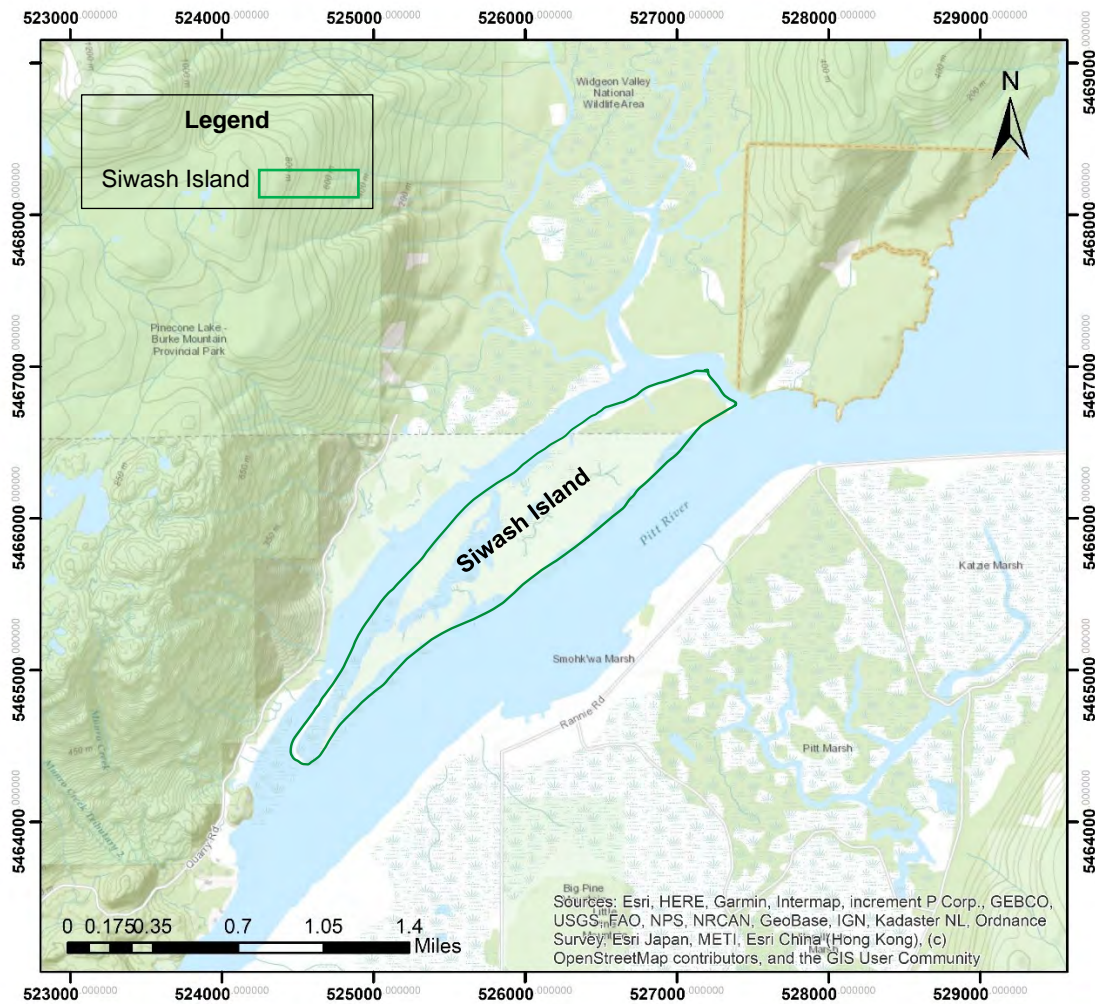


Figure 1 Study area map

## **Chapter 2.**

### **Goals and Objectives**

#### **2.1. Research Questions:**

Amidst emerging twenty-first century threats associated with SLR, the following research questions guide my investigation into Siwash Island's resilience and vulnerabilities in the face of SLR and changing sedimentation processes.

- 1- How does Siwash Island respond to SLR over the next 80 years? Does it persist or get drowned?
- 2- How does sediment concentration and tidal range influence the future modeled behavior of Siwash Island?

#### **2.2. Goals:**

- 1- To evaluate how resilient the tidal wetland ecosystem of Siwash Island is to SLR.
- 2- To assess how sedimentation processes shape the response of Siwash Island to sea level rise.
- 3- To provide information that can be used to help develop more comprehensive strategies for the conservation, restoration, and adaptive management of Siwash Island.

#### **2.3. Objectives:**

- 1- Conduct a comprehensive analysis regarding the evolution of Siwash Island due to SLR.
- 2- Develop a numerical model to simulate the response of Siwash Island to different scenarios of sea level rise and sedimentation.

- 3- Identify possible conservation and adaptation strategies that can improve the resilience of Siwash Island to climate change and SLR.

By understanding my research questions, goals and objectives, this research aims to provide useful information related to the future of tidal marsh ecosystems like Siwash Island and the factors that will influence their persistence, evolution, and ecological function in the context of sea level rise. This knowledge will be important in guiding future conservation, management, and restoration strategies to protect these critical coastal habitats.

## Chapter 3.

### Material and Methods

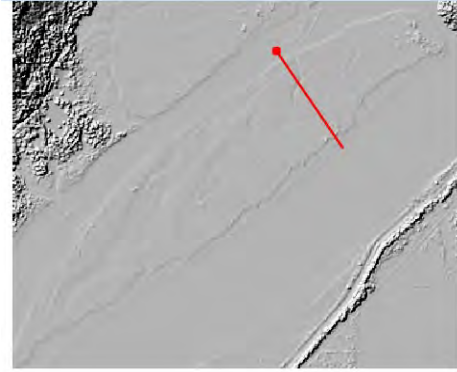
#### 3.1. Study Area

Siwash Island (Fig.1) is situated at the southern end of the Widgeon Marsh Regional Park Reserve (49°20'34"N and 122°38'55"W) (Fig. 1). The area is of great cultural and spiritual significance to multiple First Nations within the area, including Katzie First Nation, Kwikwetlem First Nation, Stó:lō Nation, Stó:lō Tribal Council, Tsawwassen First Nation, Soowahlie First Nation, Seabird Island Band, Shxw'ow'hamel First Nation, and Skawahlook First Nation (Evely, 2016). The total area of Siwash Island is approximately 250 hectares, and it functions as different types of tidal wetlands namely Swamp horsetail - Beaked sedge marsh (SH), Generic marsh (GM), Reed canarygrass marsh (RG), Sweet gale shrub swamp (GB), and Pacific crabapple shrub swamp (CB), with soils and sediment supplied by the Pitt River, with a mixture of floodplain deposits (Evely, 2016). Soils mapped at Siwash Island include Addington (AG), Sturgeon (SG), and Widgeon (WG), and all are poor in drainage and subject to flooding (Evely, 2016). The dominant vegetation is Reed canarygrass (*Phalaris arundinacea*) and breeding wildlife include the American Bittern (*Botaurus lentiginosus*) and tailed frog (*Ascaphus*), both of which are blue-listed species (Evely, 2016).

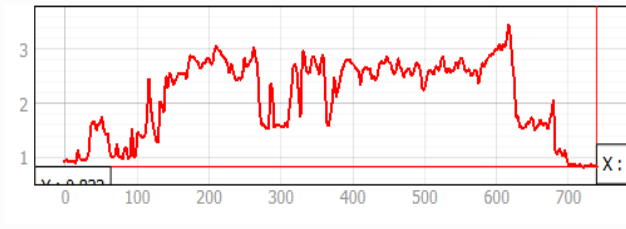
#### 3.2. Cross-section Analysis

Cross-section analyses are used to identify the topographic characteristic of Siwash Island. Different cross-sections across Siwash Island highlight the elevation profile of the marsh. These cross-sections indicate that the average highest elevation is 5.4 m (A: 6.2 m, B: 3.5 m, 6.5 m). As shown in Figure 2, the difference between the highest and the lowest elevation ranges from 2-3 m, and the elevation range is relatively consistent across all three cross-sections. This consistency implies that Siwash Island formed through deposition processes over the last few thousand years.

A



B



C

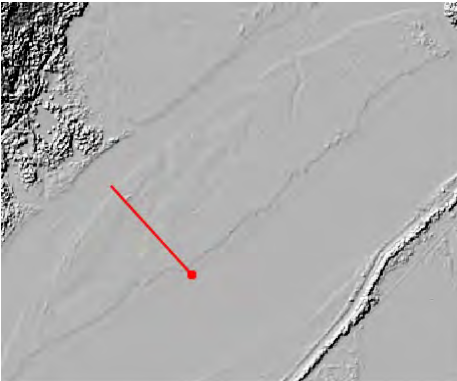


**Figure 2 Three cross-sections across Siwash Island**

### 3.3. MarshMorpho2D Model

As there has been a fast rate of tidal wetlands loss in recent decades, many models have been introduced to predict patterns of wetland loss and their extent in the next century (Mariotti, 2020; Wiberg et al, 2020). Considering all models, MarshMorpho2D model is the one that combines previous models and incorporates factors such as suspended sediment concentration (SSC), sea level rise, wave dynamics, mass-conservation, edge erosion, pond dynamics, and upland migration of tidal wetland (Table 1) (Mariotti, 2020). It assesses vegetated regions, taking elevation into account in reference to mean sea level, and it examines the reason behind the decline and increase of tidal wetland. Regions above mean sea level is vegetated, whereas areas below mean sea level rise are unvegetated. Instead of considering inter-tidal variability in the model, tide-averaged flow is used. Pond dynamics, which include pond formation, pond expansion and pond merging, were disabled in this study to prevent interference of ponds on the formation of tidal channels (Hutchins, 2021; Anderson, 2022). Wave dynamics are uncertain at Siwash Island, so we used a small weight moving in a dominant direction. For my analysis I used MarshMorpho2D model version 2.0 programmed in MATLAB® version R2021a (9.10.0.1602886), and available on the Community Surface Dynamics Modelling System website (CSDMS).

To run simulations of projects conditions, first, a digital elevation model (DEM) was developed in ArcGIS Pro 3.1.0 using LiDAR data which was downloaded from the LidarBC- open LiDAR data portal. In creating the DEM for this project six LiDAR datasets with the projected coordinate system NAD 83 CSRS UTM Zone 10N were used, with the following tile names: 092g037\_4\_1\_2, 092g037\_4\_2\_1, 092g037\_4\_2\_2, 092g037\_2\_3\_4, 092g037\_2\_4\_3, 092g037\_2\_4\_4, 092g037\_2\_3\_2, 092g037\_2\_4\_1, 092g037\_2\_4\_2. In the process of creating the DEM, the initial step was to convert LiDAR datasets to LAS dataset in ArcGIS Pro. Subsequently, these datasets were transformed to raster format. Finally, the raster datasets were merged, and DEM was created. The merged LiDAR datasets used are shown in Figure 3. After processing the DEM, a mask layer was created in MATLAB that indicates which areas of the topographic extents are marsh vs. open water. The mask layer regions of open water are not subject to change during the simulations.

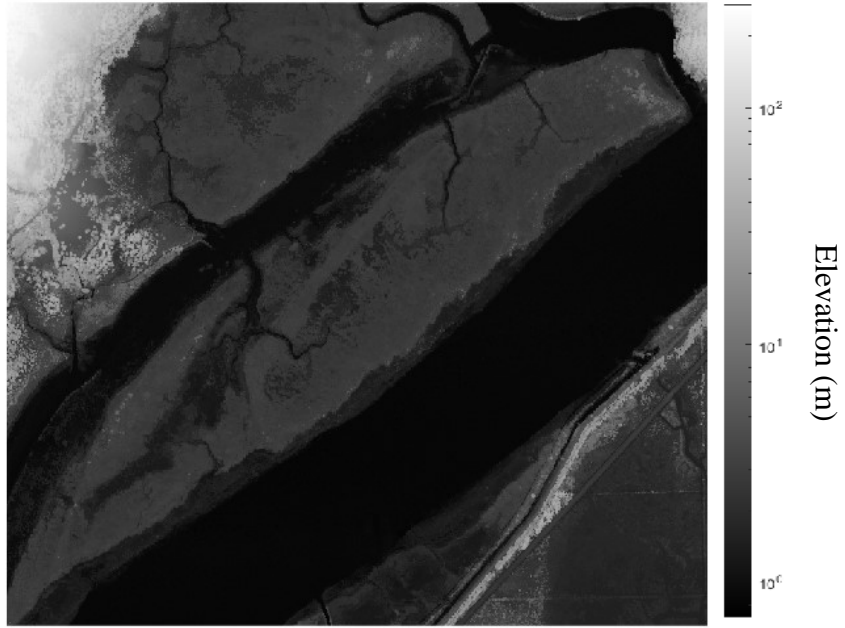


**Figure 3** Digital Elevation Model (DEM) of Siwash Island and surrounding area

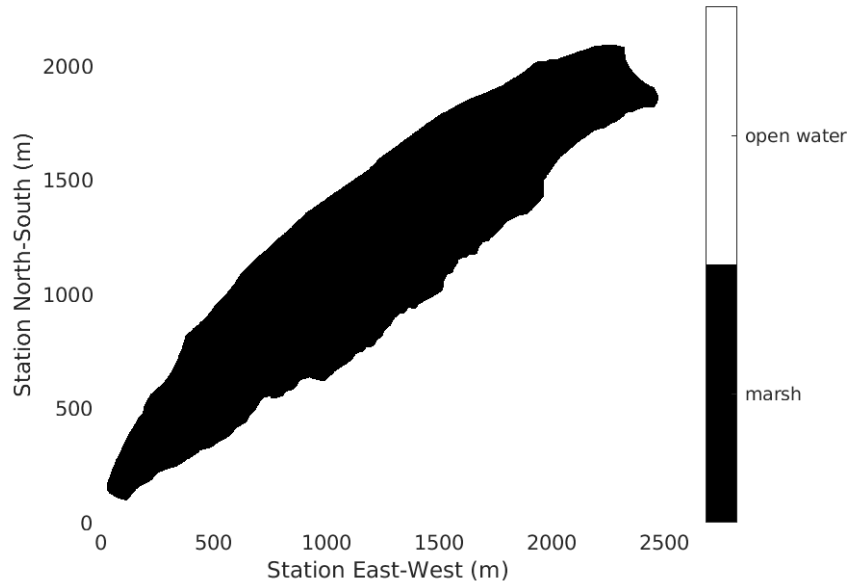


**Figure 4** Graphic representing open water (inactive cells) and marsh (active cells) used for each simulation. All cells located in black section experience changes throughout the simulations.

**Table 1** List of Parameters utilized in calibration of model MarshMorpho2D v.2.0 by G.Marriotti (2020). Site values are the ones that are used in this research.

Parameter	Description	Reference Values	Site Values
M	Number of columns in DEM	300	1274
N	Number of rows in DEM	500	1129
X	Length of site (m)	500	2548
Y	Width of site (m)	300	2258
Z	Area of site (m <sup>2</sup> )	500*300	2548*2258
Rho	Water density (kg/m <sup>3</sup> )	1030	1000
Msl	Mean sea level	2.5	0.9
Trange	Tidal range (m)	0.7	[1.5, 2.0]
Ttide	Tidal period (hrs/day)	12.5	12.25
Wind	Wind speed (m/s)	7	2
gR	Sea level rise (mm/yr)	[1, 2.5, 5, 7.5, 10]	[12.5, 25]
gC	Suspended sediment concentration (g/m <sup>3</sup> )	[60, 30, 15, 7.5]	[5, 20, 30]
taucr	Critical shear stress value	0.2	0.2

To forecast marsh evolution under different scenarios, a range of values are used to represent certain input parameters. These values are then combined in different combinations for each simulation (Tables 1 and 2). The first parameter is the rate of sea level rise, for which two scenarios were used based on global mean sea level (GMSL) rise scenarios: 1 m of SLR by the year 2100 and 2 m of SLR by the year 2100, which has been suggested in the framework of Sweet et al. (2017). An increase in sea level of 1 m and 2 m by the year 2100 aligns with 12.5 and 25 mm per year, respectively. Both scenarios are characterized by RCP 8.5 of global greenhouse gas emissions (Sweet et al, 2017).

The second parameter is the suspended sediment concentration (SSC), which is assumed to consist of mud sized particles in this model (Mariotti and Finotello, 2023). Selected suspended sediment concentrations for this study are 5 g/m<sup>3</sup>, 20 g/m<sup>3</sup>, 30 g/m<sup>3</sup> (Hutchins, 2021; Anderson, 2022). These values of SSC during tidal flow are considered as low, intermediate, and high in the study area (Anderson, 2022). Based on the study performed by Ashley in 1977, the Pitt River experiences relatively low suspended sediment (5 mg/m<sup>3</sup>) because it drains only Pitt Lake and few sluggish streams.

The other factor that has strong control on the stability of coastal marshes is tidal range (TR) and the values used to represent tidal range in this study are 1.5 m (microtidal marsh) and 2 m (mesotidal marsh) (Friedrichs and Perry, 2001). The tidal range was varied because trial simulations revealed that Siwash Island evolution is particularly sensitive to the height of inundation.

These factors, namely sea level rise (SLR), suspended sediment concentration (SSC), and tidal ranges (TR) were combined in different scenarios (Table 2), leading to in-depth analysis for marsh evolution at Siwash Island.

**Table 2** List of scenarios that were run using MarshMorpho2D v.2.0 developed by G.Mariotti (2020).

	Scenario 1			Scenario 2			Scenario3		
	SLR	SSC	TR	SLR	SSC	TR	SLR	SSC	TR
Simulation 1	12.5	5	1.5	12.5	5	2	25	20	1.5
Simulation 2	12.5	20	1.5	12.5	20	2	25	20	2
Simulation 3	12.5	30	1.5	12.5	30	2			

\*SLR= Sea Level Rise (mm/yr), SSC= Suspended Sediment Concentration (g/m<sup>3</sup>), TR= Tidal Range (m)

## Chapter 4.

### Results

Visual analysis of the MarshMorpho2D simulations indicate the pattern of Siwash Island's development over time, which I describe below by scenarios (Table 2).

#### 4.1. Scenario 1:

In the first Scenario, the SLR and TR are held constant (12.5 m and 1.5 m, respectively), but different SSC are considered 5, 20, 30 g/cm<sup>3</sup>.

##### 4.1.1. Elevation

Projected elevations and channel configurations over 80 years for 12.5 mm/yr SLR and three different SSC (5, 20, and 30 mg/L) are shown in Figures 5-7. The topographic evolution of Siwash Island is visually identical across the three SSC scenarios, and includes one dominant channel trending north to southwest, and two lesser channels situated to the north with a similar spatial orientation. The dominant channel also includes a tributary channel that trends northwest to southeast, situated roughly a few hundred meters from the mouth. Sediment deposition during the simulations is focused on the marsh surfaces adjacent to the dominant channel, as well as just north of the dominant channel along the northern shore and within the interior of the Island. Deposition in these areas approaches and exceeds 0.5 m of sediment. A lesser magnitude of deposition occurs on the northern tip of the Island, and the southern tip shoreline regresses roughly 30-50 meters from its initial position.

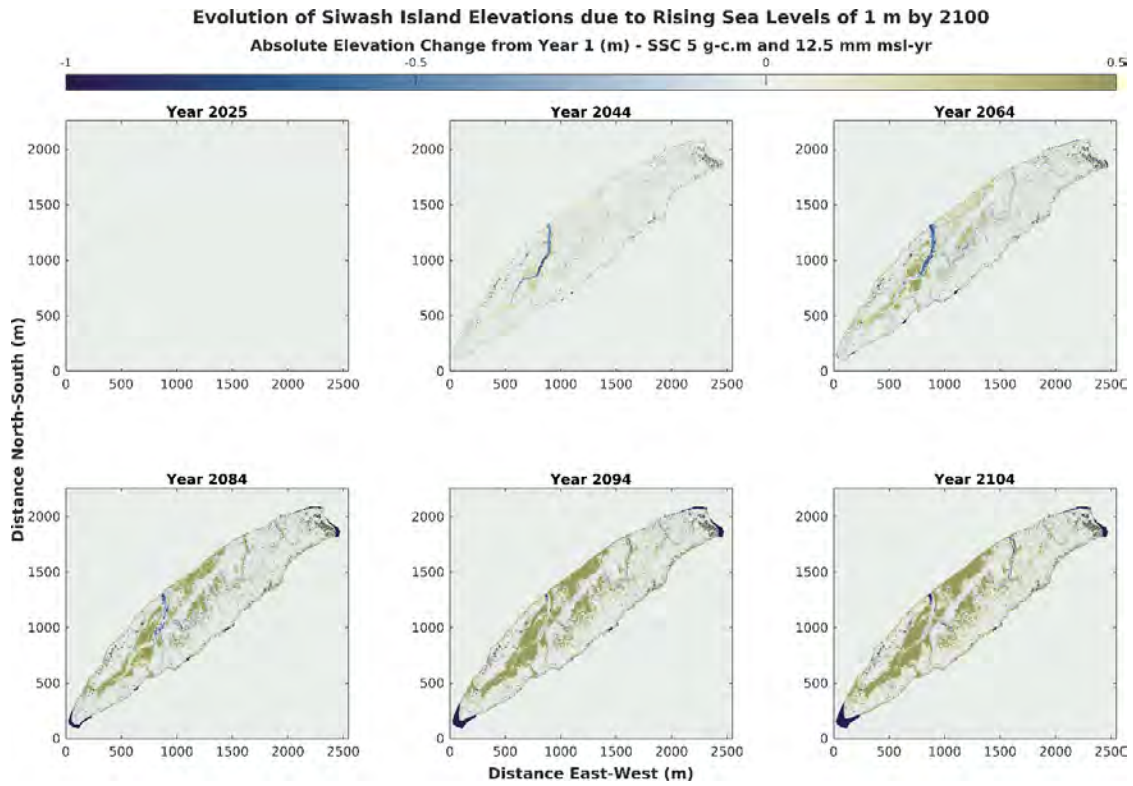


**Figure 5** Results from simulating Siwash Island with G.Mariotti's MarshMorpho2D model (2020). The plots highlight patterns of Siwash Island response through time in the model with the simulation of 12.5 mm/yr of SLR, 1.5 m of TR, and 5 g/cm<sup>3</sup> of SSC.

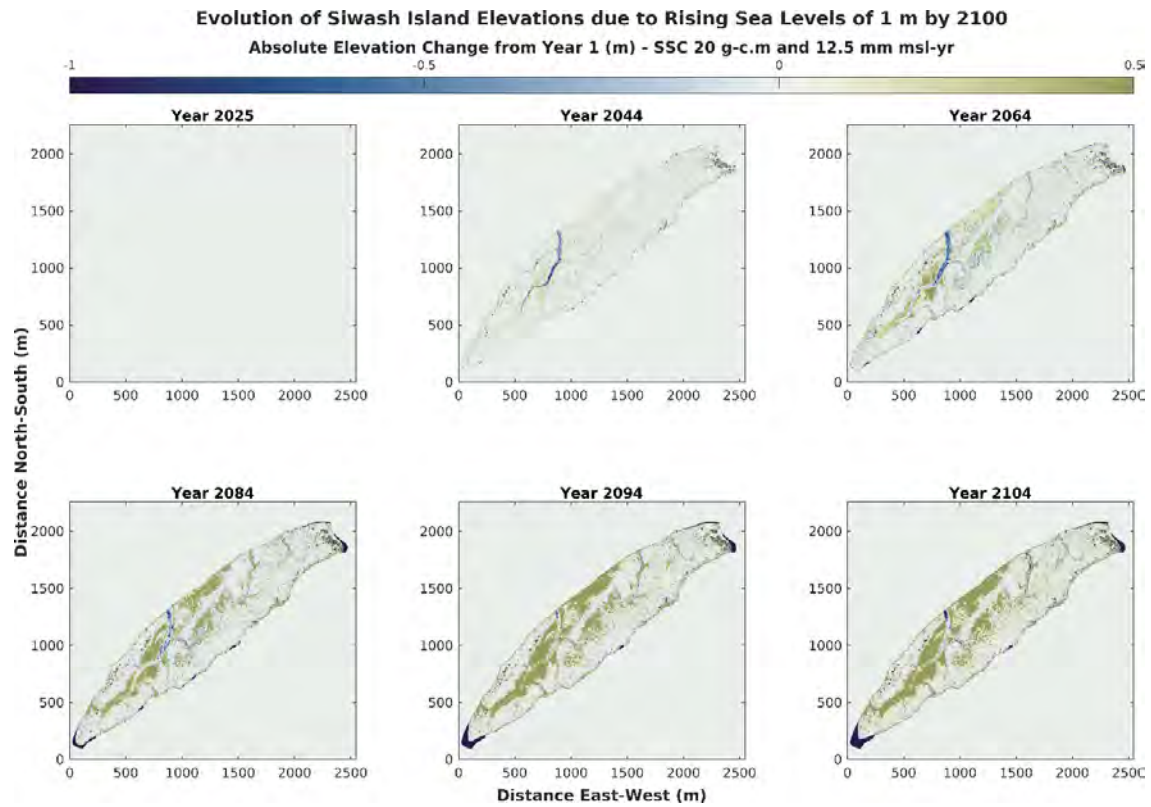


**Figure 6** Results from simulating Siwash Island with G.Mariotti's MarshMorpho2D model (2020). The plots highlight patterns of Siwash Island response through time in the model with the simulation of 12.5 mm/yr of SLR, 1.5 m of TR, and 20 g/cm<sup>3</sup> of SSC.

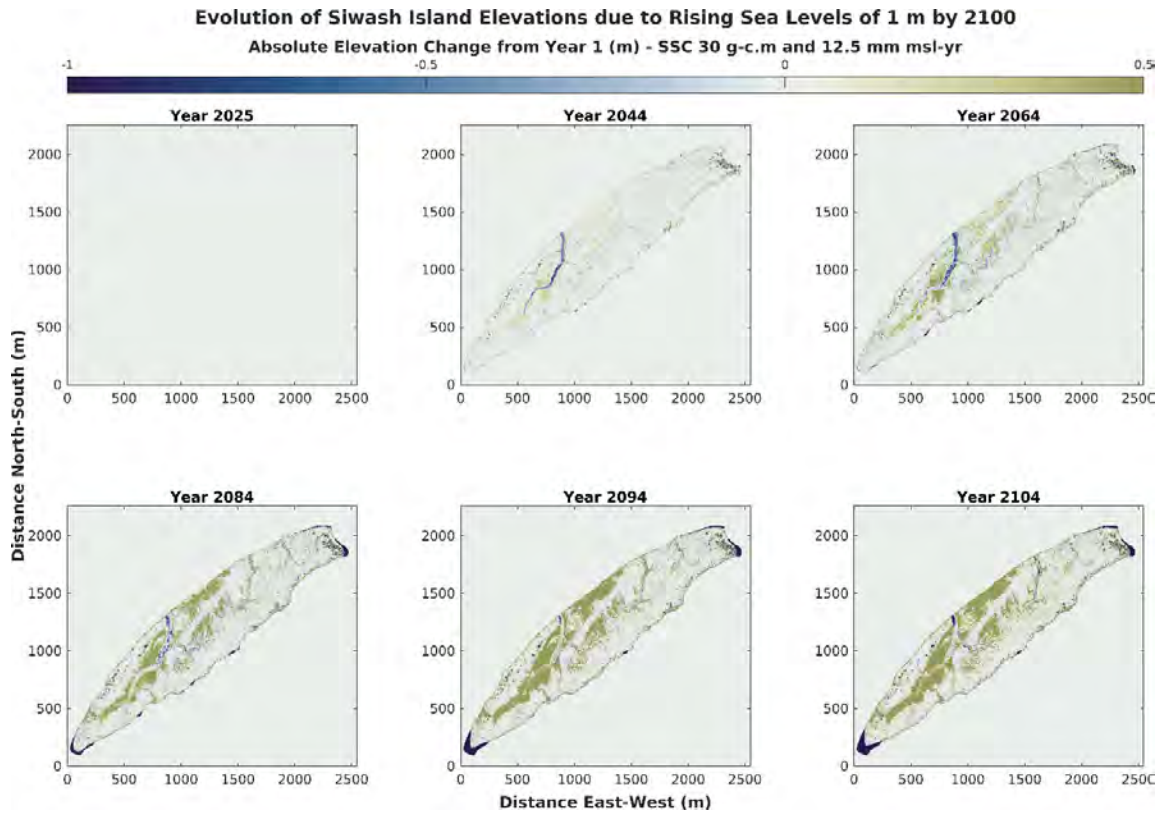


**Figure 7** Results from simulating Siwash Island with G.Mariotti's MarshMorpho2D model (2020). The plots highlight patterns of Siwash Island response through time in the model with the simulation of 12.5 mm/yr of SLR, 1.5 m of TR, and 30 g/cm<sup>3</sup> of SSC.

### **4.1.2. Relative Elevation**

The projected relative change in elevation for Siwash Island between the year 2025 and 2104 in relation to average sea level is shown in Figure 8-10. Scaling the projected elevations on the island to the corresponding average sea level each year in the simulations illustrates whether the overall marsh topography and bathymetry is keeping pace with projected increases of sea level. In general, the main tidal channel deepens, and the out of channel areas are eroded and flattened to a spatially more homogeneous condition, except for the highest areas which lie 2-4 meters above sea level at the beginning of the simulations. More specifically, as the simulations progress toward 2104, the out of channel topography tends to the average sea level elevation. The southern tip of Siwash Island also erodes and is inundated by the rising sea level, with bathymetry at the end of the simulations consistently 1 or more meters below the average sea level.

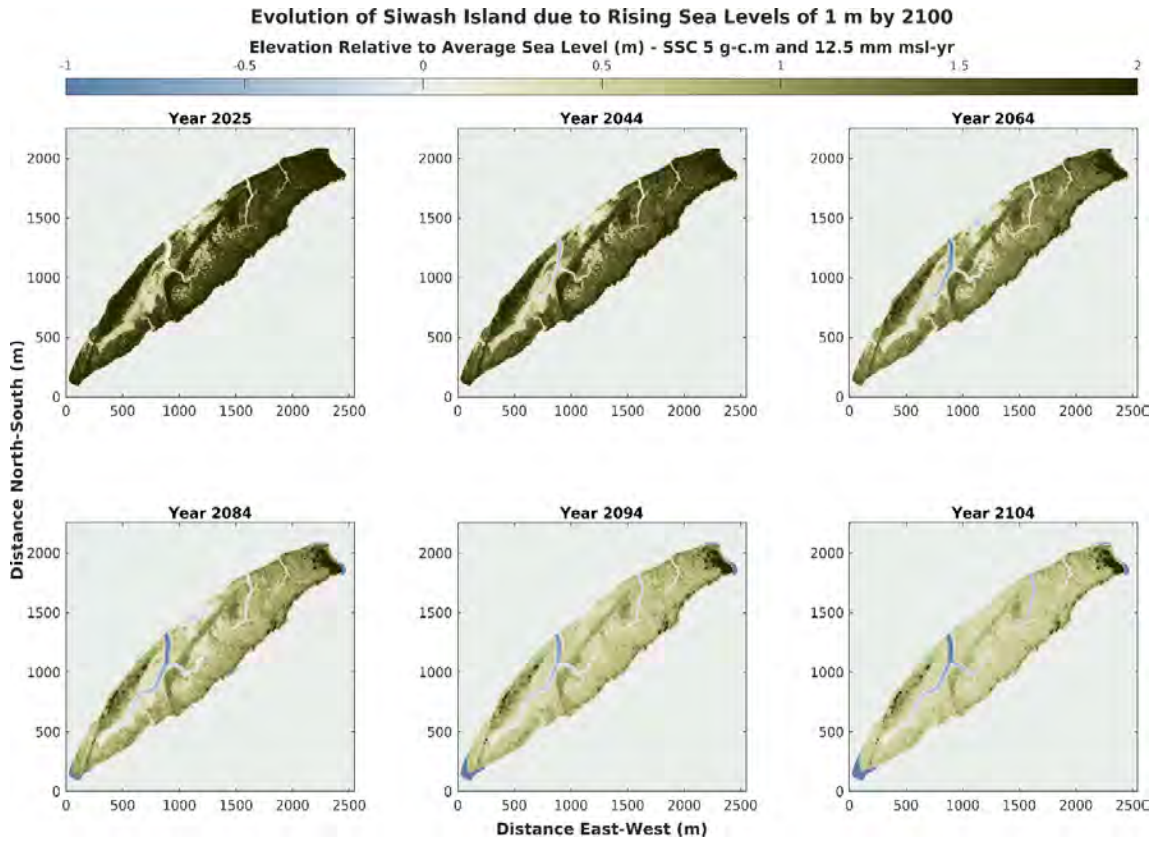


**Figure 8** Results from simulating Siwash Island with G.Mariotti's MarshMorpho2D model (2020). These six subplots show elevation relative to average sea level with the simulation of 12.5 mm/yr of SLR, 1.5 m of TR, and 5 g/cm<sup>3</sup> of SSC.

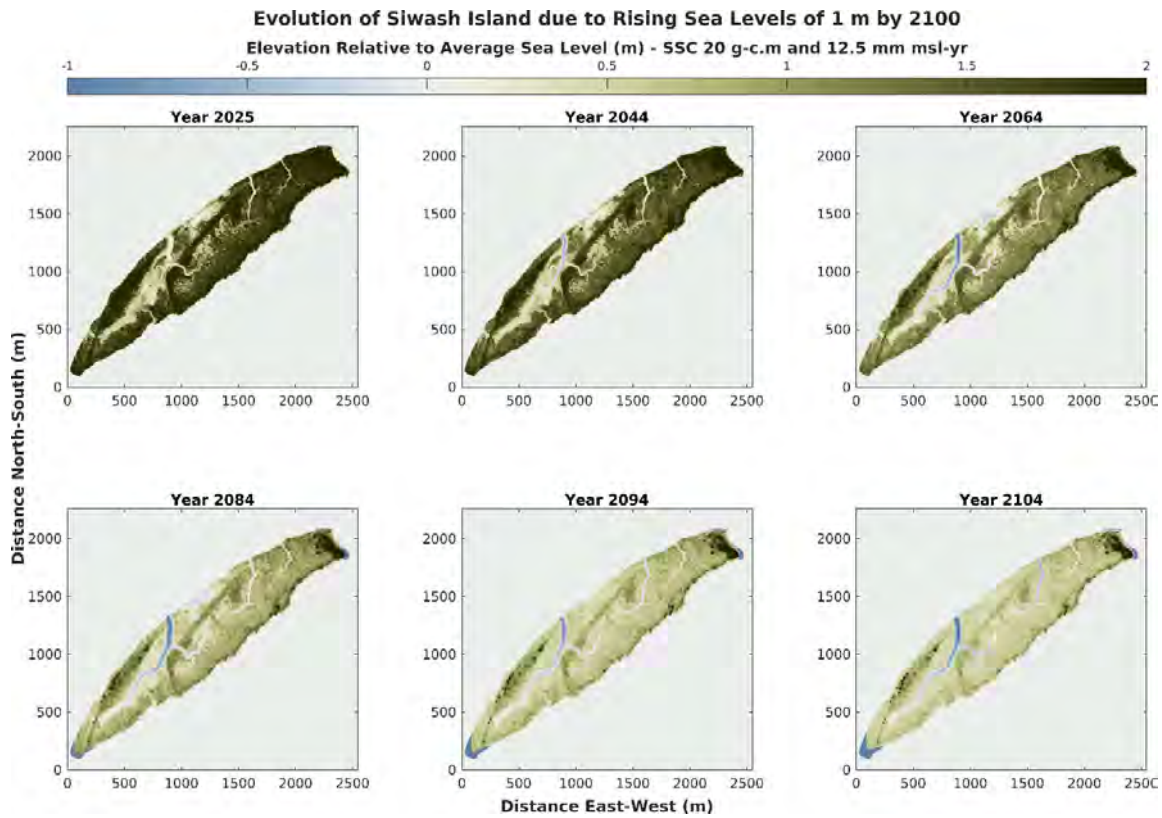


**Figure 9** Results from simulating Siwash Island with G.Mariotti's MarshMorpho2D model (2020). These six subplots show elevation relative to average sea level with the simulation of 12.5 mm/yr of SLR, 1.5 m of TR, and 20 g/cm<sup>3</sup> of SSC.

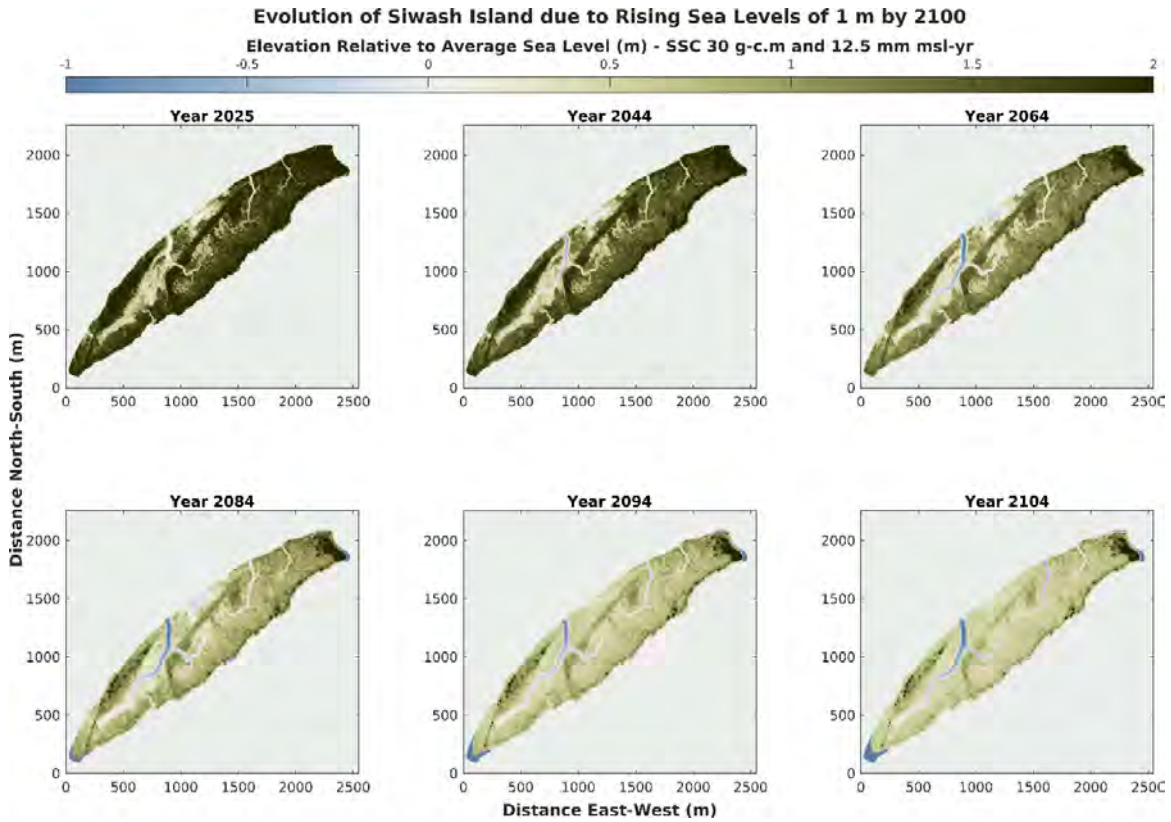


**Figure 10** Results from simulating Siwash Island with G.Mariotti's MarshMorpho2D model (2020). These six subplots show elevation relative to average sea level with the simulation of 12.5 mm/yr of SLR, 1.5 m of TR, and 30 g/cm<sup>3</sup> of SSC.

### **4.1.3. Suspended Sediment Concentration (SSC)**

The three sets of subplots in Figures 11, 12, and 13 highlight the projected evolution of SSC in accordance with simulations using SLR value of 12.5 mm/yr, TR value of 1.5 m, and SSC values of 5, 20, 30 g/cm<sup>3</sup> respectively. Figures 11, 12, and 13 illustrate SSC ranging from 0-5 g/cm<sup>3</sup>, 0-20 g/cm<sup>3</sup>, and 0-30 g/cm<sup>3</sup>. At the start of the simulations, the concentration of suspended sediment is high in the dominant channel trending north to southwest and nearby areas. Over time, the concentration of suspended sediment disperses not only in tidal channels, but also in more locations of Siwash Island, along the northern shore, within the interior of the Island and in lesser channel in the north of the island. By 2094, SSC is higher near in tidal channels, adjacent to the channels, and the southern tip of Siwash Island, ranging between 2.5 and 5 g/cm<sup>3</sup>, before decreasing in 2104. Figure 11 shows the higher concentration of SSC in SSC and nearby area in comparison to other simulations.

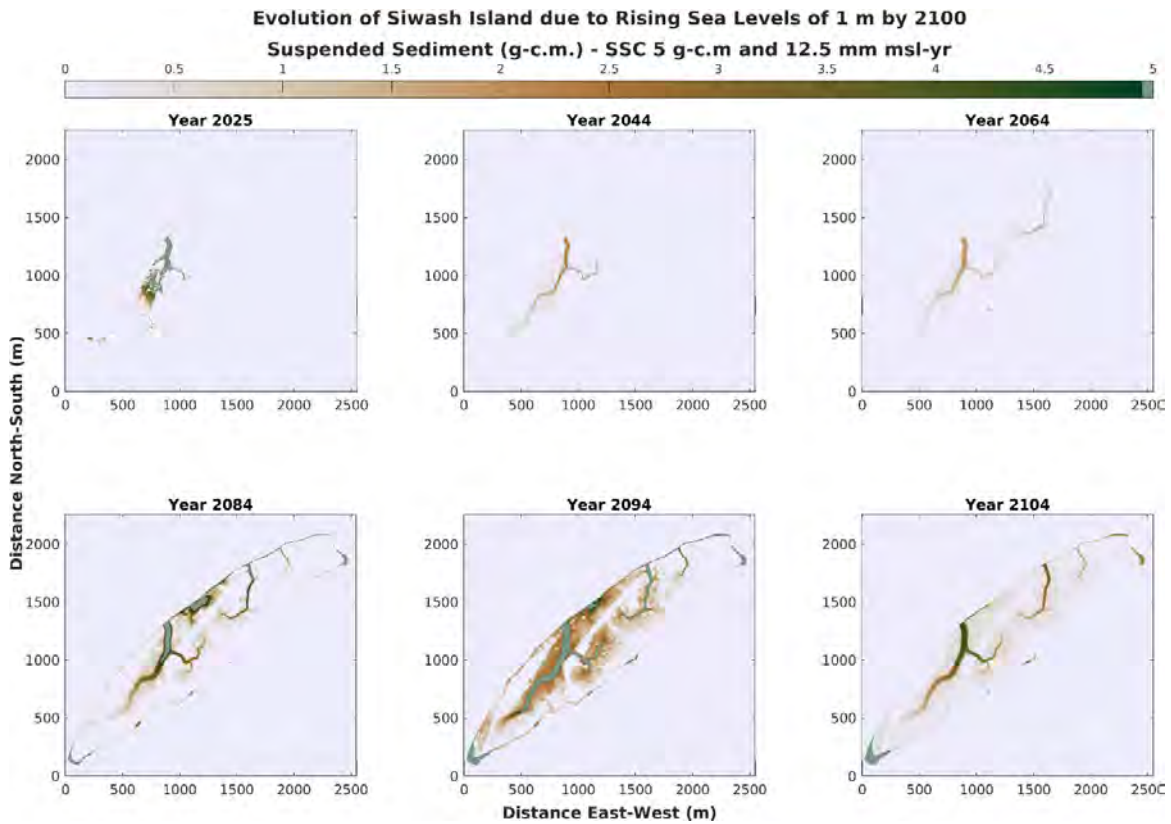


**Figure 11** Results from simulating Siwash Island with G.Mariotti's MarshMorpho2D model (2020). These six subplots show the evolution of suspended sediment concentration over time with the simulation of 12.5 mm/yr of SLR, 1.5 m of TR, and 5 g/cm<sup>3</sup> of SSC.

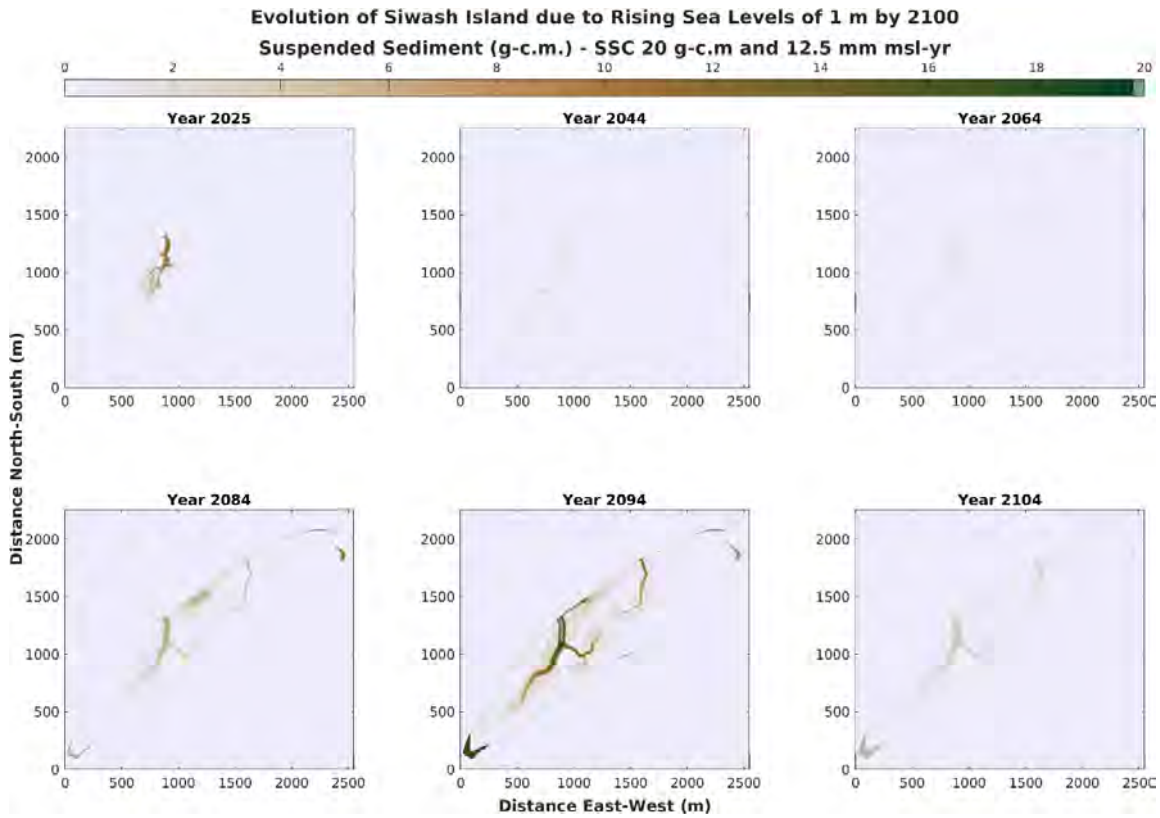


**Figure 12** Results from simulating Siwash Island with G.Mariotti's MarshMorpho2D model (2020). These six subplots show the evolution of suspended sediment concentration over time with the simulation of 12.5 mm/yr of SLR, 1.5 m of TR, and 20 g/cm<sup>3</sup> of SSC.

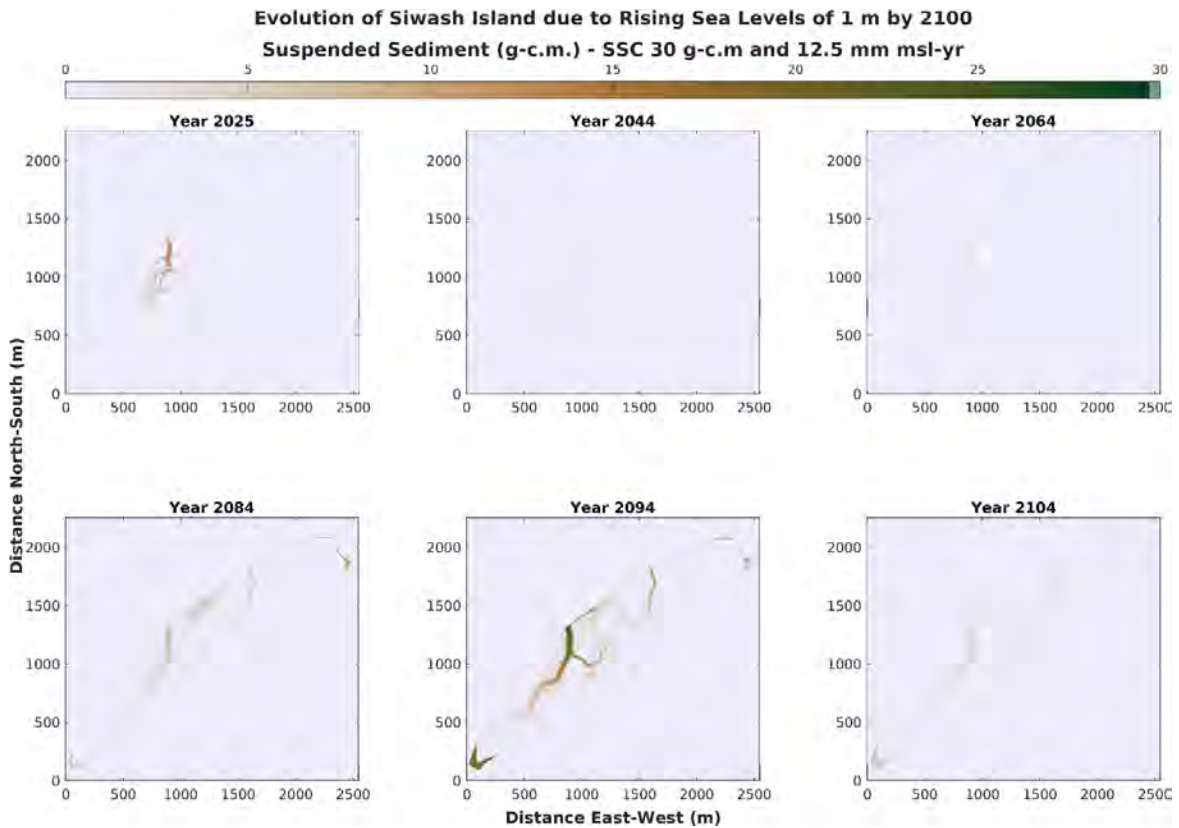


**Figure 13** Results from simulating Siwash Island with G.Mariotti's MarshMorpho2D model (2020). These six subplots show the evolution of suspended sediment concentration over time with the simulation of 12.5 mm/yr of SLR, 1.5 m of TR, and 30 g/cm<sup>3</sup> of SSC.

#### 4.1.4. Vegetation Cover

Another outcome of MarshMorpho2D model is vegetation cover that illustrates how it changed over time until 2104 that are shown in Figure 14-16 for 12.5 mm/yr SLR, 1.5 m TR, and three different SSC (5, 20, 30 g/cm<sup>3</sup>). the outcomes for vegetation changes between simulations of scenario 1 with using different SSC values, while keeping all other parameter constant, are identical. Siwash Island experience vegetation loss over the time until 2104, decreasing approximately 25% over 80 years.

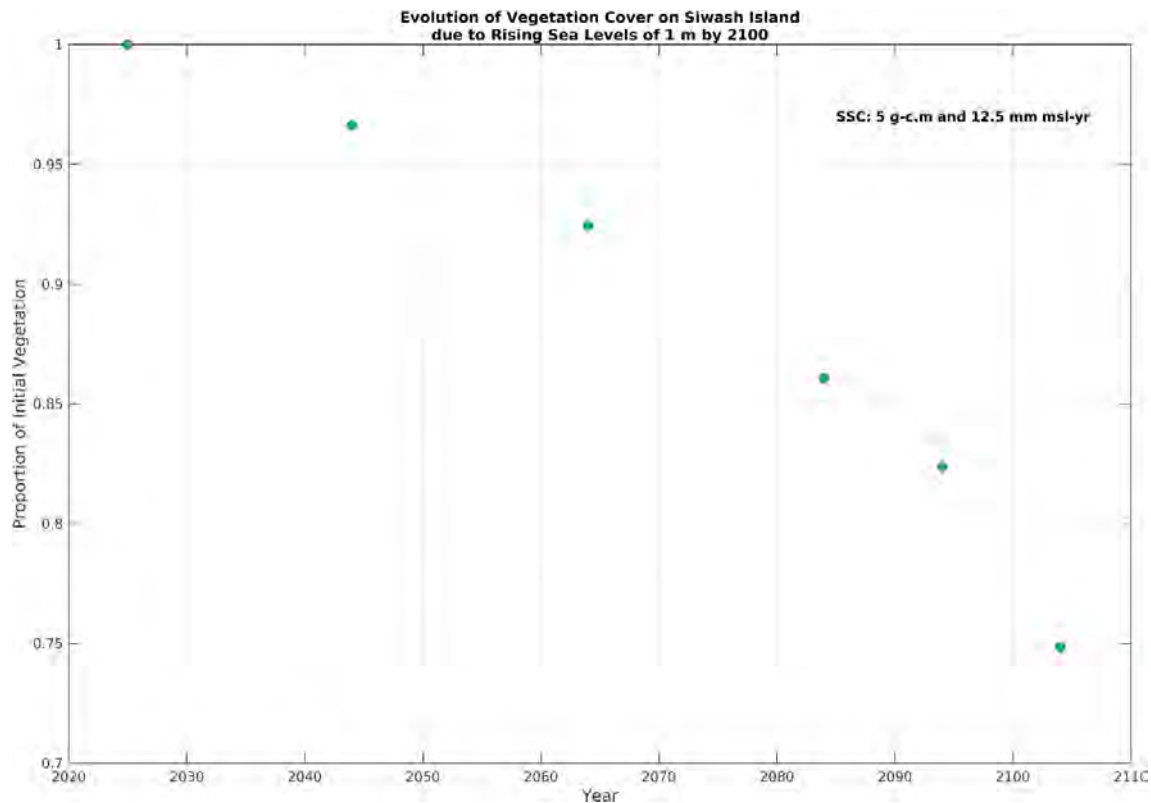


**Figure 14** Results from simulating Siwash Island with G.Mariotti's MarshMorpho2D model (2020). This plot shows the evolution of vegetation cover over time with the simulation of 12.5 mm/yr of SLR, 1.5 m of TR, and 5 g/cm<sup>3</sup> of SSC.

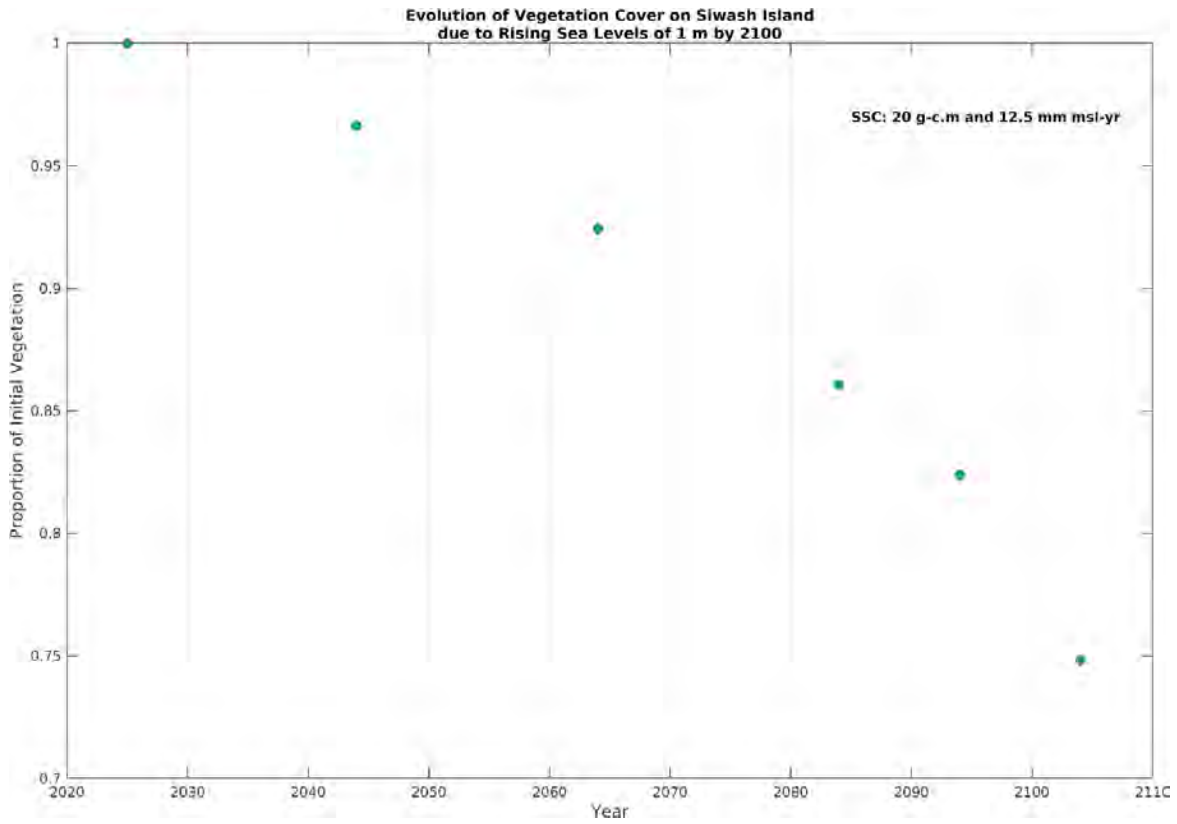


**Figure 15** Results from simulating Siwash Island with G.Mariotti's MarshMorpho2D model (2020). This plot shows the evolution of vegetation cover over time with the simulation of 12.5 mm/yr of SLR, 1.5 m of TR, and 20 g/cm<sup>3</sup> of SSC.

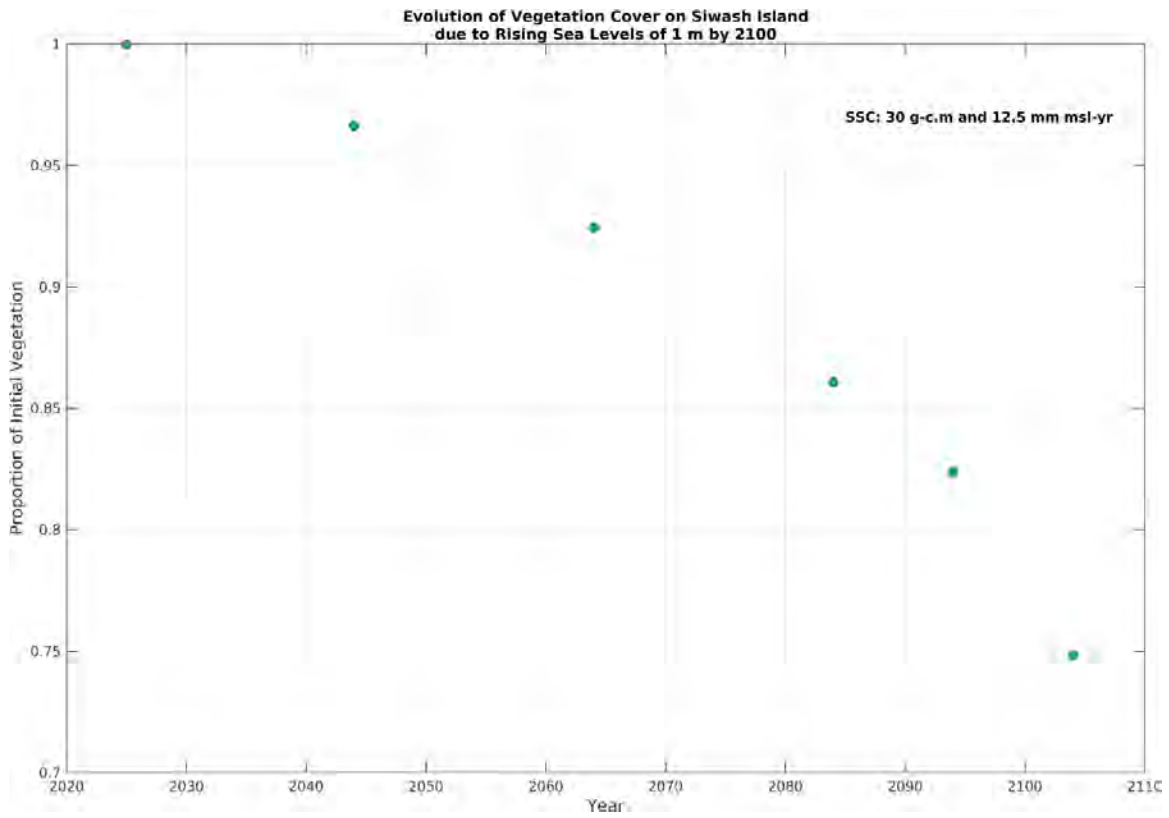


**Figure 16** Results from simulating Siwash Island with G.Mariotti's MarshMorpho2D model (2020). This plot shows the evolution of vegetation cover over time with the simulation of 12.5 mm/yr of SLR, 1.5 m of TR, and 30 g/cm<sup>3</sup> of SSC.

### 4.1.5. Velocity

Projected velocity for each simulation of scenario 1 for year between 2025 and 2104 is shown in Figures 17-19. At the start of the simulations, velocity is relatively low, and more observable in the dominant channel, situated north to southwest of Siwash Island; however, as sea level rises over time, since 2084, the velocity increases across the tidal channels, including the dominant channel and its tributary channel, as well as the two lesser channels situated to the north part of the island. Additionally, there will be a noticeable increase in velocity at the southern tip and one spot in northern tip of Siwash Island from 2084.

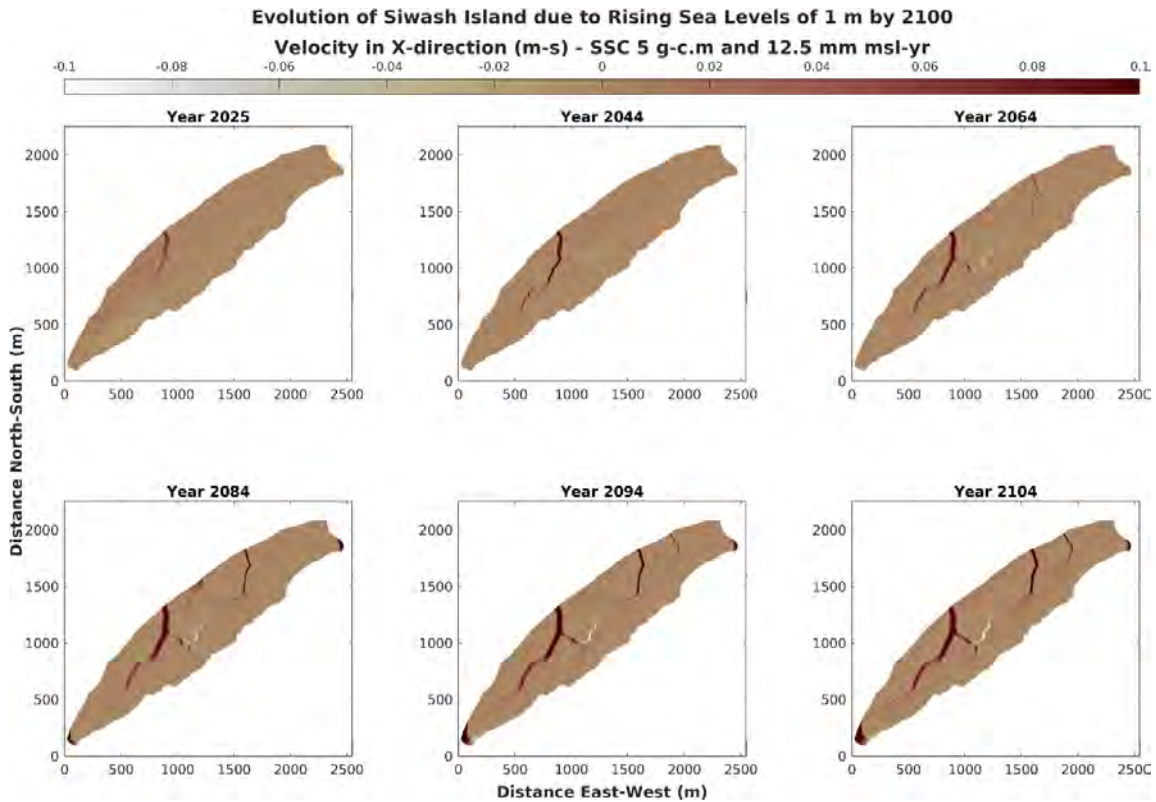


**Figure 17** Results from simulating Siwash Island with G.Mariotti's MarshMorpho2D model (2020). These six subplots show the changes in velocity until 2104 with the simulation of 12.5 mm/yr of SLR, 1.5 m of TR, and 5 g/cm<sup>3</sup> of SSC.

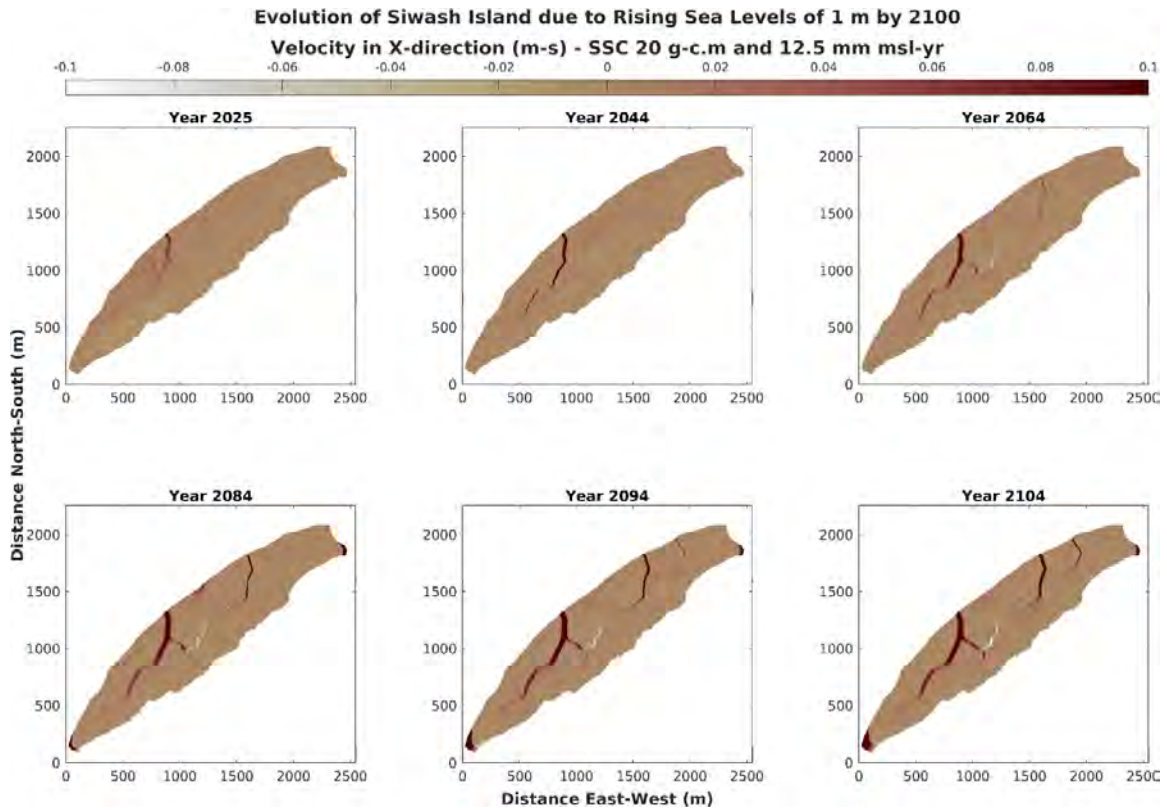


**Figure 18** Results from simulating Siwash Island with G.Mariotti's MarshMorpho2D model (2020). These six subplots show the changes in velocity until 2104 with the simulation of 12.5 mm/yr of SLR, 1.5 m of TR, and 20 g/cm<sup>3</sup> of SSC.

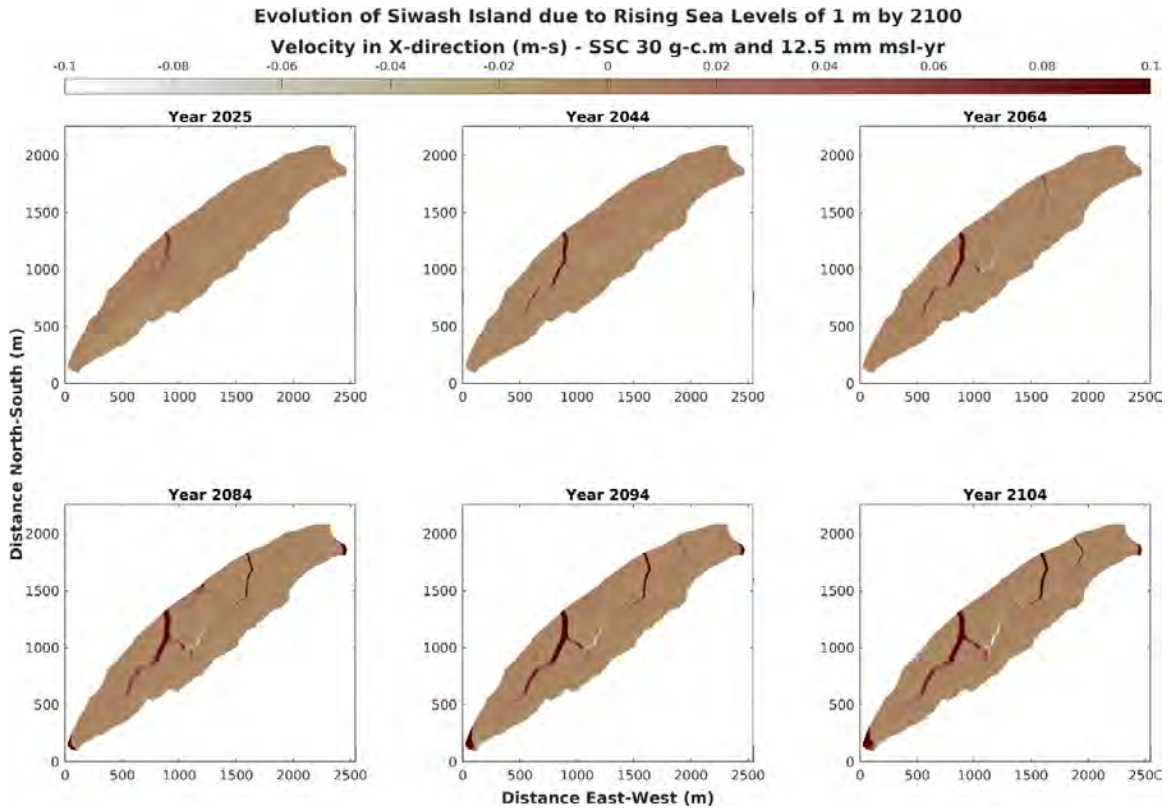


**Figure 19** Results from simulating Siwash Island with G.Mariotti's MarshMorpho2D model (2020). These six subplots show the changes in velocity until 2104 with the simulation of 12.5 mm/yr of SLR, 1.5 m of TR, and 30 g/cm<sup>3</sup> of SSC.

#### 4.1.6. Water Depth

The 6 subplots in Figures 20, 21, and 22 represent the projected water depth with 12.5 mm/yr of SLR, 1.5 m of TR, and 5, 20,30 g/cm<sup>3</sup> of SSC. All the simulations of scenario 1 show the same projected increase in water depth within Siwash Island after 80 years. In the initial stages of the simulations, the water depth is relatively low across the Island, with it being more prominent in tidal channel, adjacent surfaces at the north to southwest, and north of the dominant channel along the northern shore and within the interior of Siwash Island. As time goes on, the water depth generally increases not only in tidal channels but also across the entire Siwash Island, starting at the northern shore of the Island. The southern and northern tip of marsh area has a substantial projected increase in water depth by 2104, reaching 2 meters. As sea level rises, the two lesser channels to the north of the island and the tributary channel of the main channel lengthen and deepen over time.

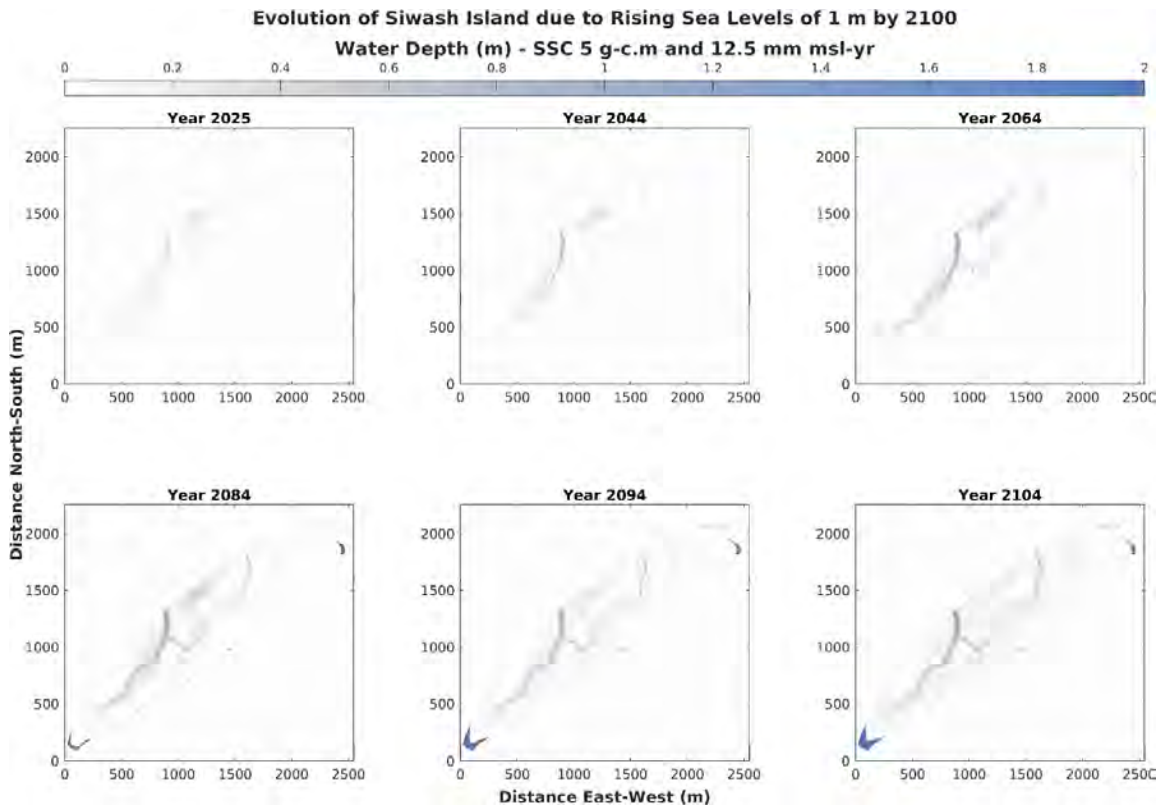


**Figure 20** Results from simulating Siwash Island with G.Mariotti's MarshMorpho2D model (2020). These six subplots show the changes in Water depth over time until 2104 with the simulation of 12.5 mm/yr of SLR, 1.5 m of TR, and 5 g/cm<sup>3</sup> of SSC.

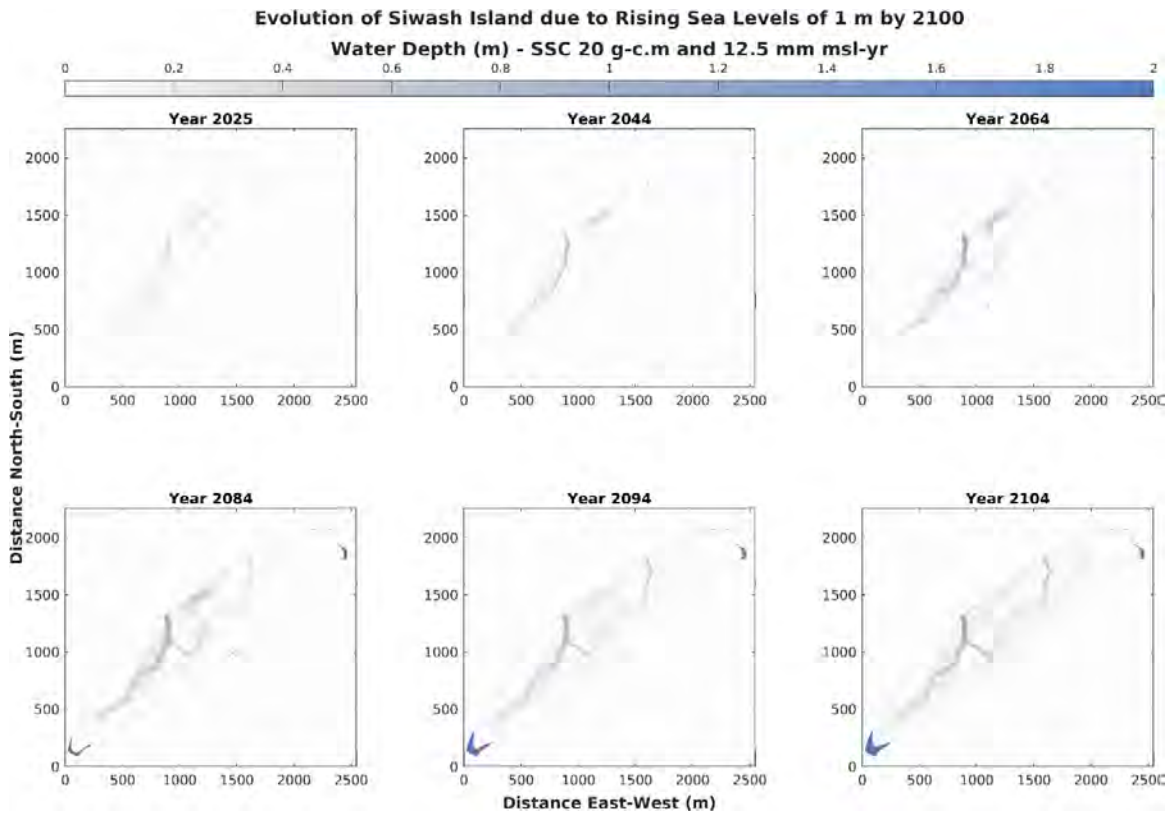


**Figure 21** Results from simulating Siwash Island with G.Mariotti's MarshMorpho2D model (2020). These six subplots show the changes in Water depth over time until 2104 with the simulation of 12.5 mm/yr of SLR, 1.5 m of TR, and 20 g/cm<sup>3</sup> of SSC.

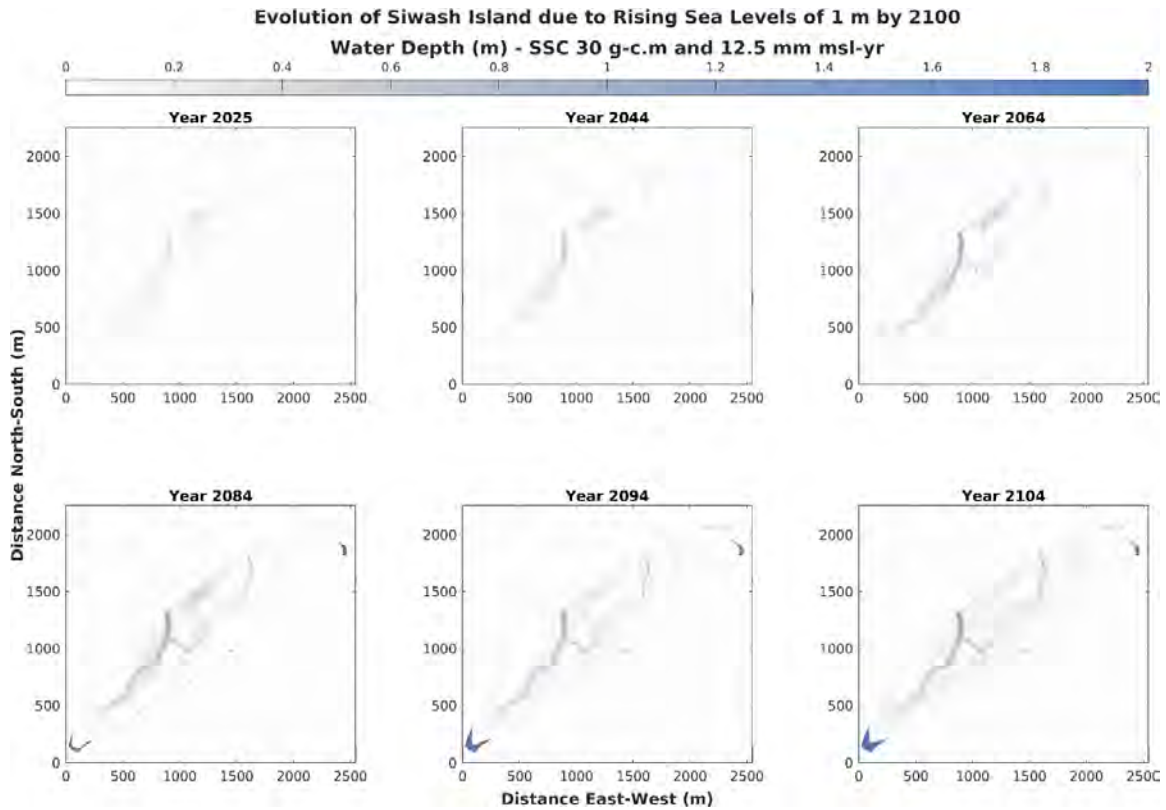


**Figure 22** Results from simulating Siwash Island with G.Mariotti's MarshMorpho2D model (2020). These six subplots show the changes in Water depth over time until 2104 with the simulation of 12.5 mm/yr of SLR, 1.5 m of TR, and 30 g/cm<sup>3</sup> of SSC.

## **4.2. Scenario 2:**

In the second Scenario, the SLR and TR are held constant (12.5 m and 2 m respectively); however different SSC are considered: 5, 20, 30 g/cm<sup>3</sup>.

### **4.2.1. Elevation Change**

In Figures 23-25, a series of subplots illustrate the projected changes in elevation and channel configurations at Siwash Island for 12.5 mm/yr SLR, 2 m of TR, and different SSC (5, 20, 30 g/cm<sup>3</sup>). The topographic evolution for all three simulations of scenario 2 represents the same conditions throughout Siwash Island, including one dominant channel trending north to southwest, and two lesser channels situated to the north with a similar orientation. The main channel also includes tributary channel situated northwest to southeast. Sediment deposition during the simulations is focused on the marsh surface adjacent to the tidal channels, as well as just north of the dominant channel along the north shore within the interior of the island, reaching and exceeding 0.5 m. Since 2084, sediment deposition occurs on almost all surface of the island reaching 0.5 m of sediment. As sea level rises, the dominant channel creates a new dominant pathway, bisecting the island. This main channel deepens and widens over time, becoming more prominent features on the island itself. The elevation of northern and southern tips of Siwash Island and channels decrease to a range of 0.5 to -1 m.

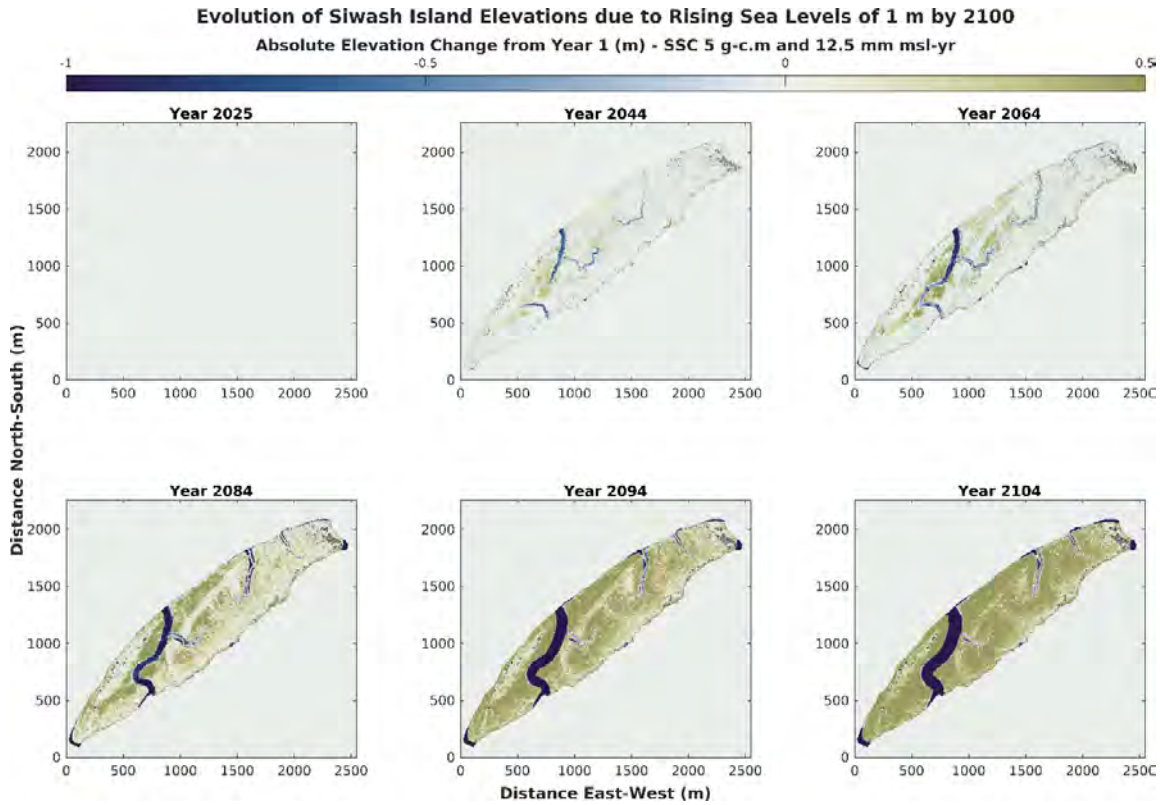


**Figure 23** Results from simulating Siwash Island with G.Mariotti's MarshMorpho2D model (2020). The plots highlight patterns of Siwash Island response through time in the model with the simulation of 12.5 mm/yr of SLR, 2 m of TR, and 5 g/cm<sup>3</sup> of SSC.

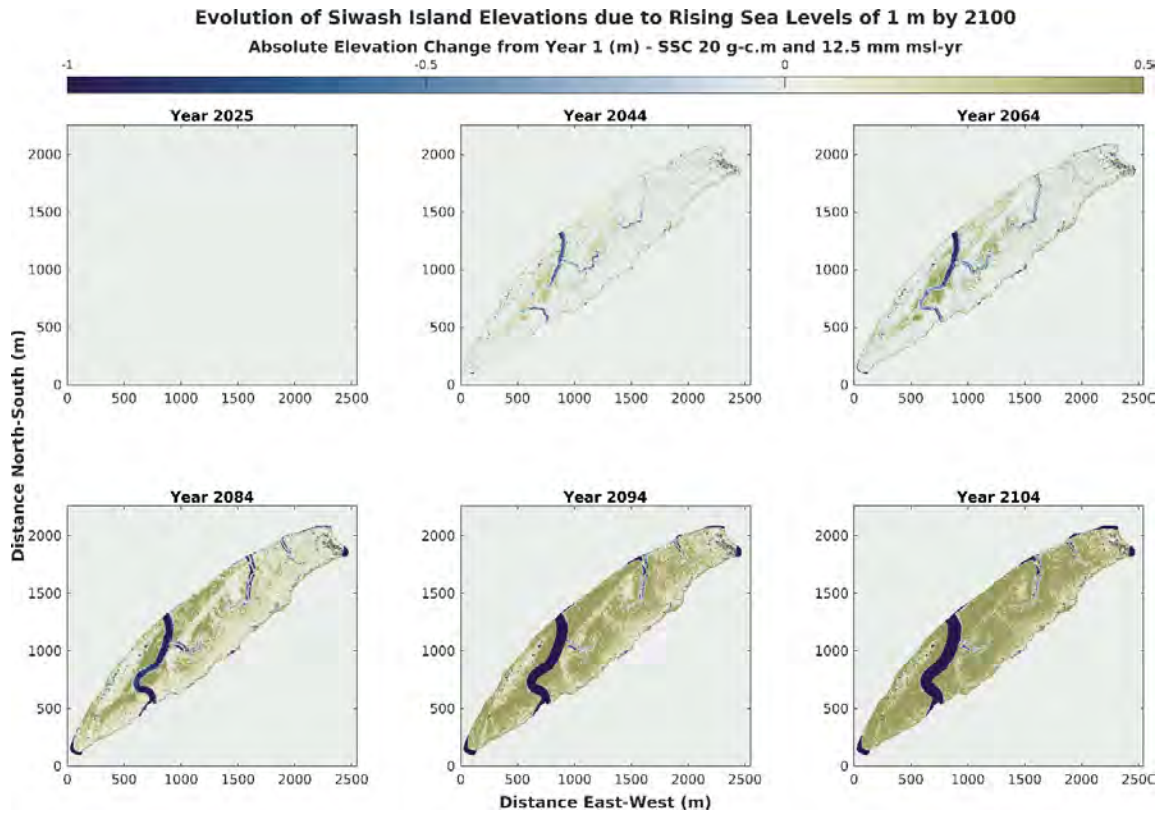


**Figure 24** Results from simulating Siwash Island with G.Mariotti's MarshMorpho2D model (2020). The plots highlight patterns of Siwash Island response through time in the model with the simulation of 12.5 mm/yr of SLR, 2 m of TR, and 20 g/cm<sup>3</sup> of SSC.

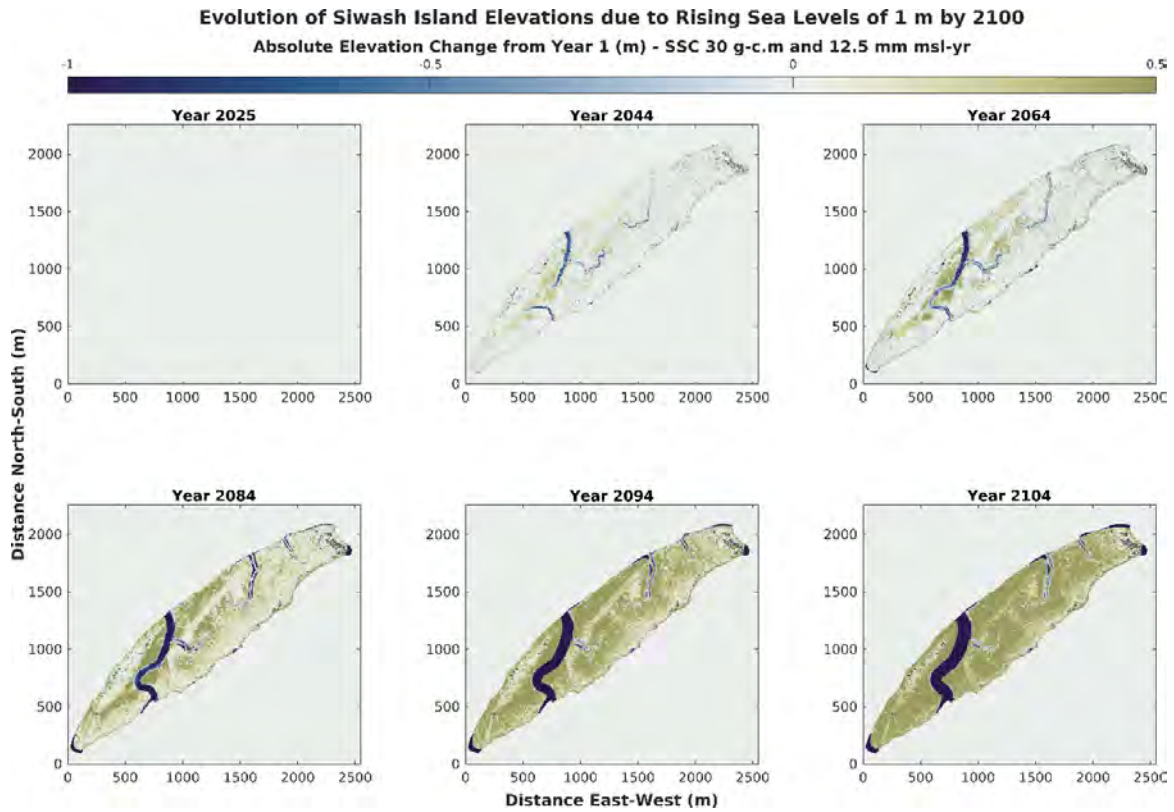


**Figure 25** Results from simulating Siwash Island with G.Mariotti's MarshMorpho2D model (2020). The plots highlight patterns of Siwash Island response through time in the model with the simulation of 12.5 mm/yr of SLR, 2 m of TR, and 30 g/cm<sup>3</sup> of SSC.

#### **4.2.2. Relative Elevation**

The projected change in relative elevation between the years 2025 and 2104 is illustrated in Figures 26-28 based on Scenario 2 with simulations of 12.5 mm/yr of SLR, 2.0 m of TR, and 5, 20, 30 g/cm<sup>3</sup> of SSC respectively. At the start of the simulation, Siwash Island's elevation ranges from 1 to 2, which is higher than the average sea level; however, as the simulation moves closer to 2104, the elevation of out of channel topography approaches near average sea level, causing the area out of channel to erode and flatten, resulting in a more spatially homogenous condition. The two lesser channels at the north of the Siwash Island deepen and lengthen, reaching 1 m below average sea level. The northern part of the Island between dominant channel and lesser channel experiences erosion and is inundated by the rising sea level, reaching approximately 1 meter below average sea level from its initial position at roughly 0.5 m. At the northern tip of Siwash Island along with some spots in the south and northwest shores still maintain an elevation of almost 2 m relative to sea level.

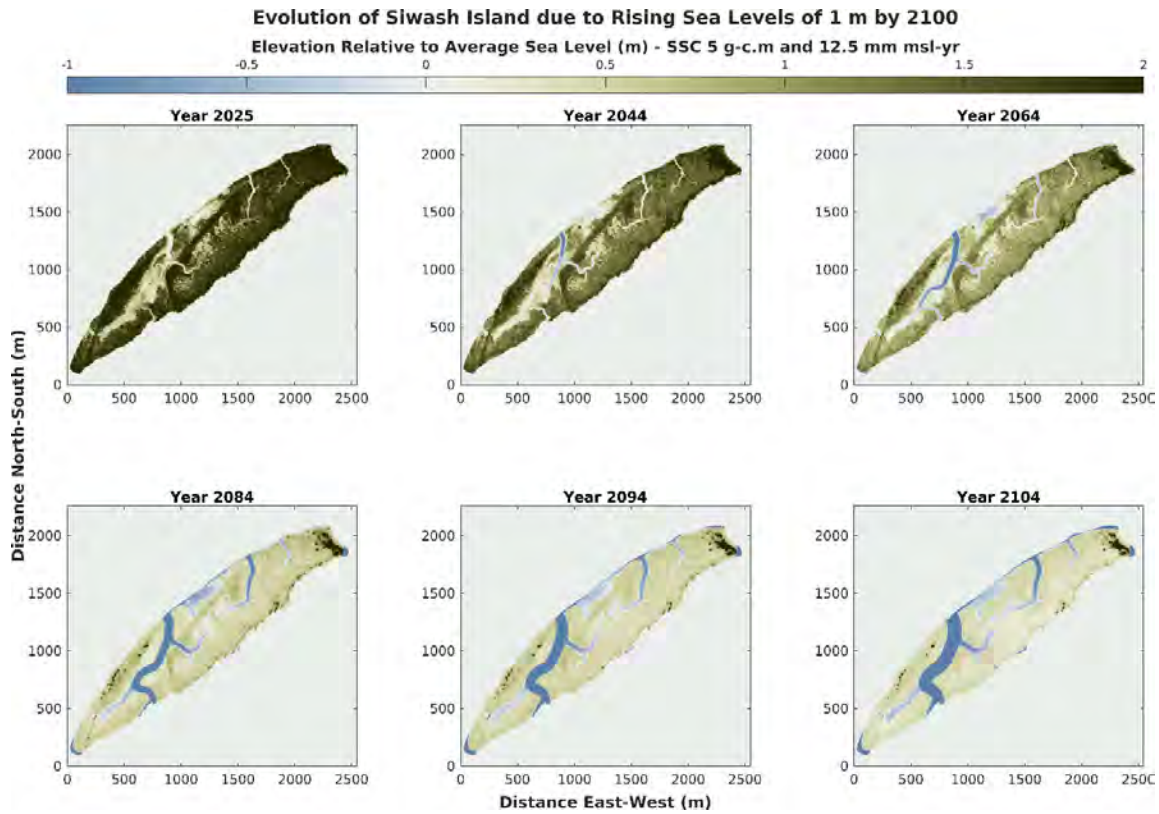


**Figure 26** Results from simulating Siwash Island with G.Mariotti's MarshMorpho2D model (2020). These six subplots show elevation relative to average sea level with the simulation of 12.5 mm/yr of SLR, 2 m of TR, and 5 g/cm<sup>3</sup> of SSC.

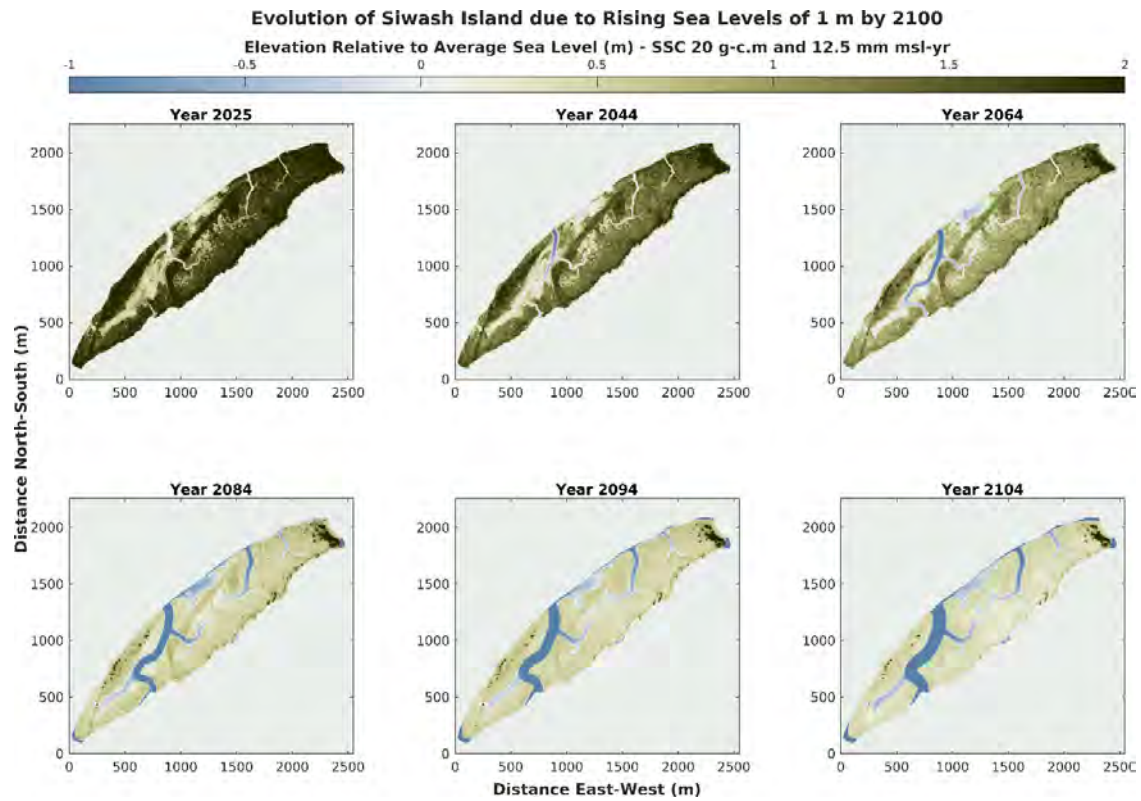


**Figure 27** Results from simulating Siwash Island with G.Mariotti's MarshMorpho2D model (2020). These six subplots show elevation relative to average sea level with the simulation of 12.5 mm/yr of SLR, 2 m of TR, and 20 g/cm<sup>3</sup> of SSC.

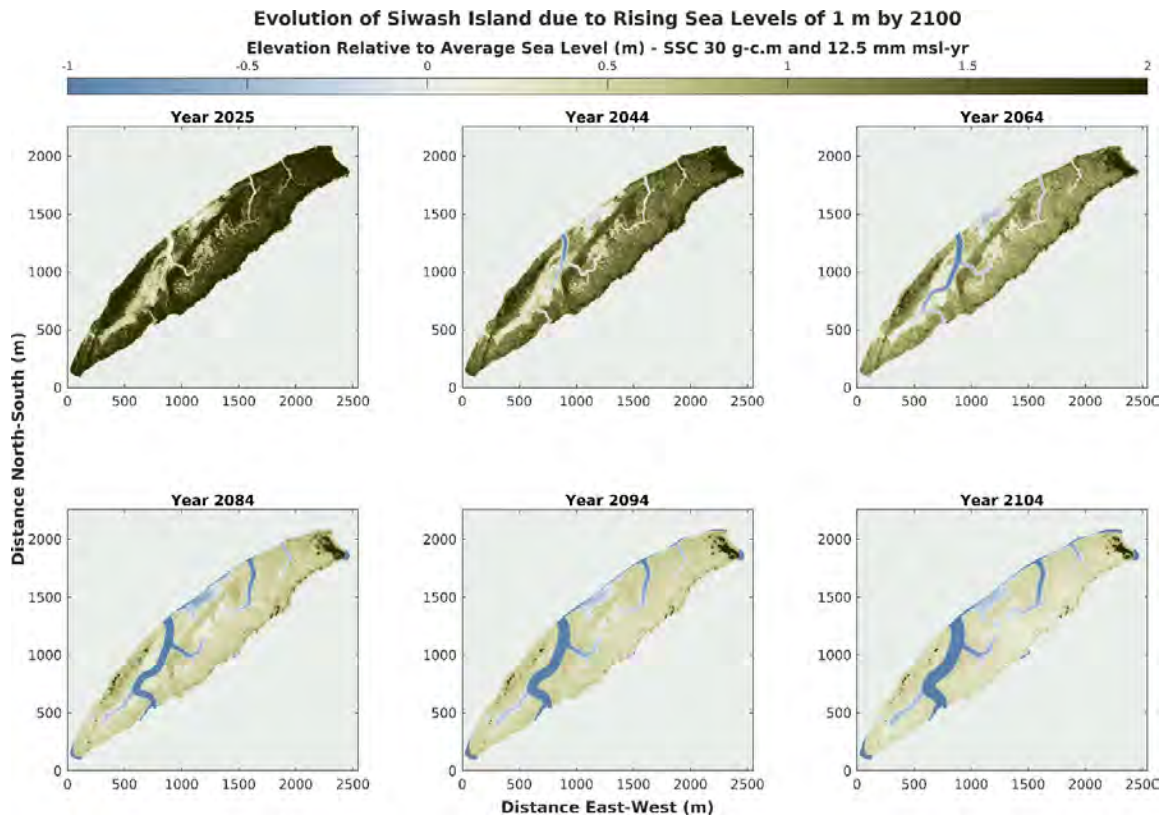


**Figure 28** Results from simulating Siwash Island with G.Mariotti's MarshMorpho2D model (2020). These six subplots show elevation relative to average sea level with the simulation of 12.5 mm/yr of SLR, 2 m of TR, and 30 g/cm<sup>3</sup> of SSC.

### 4.2.3. Suspended Sediment Concentration

Figures 29-31 illustrate the projection of suspended sediment concentration over 80 years for 12.5 mm/yr SLR, 2 m TR, and three different SSC (5, 20, 30 g/cm<sup>3</sup>) with the range of 0-5, 0-20, and 0-30 g/cm<sup>3</sup>. The concentration of suspended sediment is limited to main tidal channel and surrounding areas trending north to southwest at the beginning of the simulations, then SSC is not only dispersed in main tidal channel but also two lesser channels on the north of the island. The SSC evolution decreases in the years 2044, 2064, and 2084 in tidal channels, but an expansion of SSC throughout Siwash Island can be observed. By 2084, island is bisected based on the main channel which creates a new pathway to the south shore of the island. In the year 2094 the concentration of suspended sediment increases across the entire surface of Siwash Island and then decreases in 2104. Figure 29 shows the highest SSC in dominant and lesser channels in 2094.

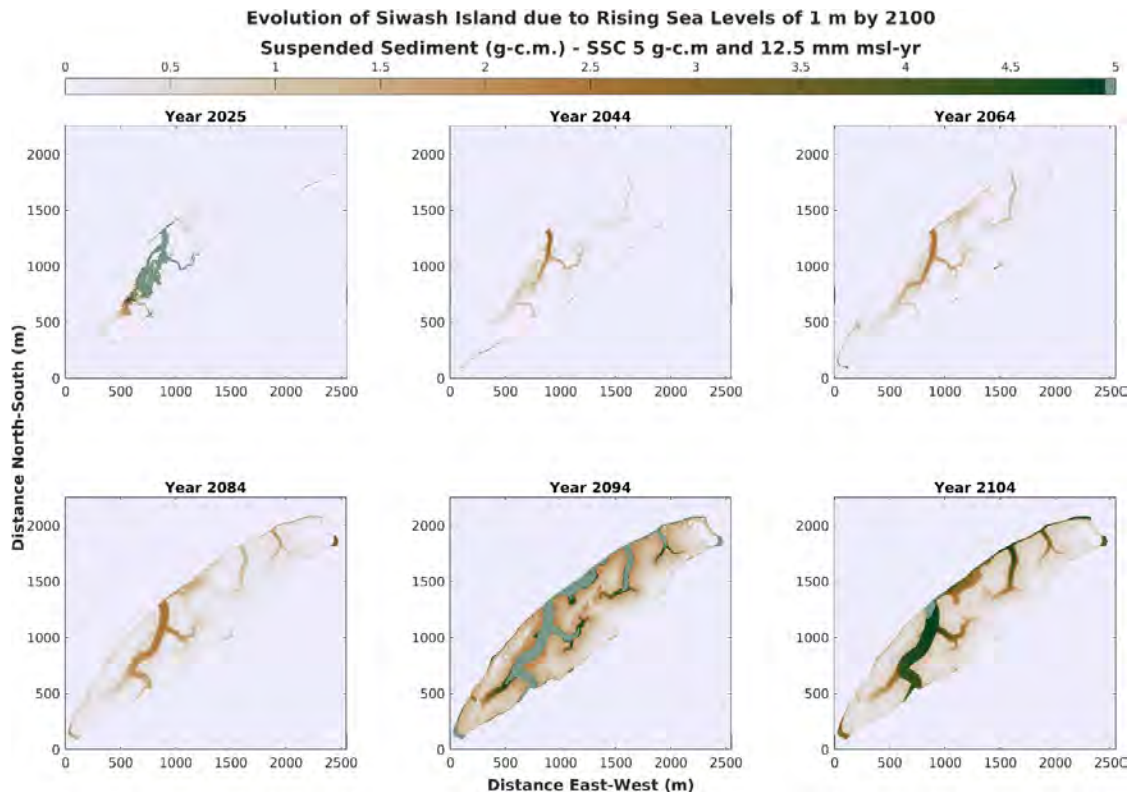


**Figure 29** Results from simulating Siwash Island with G.Mariotti's MarshMorpho2D model (2020). These six subplots show evolution of suspended sediment concentration over time with the simulation of 12.5 mm/yr of SLR, 2 m of TR, and 5 g/cm<sup>3</sup> of SSC.

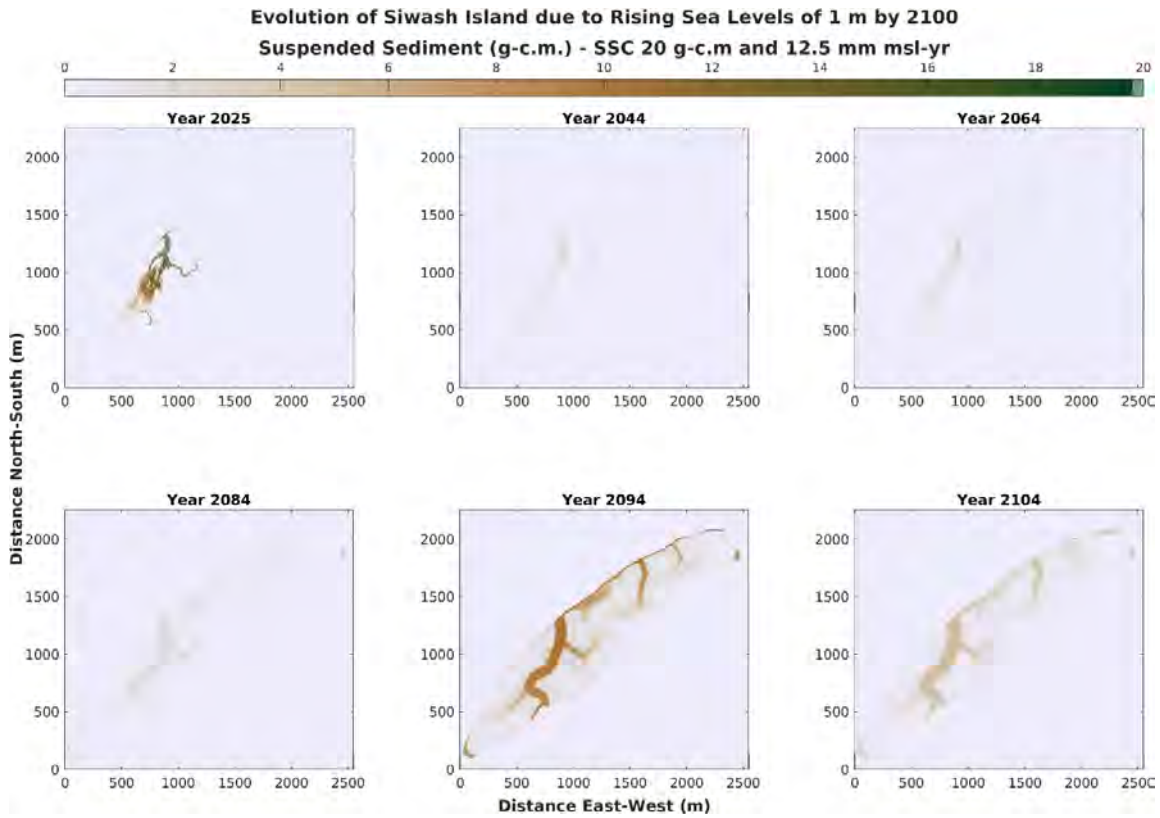


**Figure 30** Results from simulating Siwash Island with G.Mariotti's MarshMorpho2D model (2020). These six subplots show evolution of suspended sediment concentration over time with the simulation of 12.5 mm/yr of SLR, 2 m of TR, and 20 g/cm<sup>3</sup> of SSC.

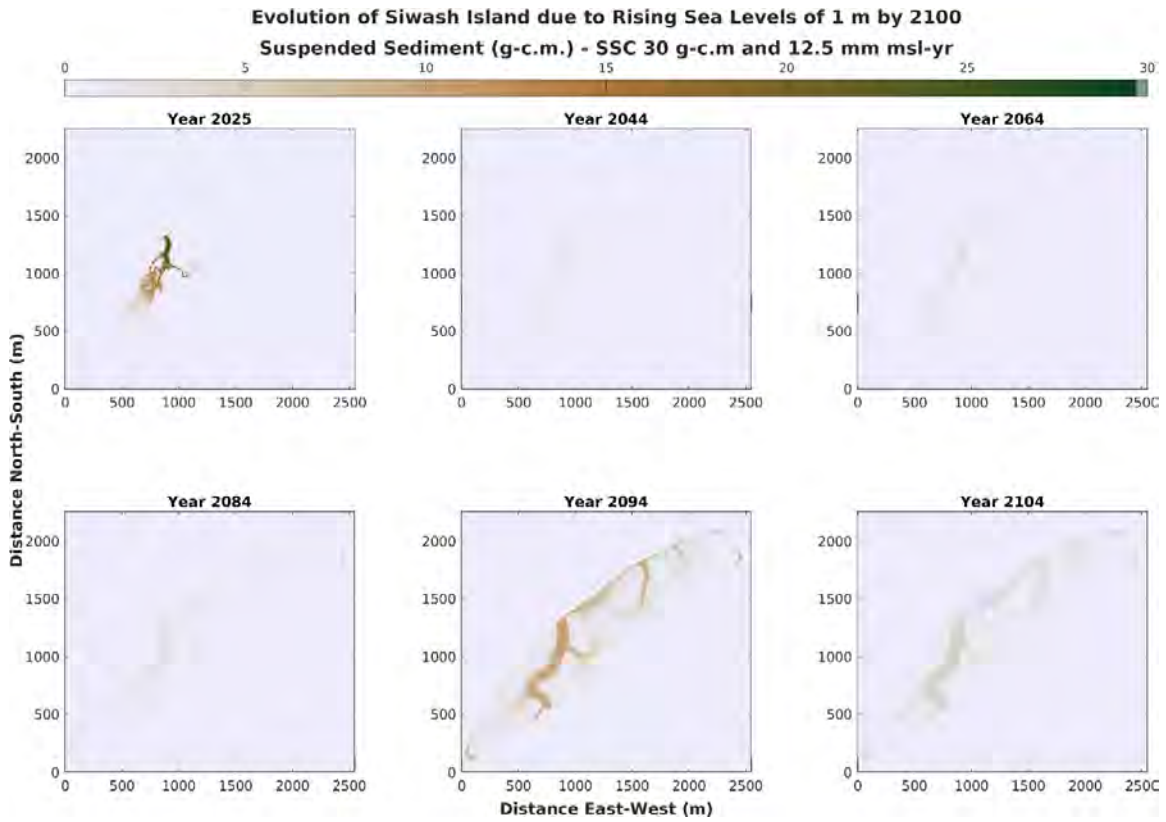


**Figure 31** Results from simulating Siwash Island with G.Mariotti's MarshMorpho2D model (2020). These six subplots show evolution of suspended sediment concentration over time with the simulation of 12.5 mm/yr of SLR, 2 m of TR, and 30 g/cm<sup>3</sup> of SSC.

#### 4.2.4. Vegetation Cover

Another result which is provided by the MarshMorpho2D model is vegetation cover, representing its evolution in Figures 32-34 over time up to 2104 for 12.5 mm/yr SLR, 2 m TR, and three different SSC (5, 20, 30 g/cm<sup>3</sup>). The evolution of vegetation cover in scenario 2 represents the same situation for all three simulations, experiencing a progressive decline in vegetation over time until 2104. While The proportion of initial vegetation in 2025 is 1, the vegetation cover decreases and reach near 0.68 at the end of 2104, decreasing approximately 32% over 80 years.

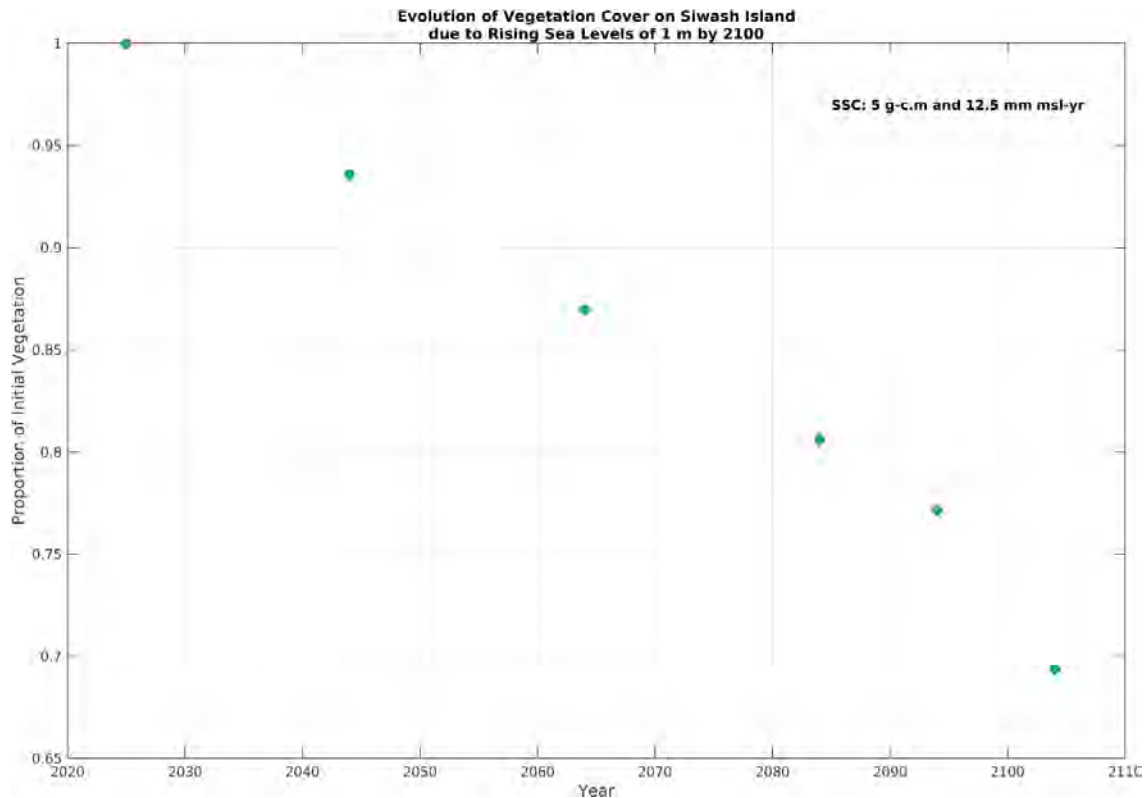


**Figure 32** Results from simulating Siwash Island with G.Mariotti's MarshMorpho2D model (2020). This plot shows evolution of vegetation cover over time with the simulation of 12.5 mm/yr of SLR, 2 m of TR, and 5 g/cm<sup>3</sup> of SSC.

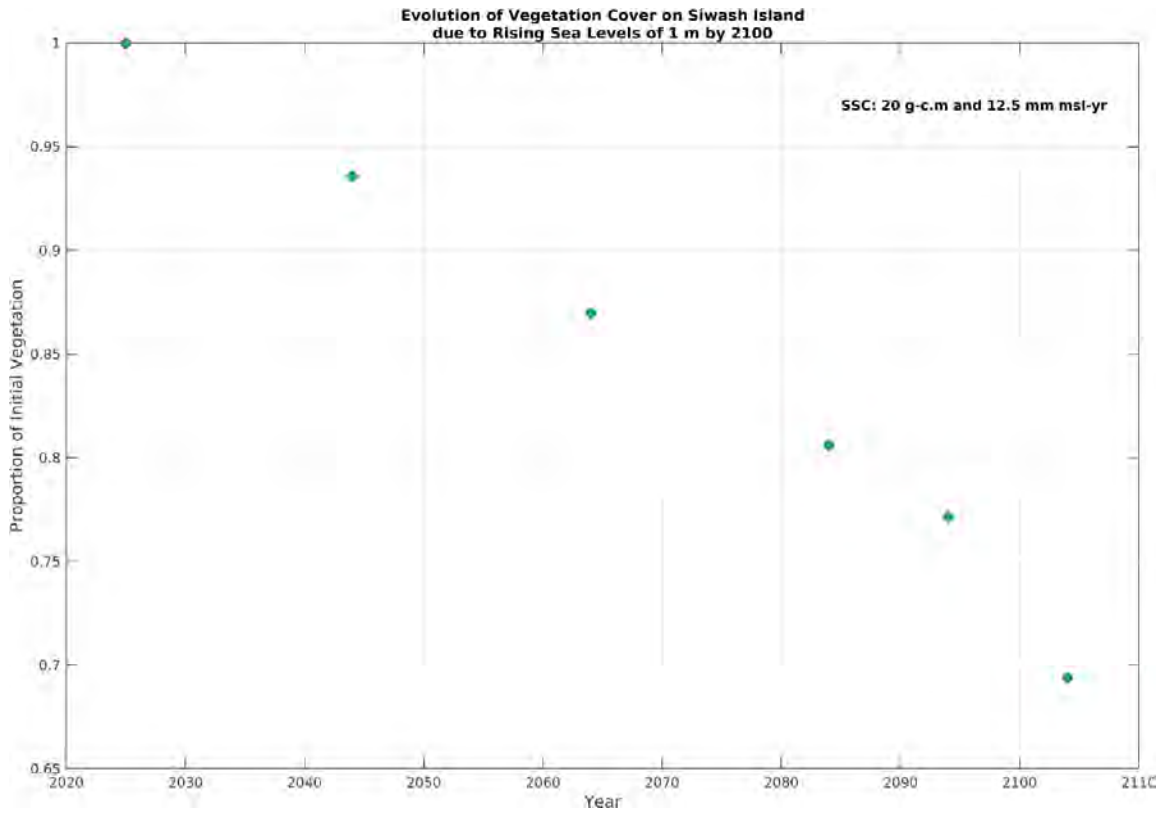


**Figure 33** Results from simulating Siwash Island with G.Mariotti's MarshMorpho2D model (2020). This plot shows evolution of vegetation cover over time with the simulation of 12.5 mm/yr of SLR, 2 m of TR, and 20 g/cm<sup>3</sup> of SSC.

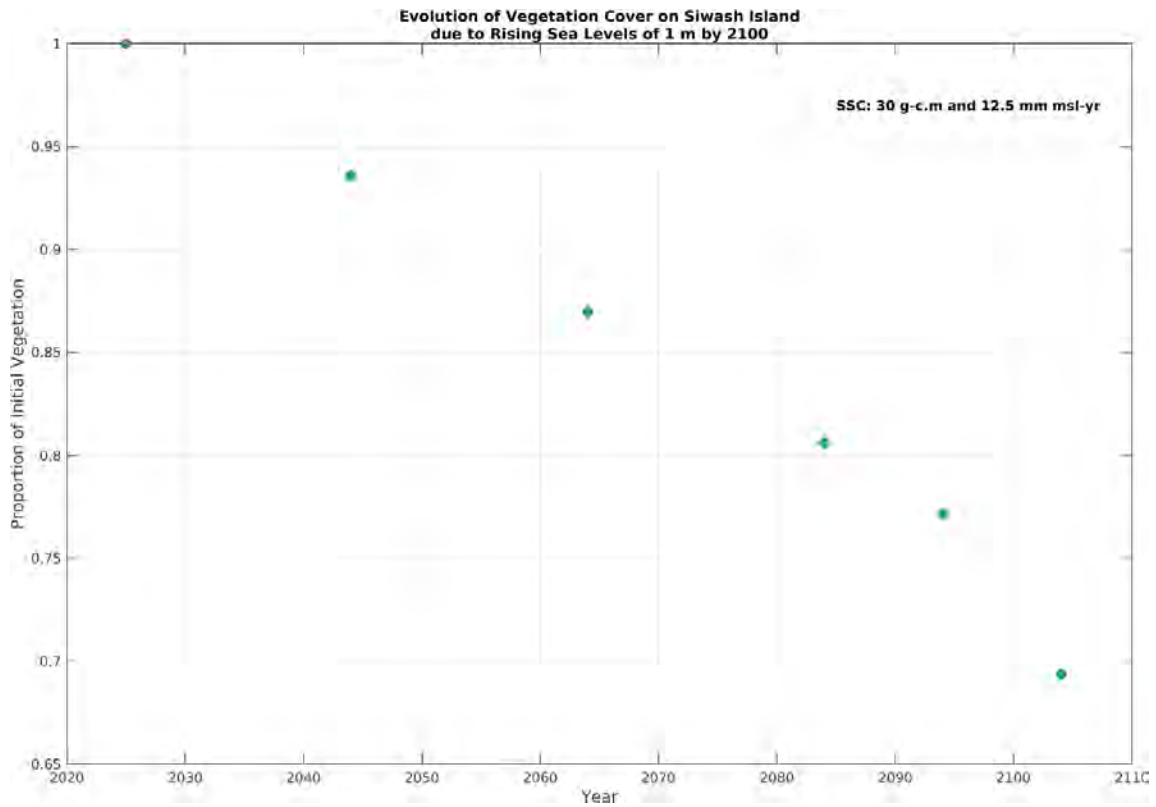


**Figure 34** Results from simulating Siwash Island with G.Mariotti's MarshMorpho2D model (2020). This plot shows evolution of vegetation cover over time with the simulation of 12.5 mm/yr of SLR, 2 m of TR, and 30 g/cm<sup>3</sup> of SSC.

### 4.2.5. Velocity

Velocity changes are also illustrated for scenario 2 (12.5 mm/yr SLR, 2 m TR, and 5, 20, 30 g/cm<sup>3</sup> SSC) in Figures 35-37. At the beginning of the simulations, the velocity is relatively modest in the dominant tidal channel trending north to southwest. As the decades progress, the dominant channel and two lesser channels on the north of island show higher velocities (0.04-0.07 m/s) and appear to deepen and lengthen over 80 years. By 2084, the dominant tidal channel finds a new pathway to southern shore of Siwash Island instead of southwest, effectively bisecting the island, and this new pathway widens over the next 20 years with a velocity of 0.1 m/s. Additionally, velocities increase at southern and northern tips of the island by 2084.

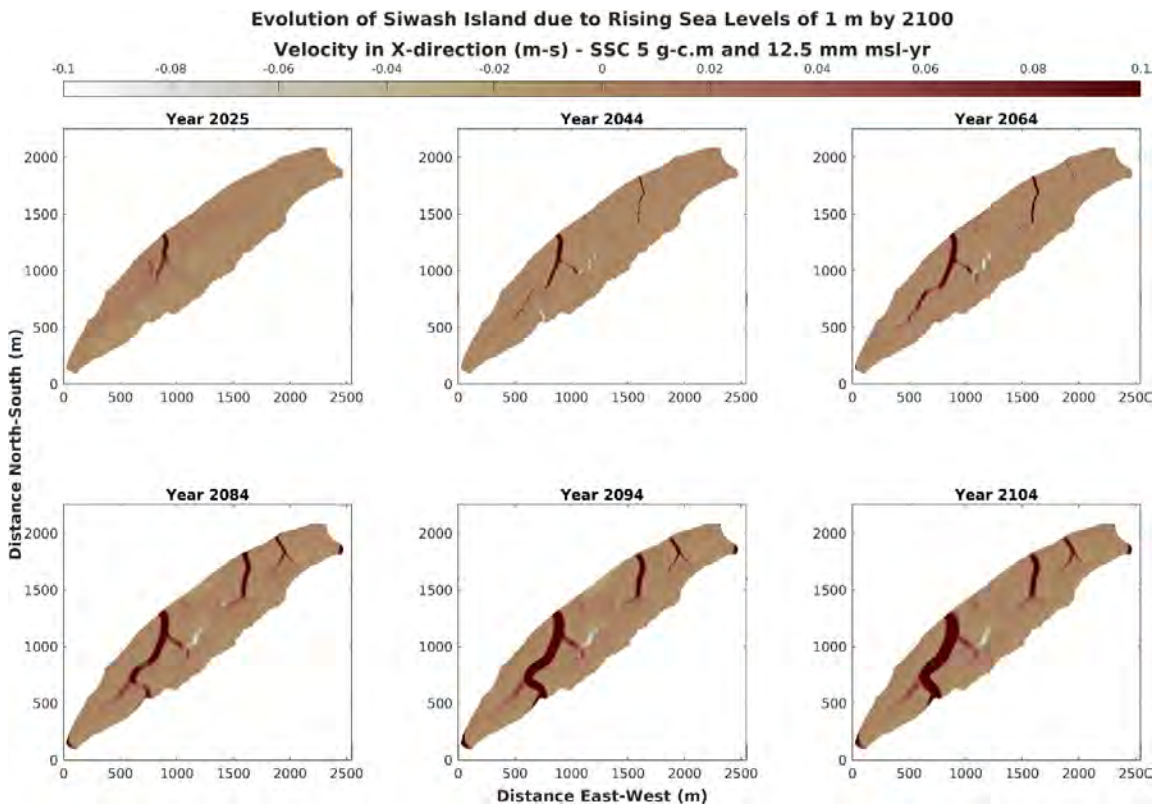


**Figure 35** Results from simulating Siwash Island with G.Mariotti's MarshMorpho2D model (2020). These six subplots show the changes in velocity over time until 2104 with the simulation of 12.5 mm/yr of SLR, 2 m of TR, and 5 g/cm<sup>3</sup> of SSC.

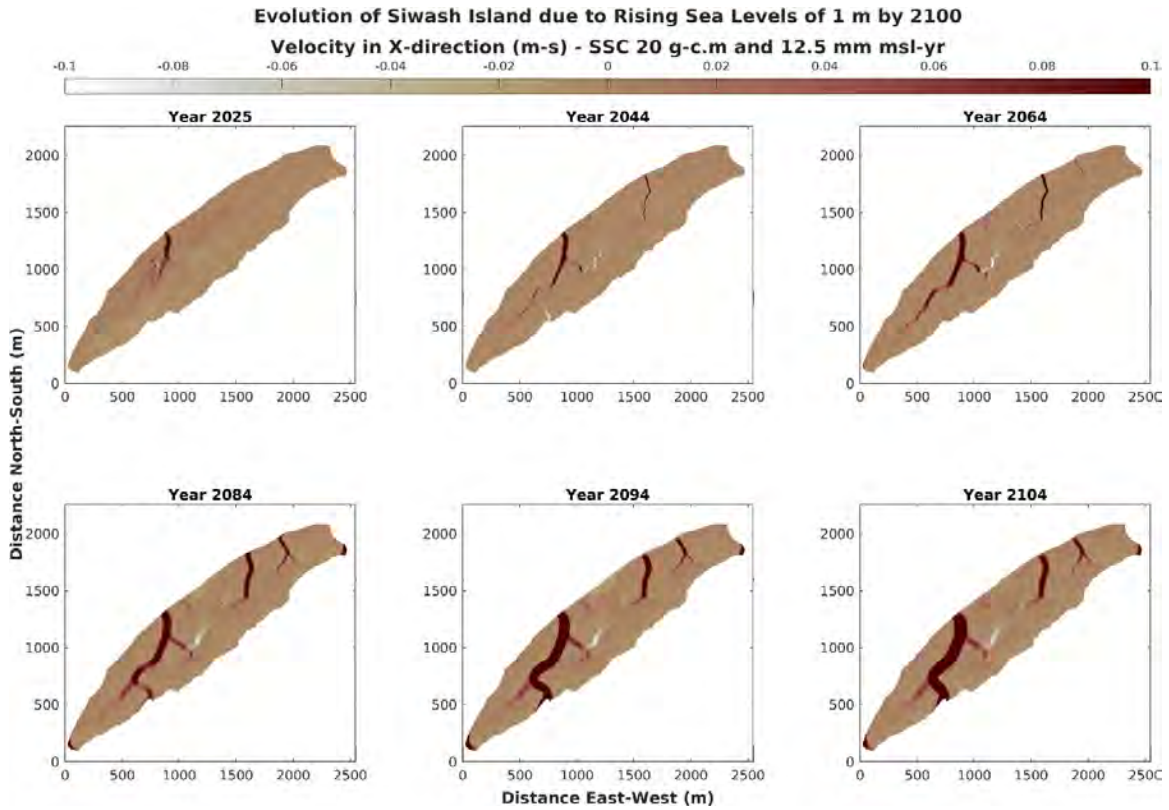


**Figure 36** Results from simulating Siwash Island with G.Mariotti's MarshMorpho2D model (2020). These six subplots show the changes in velocity over time until 2104 with the simulation of 12.5 mm/yr of SLR, 2 m of TR, and 20 g/cm<sup>3</sup> of SSC.

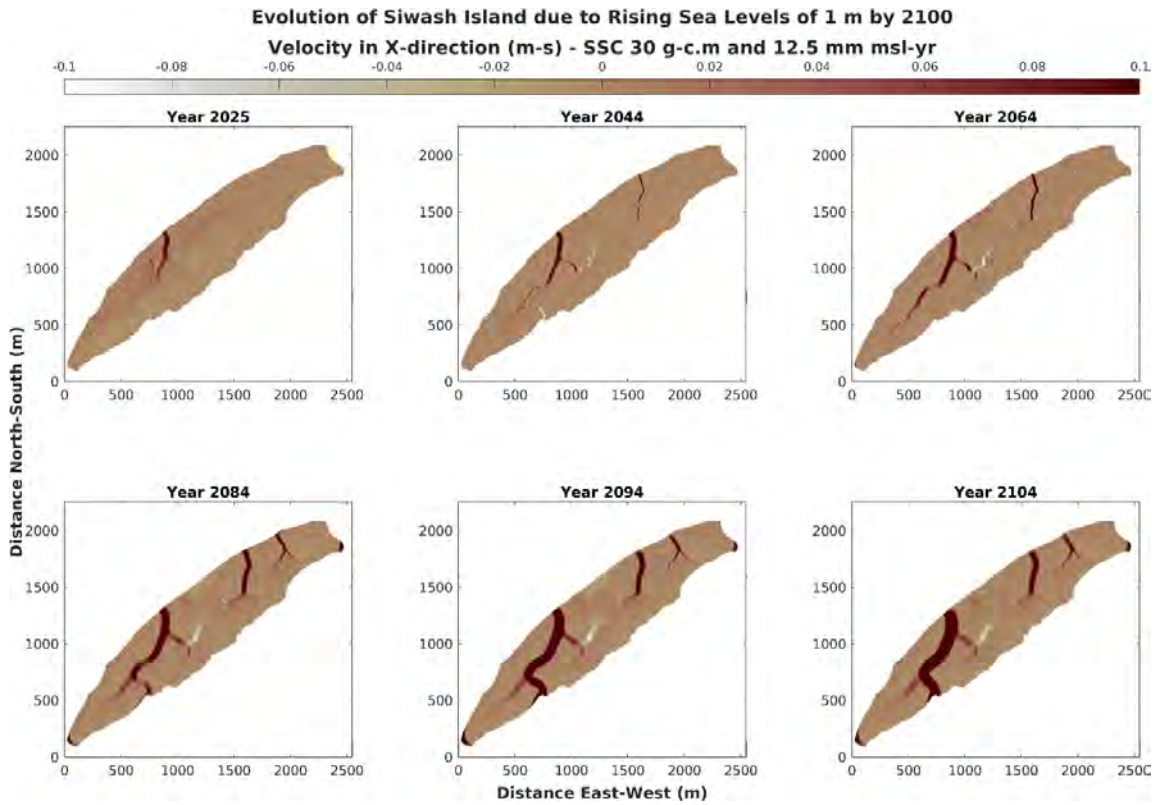


**Figure 37** Results from simulating Siwash Island with G.Mariotti's MarshMorpho2D model (2020). These six subplots show the changes in velocity over time until 2104 with the simulation of 12.5 mm/yr of SLR, 2 m of TR, and 30 g/cm<sup>3</sup> of SSC.

#### 4.2.6. Water Depth

Projected water depth over 80 years for 12.5 mm/yr SLR, 2 m TR, and three different SSC (5, 20, 30 g/cm<sup>3</sup>) are shown in Figures 38-40. Despite variations in SSC across different simulations of scenario 2, the water depth remains unchanged and consistent across all simulations. Siwash island represents relatively shallow depth of water at the start of the simulations, particularly more noticeable in the dominant channel trending north to southwest of the island, lesser channels at the north, and north of dominant channel along the northern shore and within the interior of the island. Over time, the depth gradually increases, extending beyond just the tidal channels, but it is more noticeable adjacent to tidal channel not all over the marsh. By 2084, the entire Siwash Island experiences water depth ranging from 0.6-0.8 m, although the dominant channels reach depth of 2 m and make new pathway to southern shore of the island. Additionally, the water depth reaches 2 m at the northern and southern tips of Siwash Island in 2104.

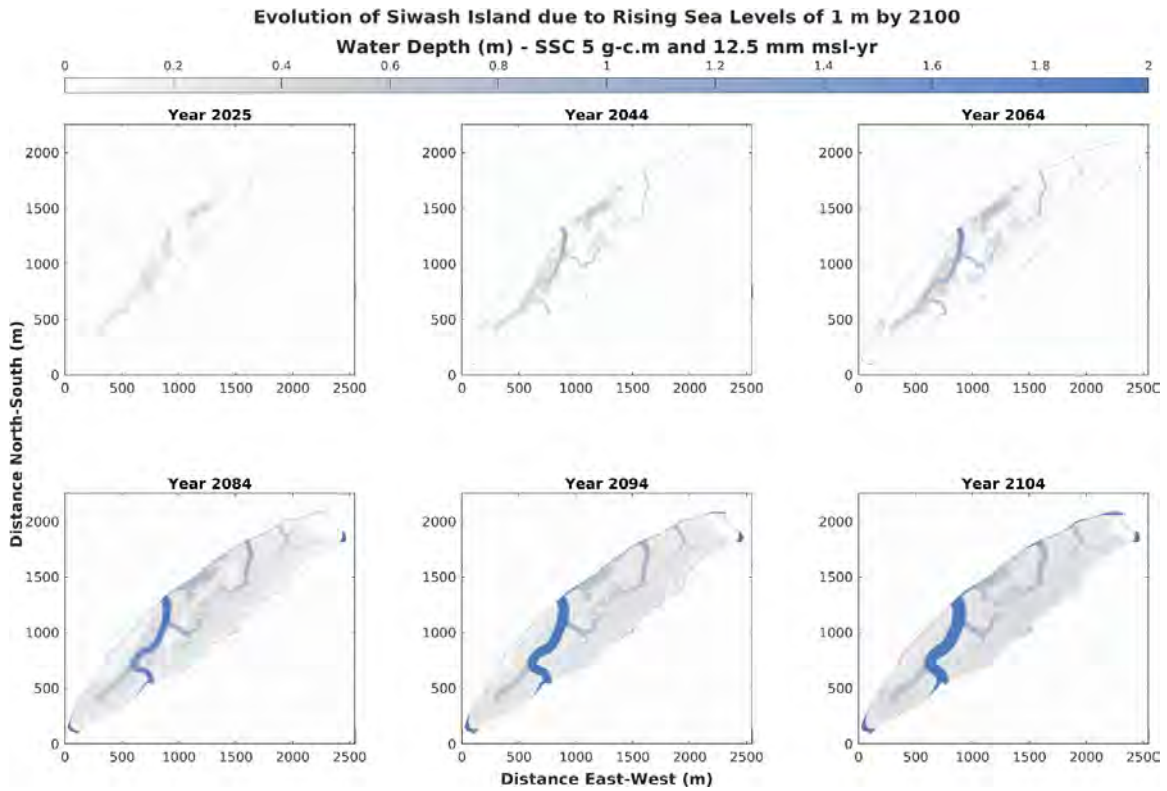


**Figure 38** Results from simulating Siwash Island with G.Mariotti's MarshMorpho2D model (2020). These six subplots show the changes in water depth over time until 2104 with the simulation of 12.5 mm/yr of SLR, 2 m of TR, and 5 g/cm<sup>3</sup> of SSC.

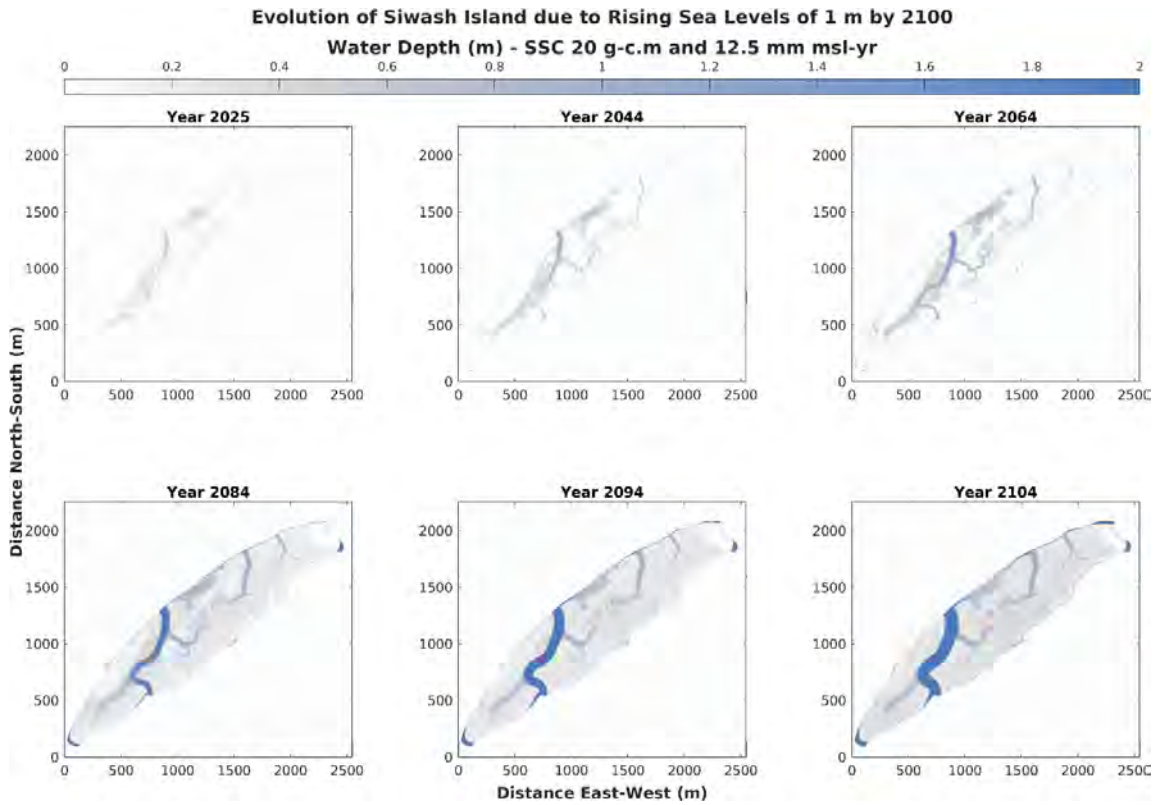


**Figure 39** Results from simulating Siwash Island with G.Mariotti's MarshMorpho2D model (2020). These six subplots show the changes in water depth over time until 2104 with the simulation of 12.5 mm/yr of SLR, 2 m of TR, and 20 g/cm<sup>3</sup> of SSC.

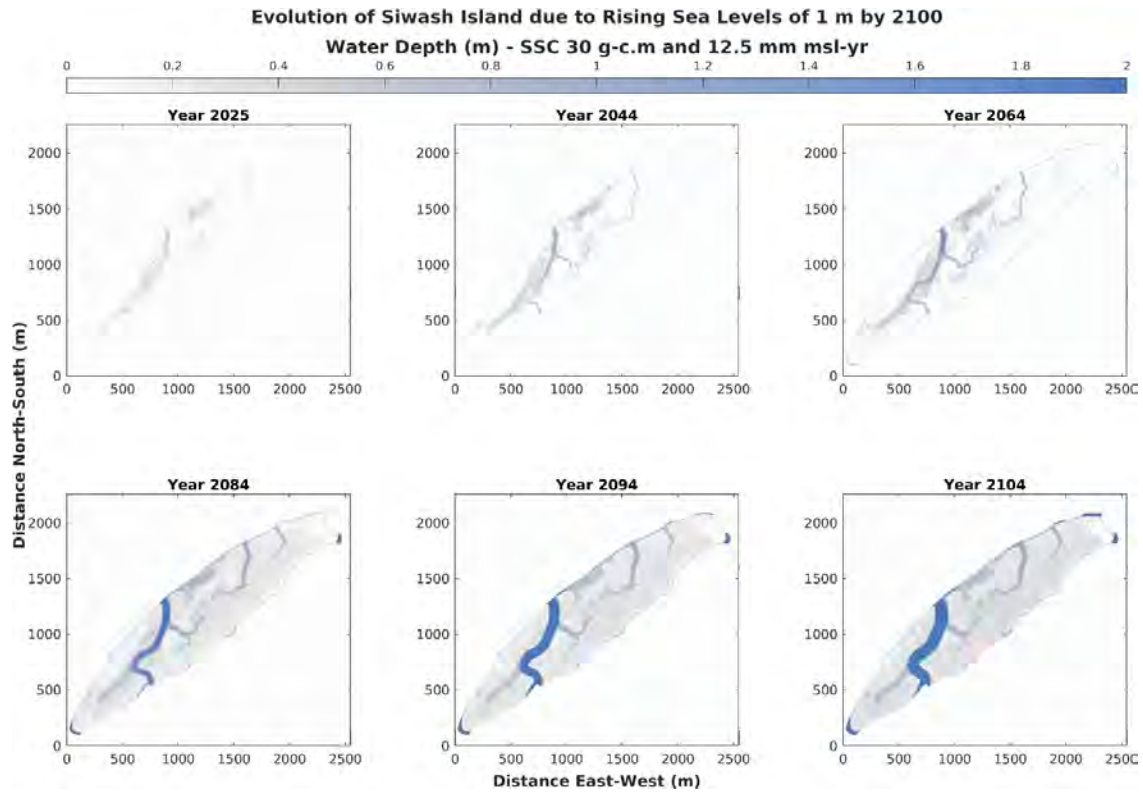


**Figure 40** Results from simulating Siwash Island with G.Mariotti's MarshMorpho2D model (2020). These six subplots show the changes in water depth over time until 2104 with the simulation of 12.5 mm/yr of SLR, 2 m of TR, and 30 g/cm<sup>3</sup> of SSC.

### **4.3. Scenario 3:**

two simulations in scenario 3 were conducted in MarshMorpho2D model. The First simulation is sea level rise (SLR) value of 25 mm/yr, suspended sediment concentration (SSC) value of 20 g/cm<sup>3</sup>, and tidal range (TR) value of 1.5 m, while the second simulation includes SLR value of 25 mm/yr, SSC value of 20 g/cm<sup>3</sup>, TR value of 2 m. The difference between two simulations in scenario 3 would be changes in tidal range.

#### **4.3.1. Elevation**

Figures 41 and 42 represent the projection of topographic evolution on Siwash Island with tidal ranges of 1.5 m and 2 m, respectively, and SLR of 25 mm/yr. Figure 41 illustrates a dominant channel trending north to southwest of Siwash Island with the elevation of -0.2 to -0.4 m. Additionally, the dominant channel includes a tributary channel that trend northwest to southeast, situated approximately a few hundred meter from the mouth, with the elevation up to -0.2 m. By 2064, the two lesser channels at the north are more noticeable, and sediment deposition occurs not only adjacent to tidal channels, but also on all marsh surfaces. Deposition also occurs at the end of the dominant channel, with accumulations reaching 0.2 m of sediment. By 2084, the sediment deposition occurs across the surface of the island, and a lesser channel is created in the south part of the island; subsequently, the dominant channel finds a new pathway to the south, bisecting the island, and this new channel widen and deepen, reaching depth of -1 by the end of simulation. The most sediment deposition occurs near tidal channel, the previous location of dominant channel and the north of dominant channel along the northern shore and within the interior of the island., reaching 1 m. On the other hand, depth of southern and northern tips of the island reaches -1 m.

In Figure 42, by 2044, lesser channels at the north and south of the island become noticeable, and sediment deposition occurs adjacent to tidal channels and northern tip of the island. In 2064, the dominant channel finds its pathway to the south and bisects the island, as compared to Figure 41, which shows the island bisected in 2094. Over time, the dominant channel becomes deeper and wider, but more sediment deposition occurs near channels, on the north shore of the island, and previous location

of dominant channel. More areas of marsh surface experience sediment deposition, with accumulation reaching 1 m.

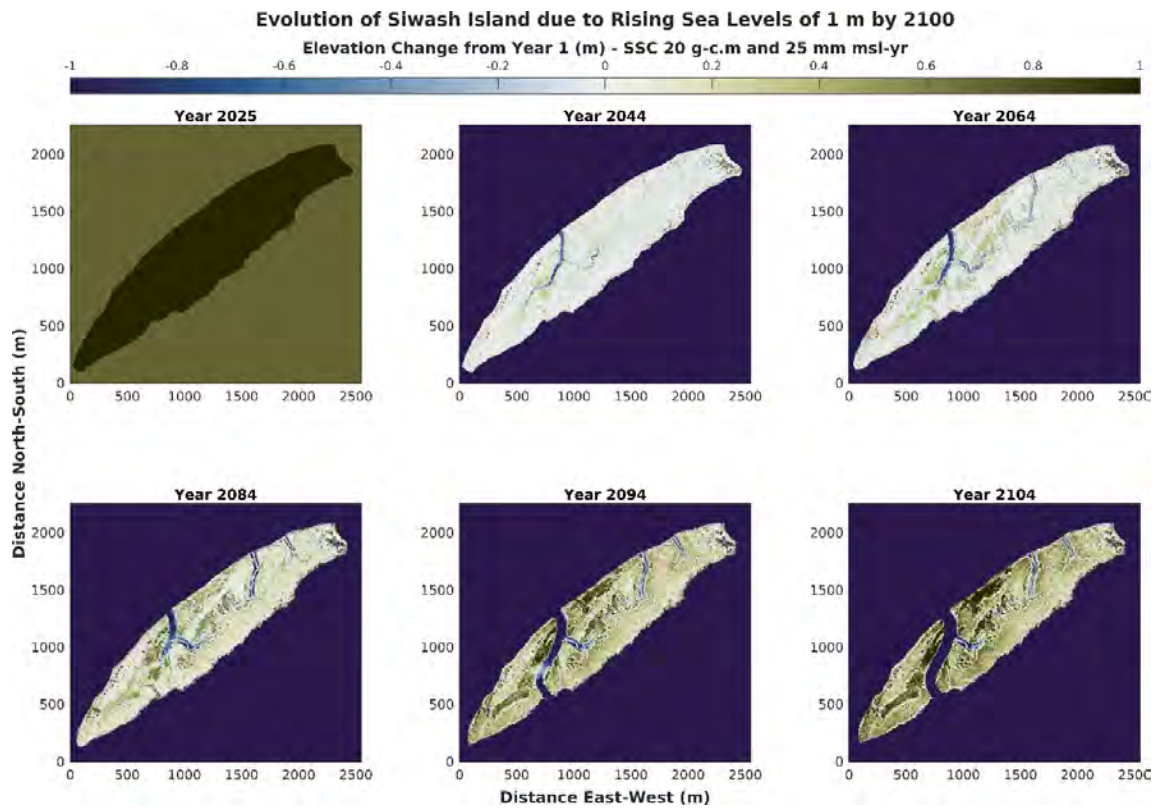


**Figure 41** Results from simulating Siwash Island with G.Mariotti's MarshMorpho2D model (2020). The plots highlight patterns of Siwash Island response through time in the model with the simulation of 25 mm/yr of SLR, 1.5 m of TR, and 20 g/cm<sup>3</sup> of SSC.

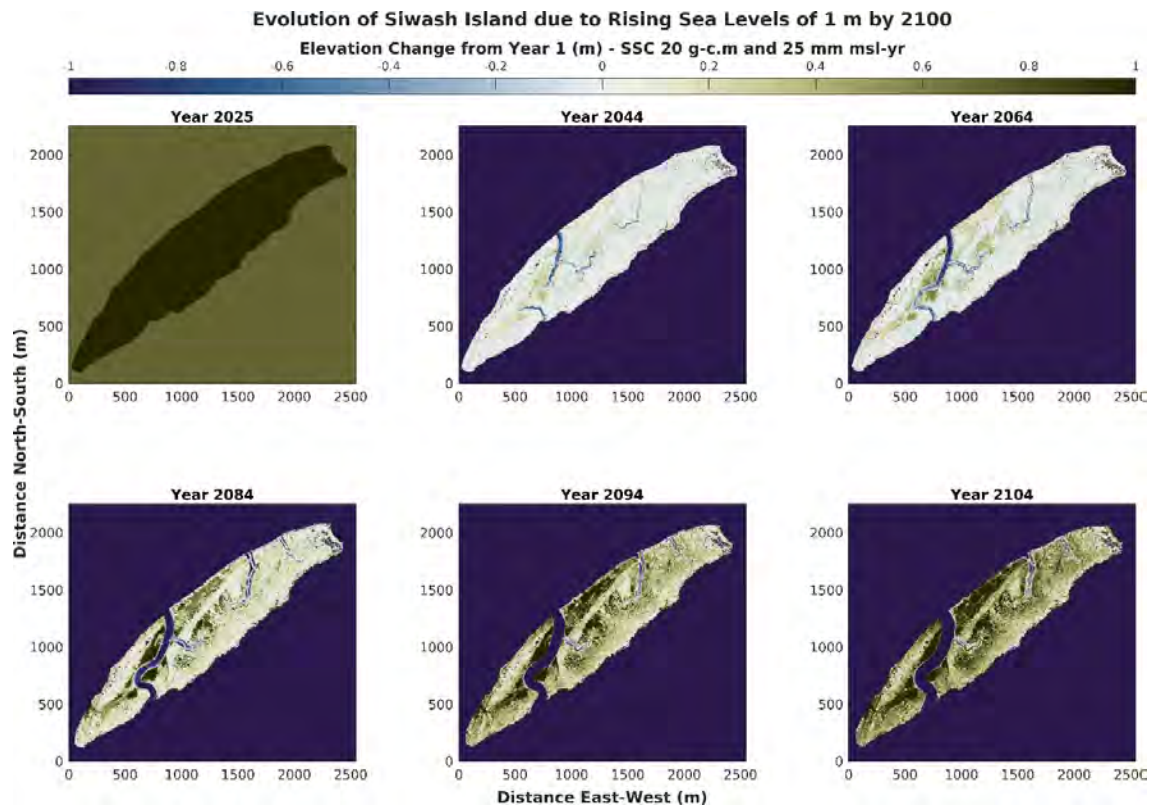


**Figure 42** Results from simulating Siwash Island with G.Mariotti's MarshMorpho2D model (2020). The plots highlight patterns of Siwash Island response through time in the model with the simulation of 25 mm/yr of SLR, 2 m of TR, and 20 g/cm<sup>3</sup> of SSC.

### 4.3.2. Relative Elevation

Figures 43 and 44 illustrate the projection of relative Elevation on Siwash Island based on two simulations of scenario 3, with Figure 43 showing the outcome of the first simulation (Tidal range= 1.5 m), and Figure 44 highlighting the outcome of second simulation with tidal range of 2 m. As shown in Figures 43 and 44, the elevation relative to sea level decreases over time. The range of elevation in 2025 at the start of the simulations is approximately 1.5-2 m. In Figure 43, the elevation of tidal channels of both the dominant and lesser channels decreases, reaching 2 m and 1 m below average sea level, respectively. The dominant channel, trending north to southwest, finds a new pathway to south and bisects the island in 2094. The only part with an elevation of 2 m is a small spot at the northeast of the island, but the other part is either near or below the average sea level.

In Figure 44, the dominant channel finds a new pathway to south by 2084, deepening and widening until the end of simulations. The parts below average sea level consist of tidal channels and some areas at the north shore of the island. The elevation of the other parts of the island indicates a range of 0.3-0.5 m with some spots reaching 2 m at the northern tip and the edge of south and northwest of the island.

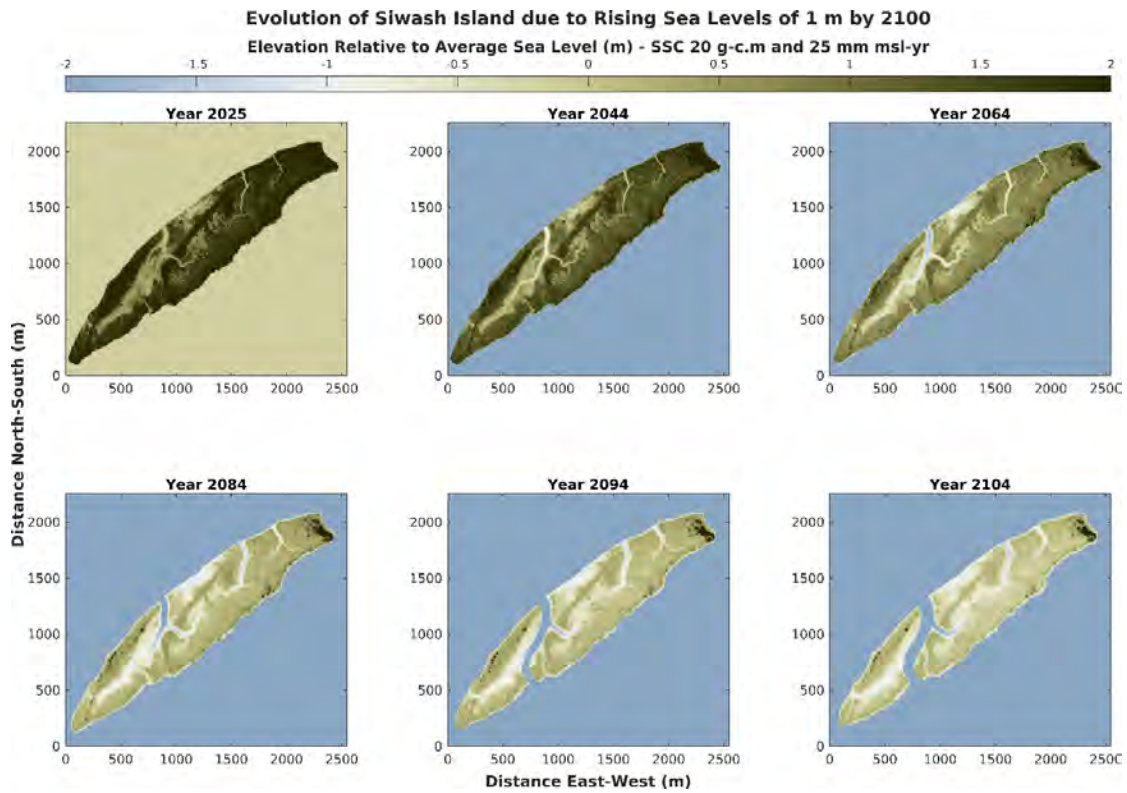


**Figure 43** Results from simulating Siwash Island with G.Mariotti's MarshMorpho2D model (2020). These six subplots show elevation relative to average sea level with the simulation of 25 mm/yr of SLR, 1.5 m of TR, and 20 g/cm<sup>3</sup> of SSC.

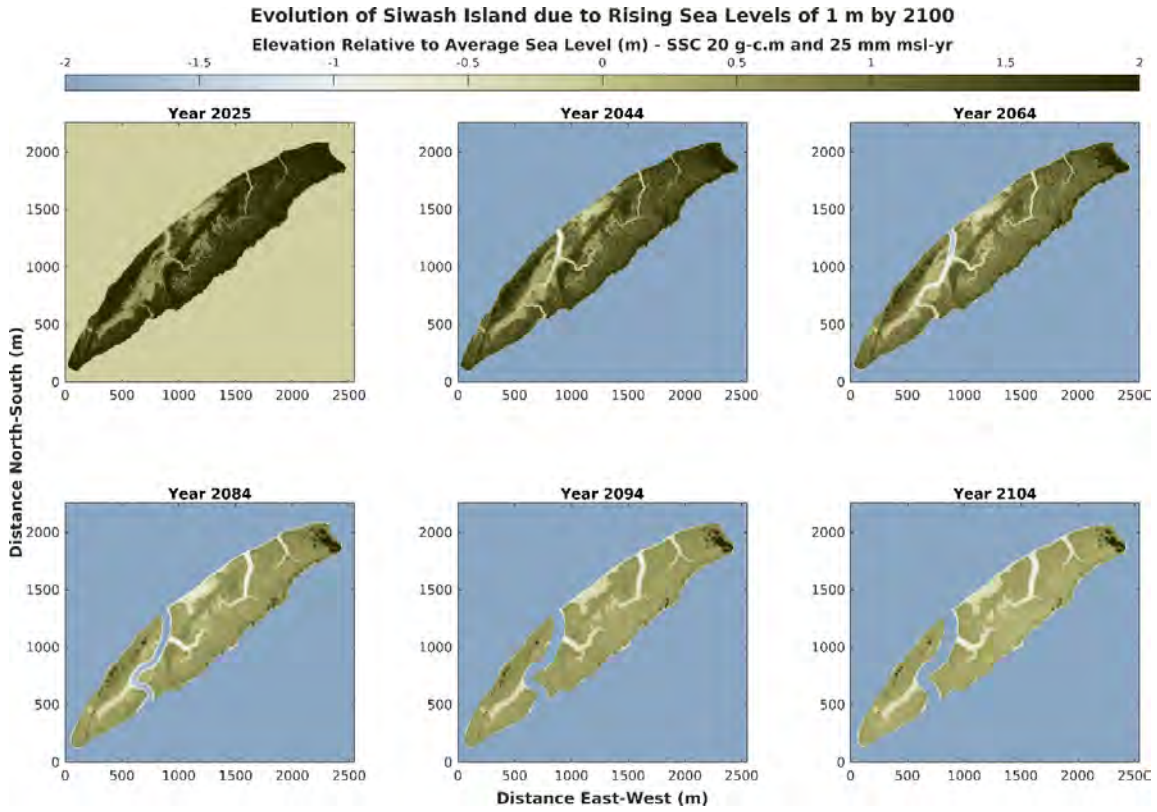


**Figure 44** Results from simulating Siwash Island with G.Mariotti's MarshMorpho2D model (2020). These six subplots show elevation relative to average sea level with the simulation of 25 mm/yr of SLR, 2 m of TR, and 20 g/cm<sup>3</sup> of SSC.

### 4.3.3. Suspended Sediment Concentration

The six subplots in Figures 45 and 46 indicate the predicted changes in suspended sediment concentration (SSC) of Siwash Island in response to two simulations of tidal range of 1.5 m and 2 m in scenario 3 up to year 2104, respectively. In 2025, SSC is more concentrated in the dominant tidal channels trending north to southwest, and their surrounding areas, which is more noticeable in simulation 2 (Figure 46) with the range of 10-20 g/cm<sup>3</sup>, while the range of SSC in other simulation is between 4 to 10 g/cm<sup>3</sup>. The concentration of SSC in dominant tidal channel decreases over time and disperses in channels and adjacent areas. The amount of SSC in tidal channels and north shore, as well as the southern and northern tips of the island in simulation 2, is more pronounced, reaching 13 g/cm<sup>3</sup> by 2094, while in simulation 1, SSC covers a larger area of the Island with the range of SSC in tidal channel at 8 g/cm<sup>3</sup>. The amount of SSC in the newly formed dominant channel is noticeable.

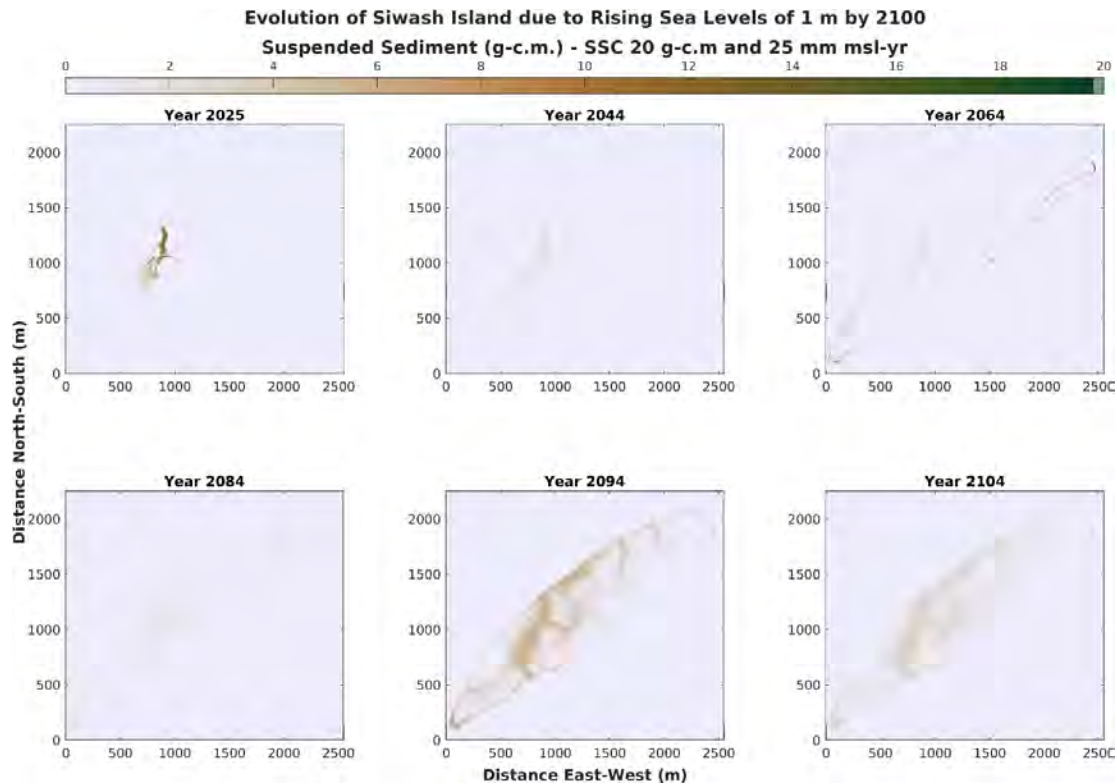


**Figure 45** Results from simulating Siwash Island with G.Mariotti's MarshMorpho2D model (2020). These six subplots show the evolution of suspended sediment concentration over time with the simulation of 25 mm/yr of SLR, 1.5 m of TR, and 20 g/cm<sup>3</sup> of SSC.

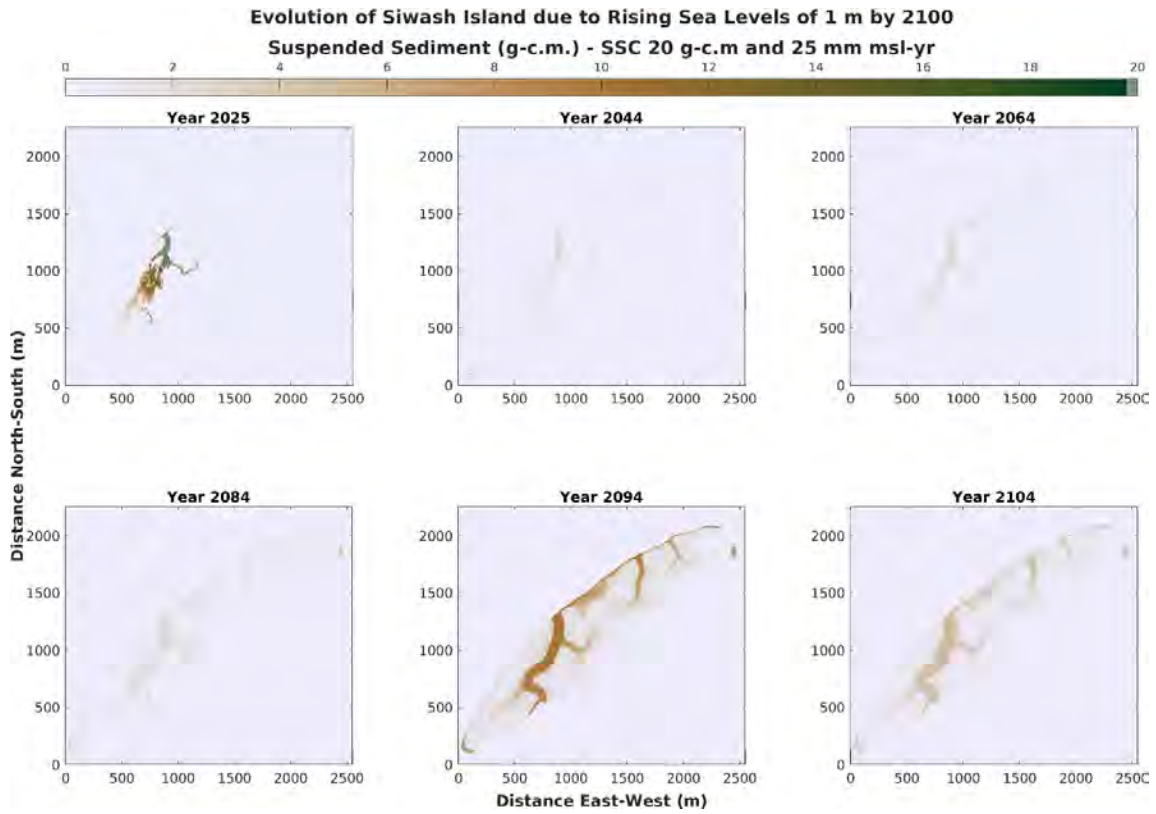


**Figure 46** Results from simulating Siwash Island with G.Mariotti's MarshMorpho2D model (2020). These six subplots show the evolution of suspended sediment concentration over time with the simulation of 25 mm/yr of SLR, 2 m of TR, and 20 g/cm<sup>3</sup> of SSC.

#### 4.3.4. Vegetation Cover

Figures 47 and 48 represent the changes in vegetation cover in accordance with scenario 3 where SLR and SSC is identical for both simulations at 25 mm/yr and 20 g/cm<sup>3</sup> respectively; however, the tidal range for Figure 47 is 1.5 m, and for figure 48, it is 2 m. vegetation loss occurs over time and the rate of decline in Figure 47 is faster and more pronounced, declining 65% compared to simulation 2 shown in Figure 48, which experience a decline of 31%.

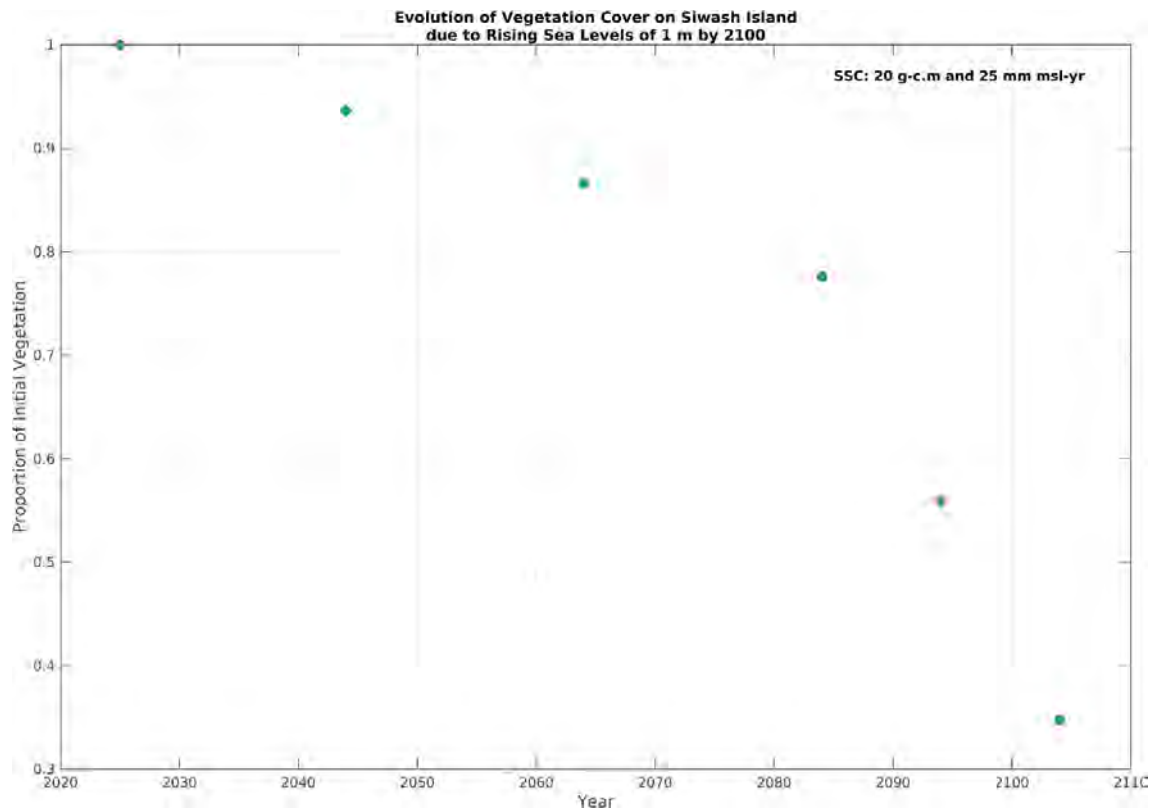


**Figure 47** Results from simulating Siwash Island with G.Mariotti's MarshMorpho2D model (2020). This plot shows the evolution of vegetation cover over time with the simulation of 25 mm/yr of SLR, 1.5 m of TR, and 20 g/cm<sup>3</sup> of SSC.

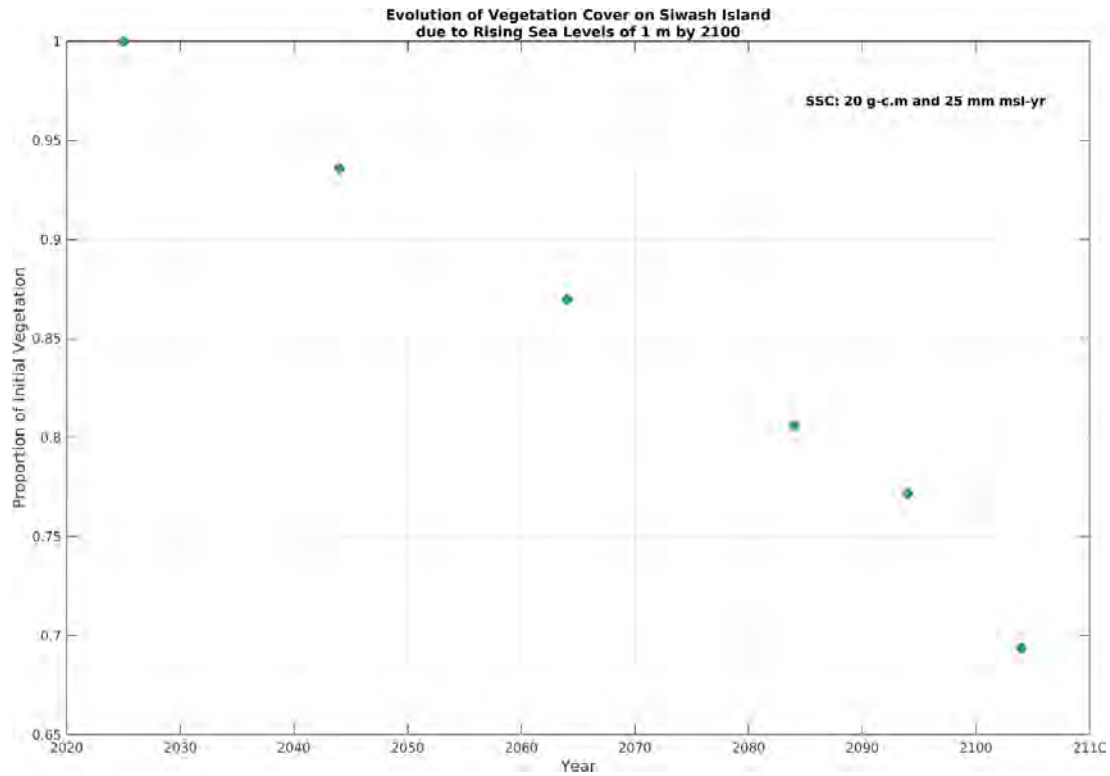


**Figure 48** Results from simulating Siwash Island with G.Mariotti’s MarshMorpho2D model (2020). This plot shows the evolution of vegetation cover over time with the simulation of 25 mm/yr of SLR, 2 m of TR, and 20 g/cm<sup>3</sup> of SSC.

### 4.3.5. Velocity

Figures 49 and 50 illustrate the projection of velocity on Siwash Island with tidal ranges of 1.5 m and 2 m, respectively, and SLR of 25 mm/yr. Figure 49 with a 1.5 m TR shows higher velocity within dominant channel in 2044, then velocity increases in lesser channels on the north and dominant channel that bisect the island in 2094, while bisecting the island by dominant channel occurs in 2084 and the channel is getting wider in Figure 50.

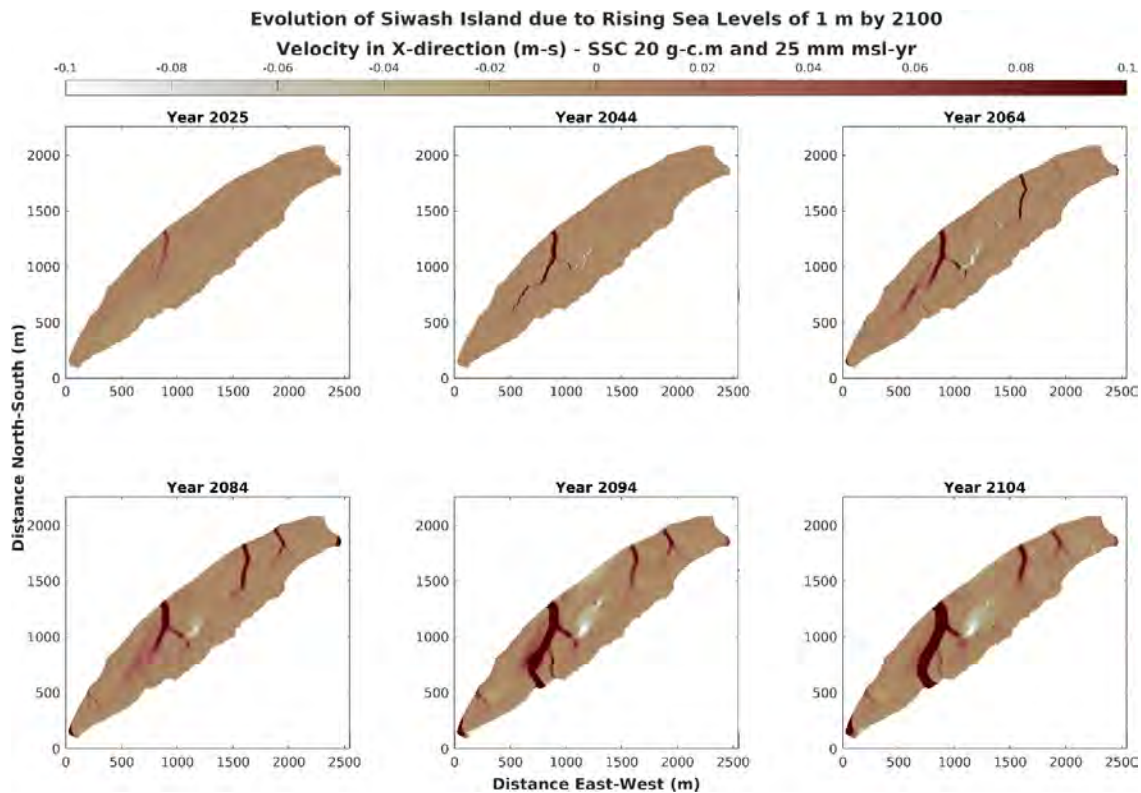


**Figure 49** Results from simulating Siwash Island with G.Mariotti's MarshMorpho2D model (2020). These six subplots show the changes in velocity over time until 2104 with the simulation of 25 mm/yr of SLR, 1.5 m of TR, and 20 g/cm<sup>3</sup> of SSC.

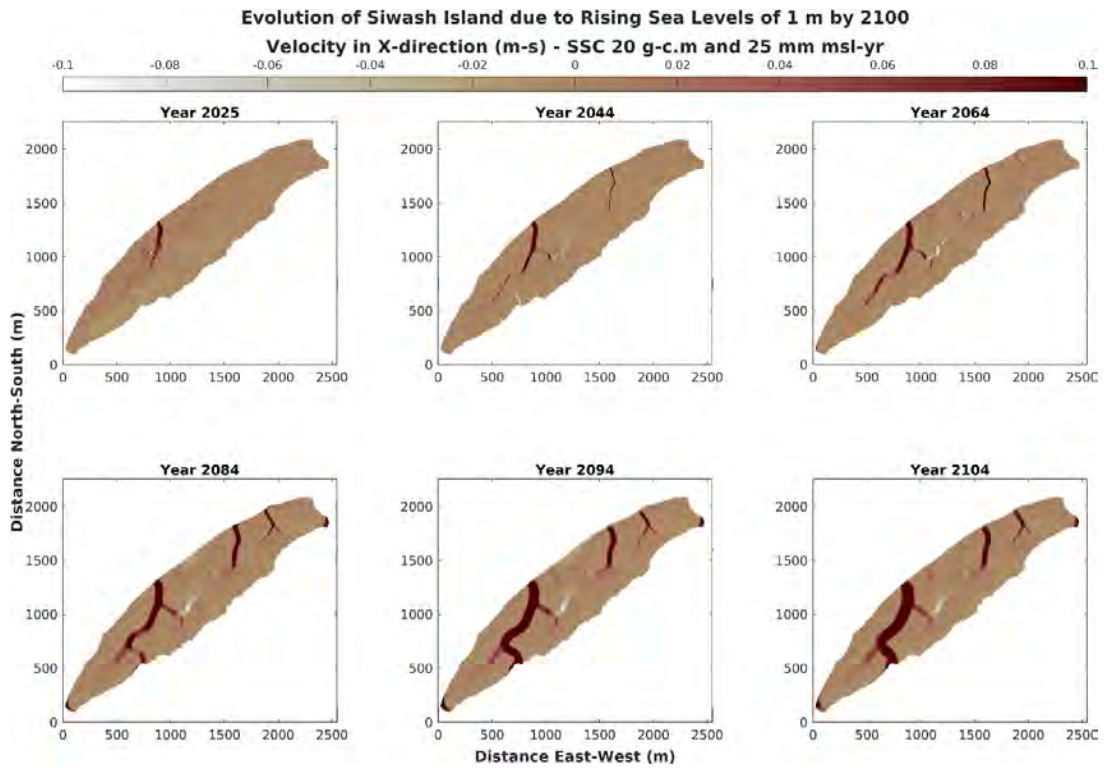


**Figure 50** Results from simulating Siwash Island with G.Mariotti's MarshMorpho2D model (2020). These six subplots show the changes in velocity over time until 2104 with the simulation of 25 mm/yr of SLR, 2 m of TR, and 20 g/cm<sup>3</sup> of SSC.

### 4.3.6. Water Depth

The two subplots in Figures 51 and 52 represent two simulations of scenario 3, Although SLR and SSC are identical in two simulations, Figure 51 and 52 illustrates TR value of 1.5 m, and 2 m respectively. At the start of the simulations, water depth is relatively low across most of Siwash Island; however, in simulation 2 (Figure 52), the water depth is greater than in Simulation 1, as shown in Figure 51. As the time goes on, the depth generally increases within tidal channels and across all Siwash Island. Tidal channels are becoming a more prominent feature on the Island itself and the dominant channel bisect the island in 2094 shown in Figure 51 and in 2084 shown in Figure 52. At the end of simulation, the water covers Siwash Island a depth of 2 m in tidal channels, as well as northern and southern tips of the island and 0.8 for the rest of the island in simulation 1, while the depth in simulation 2 (Figure 52) is lower.

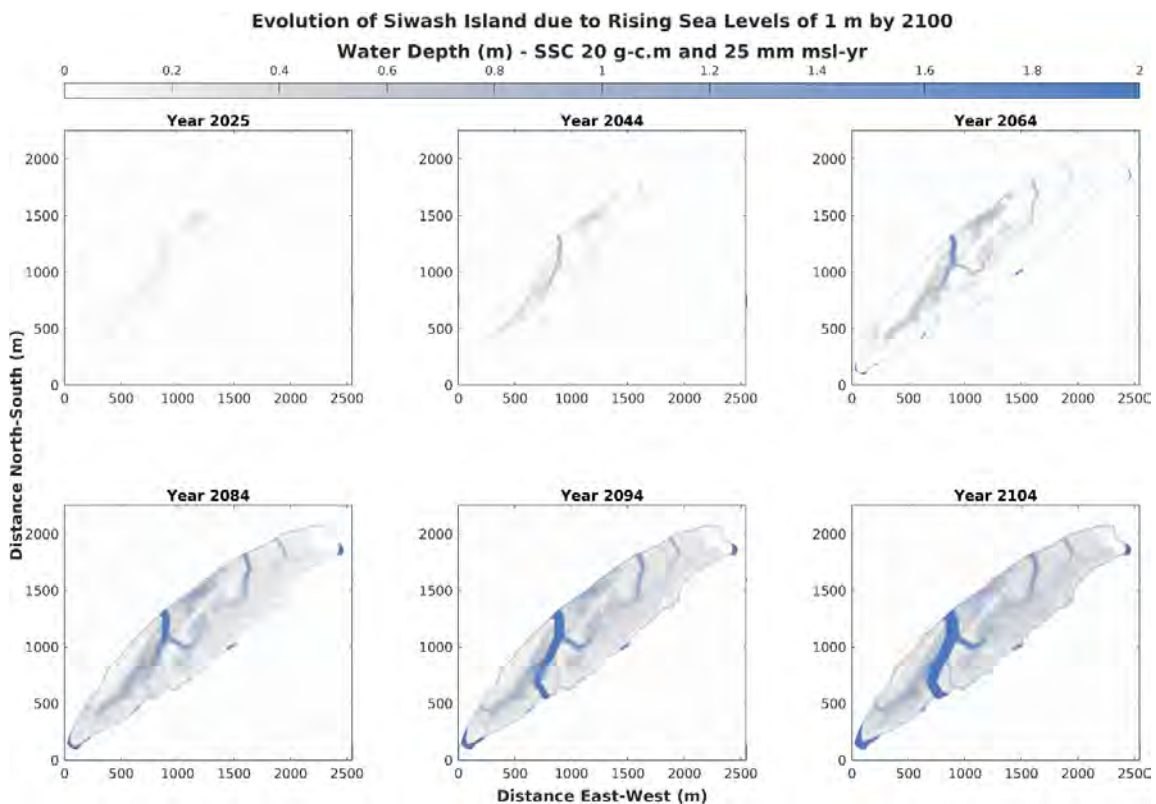


**Figure 51** Results from simulating Siwash Island with G.Mariotti's MarshMorpho2D model (2020). These six subplots show the changes in water depth over time until 2104 with the simulation of 25 mm/yr of SLR, 1.5 m of TR, and 20 g/cm<sup>3</sup> of SSC.

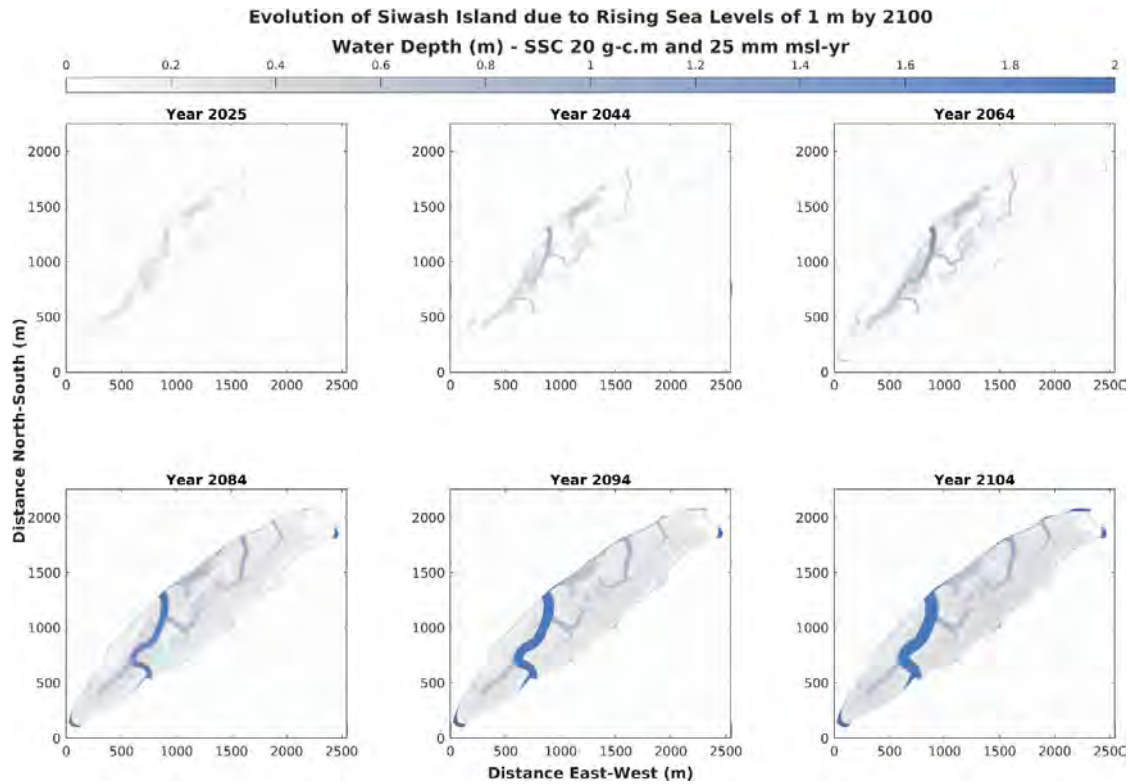


**Figure 52** Results from simulating Siwash Island with G.Mariotti's MarshMorpho2D model (2020). These six subplots show the changes in water depth over time until 2104 with the simulation of 25 mm/yr of SLR, 2 m of TR, and 20 g/cm<sup>3</sup> of SSC.

## **Chapter 5.**

### **Discussion**

#### **5.1. Differences between scenarios**

##### **5.1.1. Scenarios 1 and 2:**

In spite the fact that with different rate of SSC In scenarios, the projected evolution of Siwash Island remains the same in each scenario. The difference between Scenario 1 and scenario 2 is tidal range that is changed from 1.5 m to 2 m.

To compare the projected elevation between scenario 1 (Figures 5, 6, and 7) and scenario 2 (Figures 23, 24, and 25), it is observed that more areas of Siwash Island are affected by increasing tidal range in scenario 2. These changes are more distinguishable from the year 2084. While in scenario 1, the elevation changes are more limited around the bank of tidal channel and north shore of Siwash Island, in scenario 2, the elevation changes extend all over Siwash Island; moreover, the dominant channel trending north to southwest in Siwash Island find a new pathway to south and bisect the island and becomes a prominent feature of the Island in scenario 2 starting from the year 2084. Although there is a regression on the southern tip of the island in scenario 1, this regression happens in northern tip of the island in scenario 2.

Regarding relative elevation, scenario 2 (Figures 26-29) represents lower elevations relative to average sea level in comparison with scenario 1 (Figures 8-10) over time. The range of relative elevation spans from -2 to 2. In scenario 1, the range at the start of the simulation is between 0.7 and 2, while at the end of simulation (2104), it declines to 0.5 across Siwash Island, except for the channels which exhibit a range of -0.5 to -1; however, in scenario 2, by the end of simulation, the elevation of Siwash Island is near sea level, with the dominant channel at the west side of the Island and bisecting the island, reaching -2. The dominant channel at Siwash Island in scenario 1 deepens and lengthens over time, but in scenario 2 the dominant channel bisects the island and widens over time.

In terms of SSC evolution, where water covers more area of Siwash Island, the SSC extends over a larger area. In scenario 1 (Figures 11-13), where the tidal range is lower than scenario 2 (1.5 m compared to 2 m), shown in Figures 29-31, the SSC is concentrated more in tidal channels and surrounding areas; however, in scenario 2 SSC covers larger area of Siwash Island, indicating a higher amount of SSC.

With regard to differences between scenario 1 (Figures 14-16) and scenario 2 (Figures 32-34) in vegetation cover, there is a slight difference between them. Although the pace of vegetation loss in scenario 2 is slightly higher than in scenario 1, the difference is not very noticeable, 32% compared to 25%. Since SSC did not play a role in the resilience of the tidal wetland, this suggests that other factors may have a dominant influence on vegetation dynamics in tidal wetlands.

Velocity is a factor that can be compared between scenarios 1 and 2. As shown in scenario 2 (Figures 35-37), the velocity increases significantly in channels which is considerably higher than in scenario 1 (Figures 17-19). The southern tip of the island experiences higher velocity in scenario 1 than in scenario 2.

With respect to water depth, in scenario 1 (Figures 20-22), the rate of change in water depth is not too high and water does not cover the entire Siwash Island by the end of simulation; however, in scenario 2 (Figures 38-40), the entire area of Siwash Island is almost inundated from the year 2084, and the depth of dominant channel in scenario 2 reaches 2 m, while in scenario 1 it reaches almost 0.8 m. the water depth in the southern tip of the island reaches 2 m.

### **5.1.2. Scenario 1 and 3**

In this section simulation 2 from scenario 1 (SLR=12.5 mm/yr, SSC= 20 g/cm<sup>3</sup>, and TR= 1.5 m), shown in Figure 6, and simulation 1 from scenario 3 (SLR=25 mm/yr, SSC= 20g/cm<sup>3</sup>, and TR= 1.5m), shown in Figure 41, were examined.

Regarding elevation change, as shown in Figures, despite the fact that the elevation increases over time in both simulations, the elevation of tidal channels decreases and becomes more pronounced from the year 2094, reaching the rate of -1 in scenario 3. The increase in elevation is more noticeable from the year 2084. At the end of the simulations, in Figure 6 (scenario 1), this elevation change is more distinguishable

adjacent to dominant channel and the north shore of the Siwash Island, ranging from near sea level to 1; however, in Figure 41, the deposition of sediment occurs across the island, ranging 0.4 to 1. In scenario 3, the dominant channel finds a new pathway to south and bisects the island, however in scenario 1 this channel lengthens to the southwest.

As shown in Figures 9 and 43, elevation relative to sea level decreases over time. At the start of the simulations, elevation is higher than sea level in relation to sea level, nearly 2 m in most parts of Siwash Island, but at the end of the simulations, there are differences between those simulations with different SLR. When the SLR is 12.5 mm/yr (Figure 9), Siwash Island is still higher than average sea level, reaching 0.5 m at the surface of the Island, whereas most of the Island is inundated when the SLR is 25 mm/yr, and the dominant channel bisect the island (Figure 43). In Figure 9, elevation relative to sea level in channels shows a range of -0.7, while it is -2 in Figure 43 with an SLR of 25 mm/yr. the northern tip of the island has an elevation of 2 m in both simulations.

According to Figures 12 and 45, regarding the changes in SSC, in spite of the higher concentrations of suspended sediments in tidal channels and their surrounding areas in Figure 12, SSC is more dispersed across Siwash Island as shown in Figure 45 with an SLR of 25 mm/yr, and the higher amount of SSC is shown in channels both dominant and lesser channels. The reason behind this process may be that higher SLR rate results in greater tidal inundation of Siwash Island, enabling suspended sediments from the tidal channels to disperse more widely across the island.

Figures 15 and 47 have shown that with the increase in sea level, the rate of vegetation loss increases. At the end of simulations, the decline rate of vegetation cover in simulation 2 of Scenario 1 with an SLR of 12.5 mm/yr (Figure 15) and in simulation 1 of scenario 3 with an SLR of 25 mm/yr is 25% and 65% respectively. It indicates that higher rate of SLR can have detrimental effect on vegetation cover.

As shown in Figures 18 and 49, changes in velocity are more pronounced in subplots with an SLR of 25 mm/ yr, specifically in dominant channel. As sea level rises, the velocity also increases.

In comparison with different SLR of 12.5 mm/yr and 25 mm/yr, shown in Figures 21 and 51 respectively, at the end of simulation, the depth of water in Figures 21 ranges from 0 to 0.4 m, while in Figure 51, it ranges from almost 0.8 to 1 m. In Figure 18 the only areas that water depth reaches 2 m are the southern tip and one small spot at northern tip of the island.

## **5.2. General Interpretation of Marsh Evolution:**

The detailed examination of the evolution of the marsh on Siwash Island under various scenarios provides insight into the complex interaction between the water depth, vegetation cover, SLR, SSC, and TR. These results provide insightful information regarding how marsh ecosystems will develop in the future.

One of the most important observations is the orientation of channels in Siwash Island which all of them are north to southwest, indicating that the channelization process is mostly controlled by the existing channels. This channelization determines channel expansion and the overall morphology of the island. Channels deepen and lengthen along pre-existing paths in scenarios with lower tidal range. On the other hand, higher tidal range results in substantial channel erosion, leading to finding new pathways and bisecting the island, and temporarily stopping channel that drain in a southwest direction. This emphasizes how vulnerable marsh ecosystems are to changes in tidal dynamics.

Additionally, the effect of SLR on marsh elevation and inundation is obvious in the scenarios. Marsh elevation decreases in relation to average sea level with regard to SLR, increasing Siwash Island's inundation. The rate of sea level rise affects the extent of inundation, with higher loss of marsh elevation and vegetation cover.

The changes in SSC distribution are more pronounced under higher tidal range conditions, and the controls on SSC distribution are complex and difficult to pin down to one specific marsh evolution behavior. However, an examination of how cross-sectional changes within the main tidal channel evolve in time provides some clues to the simulated SSC dynamics. Notably, cross-sectional changes during the simulations of scenario 1 suggest that right around 2094 there is a period of tidal channel erosion, coupled with a slow down in the rate of out of channel sediment deposition, resulting in a

deeper and wider main outlet tidal channel (Figure 53). This period of erosion and slow down of out of channel deposition increases the SSC concentration at the main tidal channel outlet. Similar behaviors and explanations extend to the simulation of scenario 2.

Furthermore, water velocity is relatively stable in lower tidal range conditions, especially in channels that follow pre-existing paths. This implies that there will be a balance between channel morphology and tidal range, leading to lower degree of erosion; however, water velocity varies substantially with increasing tidal range, especially in dominant channel, breaking about greater erosive forces.

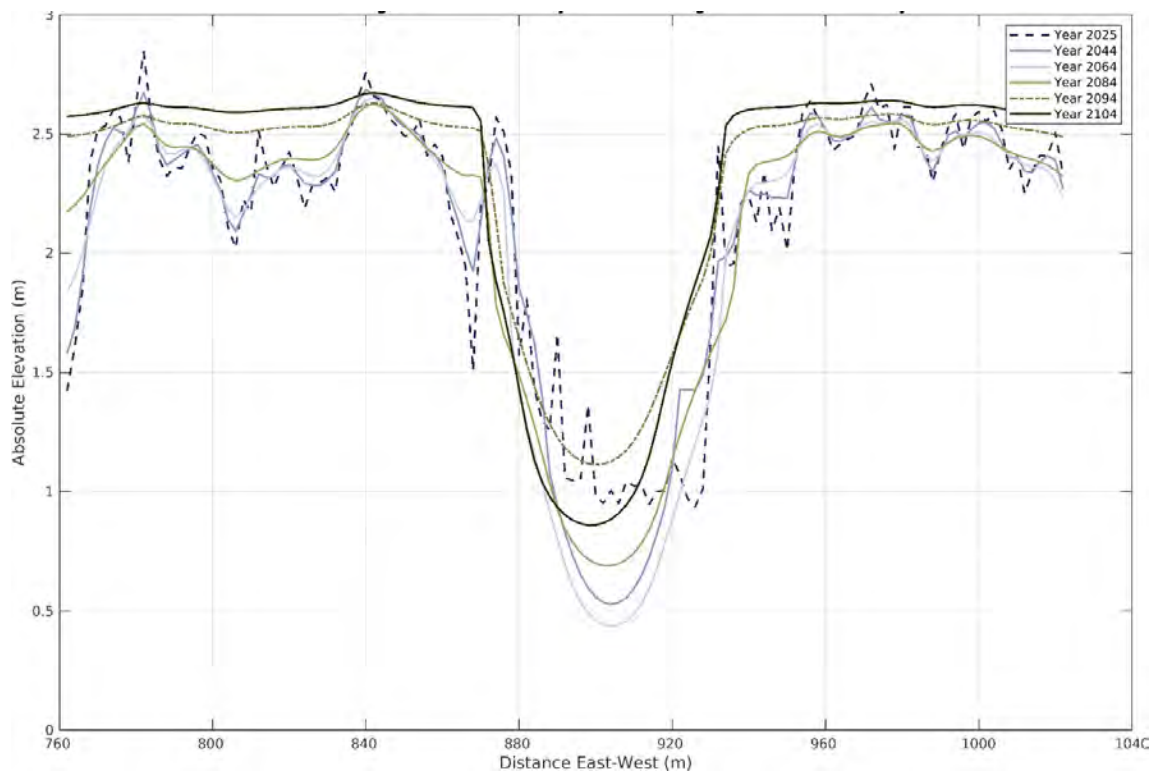


**Figure 53 Evolution of main tidal channel on Siwash Island**

### 5.3. Comparison to other studies:

Although SSC played a significant role in previous research conducted by Hutchinson (2021) and Anderson (2022), it did not play a crucial part in this study; accordingly, the primary characteristics that affect the evolution of Siwash Island are TR

and SLR. This discovery aligns with Mariotti's research in 2020, which indicated that using MarshMorpho2D results in a scenario where sea level rise leads to widening of channels, making them more pronounced; however, this is not the case regarding SSC.

On one hand, despite the higher TR shown in Figure 44, which represents relative elevation, Siwash Island appears to be more resilient compared to Figure 43, where TR is 1.5 m. This result aligns with Kirwan and Guntenspergen (2009), which demonstrates that tidal marshes in high TR are more resilient to sea level rise than tidal wetlands in low TR. On the other hand, the observation for simulations of SLR of 12.5 mm/yr indicate that Siwash Island seems to be disappearing rapidly by increasing tidal range from 1.5 m to 2 m (Figure 9 compared to Figure 30). This finding is consistent with the work of Chmura and Hung (2004), where it is found that macrotidal marshes in Canada suggests a negative relationship accretion rate and tidal range. This could indicate that in a faster rate of sea level rise, tidal wetlands can survive in tidal range of 2 m (mesotidal) than 1.5 m (microtidal) (Friedrichs and Perry, 2001).

## **5.4. Implications and Management Recommendations**

When examining the main causes of wetland loss, the focus should be on changes of vertical growth such as sediment supply and transport of material to the surface of the marshes; moreover, it is necessary to take into account the impact of climate change, including SLR. The vulnerability of tidal wetlands to sea level rise starts before any signs of tidal marshes loss become evident (Cahoon et al, 2019). If a tidal wetland appears to be healthy, it may already have difficulty to keep up with the sea level rise.

Using MarshMorpho2D model to predict the evolution of Siwash Island under various scenarios shows that it is an ideal tool for planners and carry significant implications for coastal management and adaptation strategies to address SLR impacts on tidal wetlands. In all simulations across different scenarios, Siwash Island consistently experiences a reduction in elevation relative to sea level, indicating that it will not be able to persist under any SLR conditions. Although the pace of reduction is slower in scenario 3 simulation with SLR of 25 mm/yr and TR of 2 m compared to other simulations, it still leads to decline the elevation relative to average sea level. Different levels of SSC were investigated, but they did not have impact on vertical accretion of

Siwash Island, so this factor combined with rapid SLR, makes Siwash island more vulnerable to the effects of climate change.

The rising and anticipated sea levels have raised concerns among managers and scientists about the future threats to the health of tidal marshes, so predictive models are useful for forecasting potential future changes in tidal wetlands evolution and understanding the factors involved (Fagherazzi, 2020). The reduction of vegetated area across all scenarios will result in the loss of critical functions provided by tidal marshes that carries significant implications for coastal management and conservation efforts. The decline of this ecosystem weakens its ability to act as a natural buffer against storm surges by absorbing and slowing down the movement of floodwater, increasing the vulnerability of Siwash Island to extreme weather and SLR; moreover, decline in wildlife habitat a result of marsh loss threatens the survival of numerous species, including American Bittern (*Botaurus lentiginosus*) and tailed frog (*Ascaphus*) on Siwash Island.

All things considered; these findings highlight the importance of incorporating predictive modeling tools like MarshMorpho2D into tidal marsh management framework in order to enable informed decision-making. These tools enable scientists and policymakers to simulate different scenarios and assess the potential future changes in wetlands. By predicting potential future changes on Siwash Island's evolution and understanding the factor involved, these models can guide the development of adaptive strategies aimed at strengthening the resilience of tidal wetlands in the face of SLR and changing environmental conditions; moreover, predictive modeling tools an help prioritize conservation efforts and allocate resources more efficiently by identifying areas that are most vulnerable to marsh loss and in need of immediate attention. Taking proactive measures is important for maintaining the ecological health and services of Siwash Island, guaranteeing their sustainability over the long term, and contributing to broader efforts aimed at strengthening coastal resilience.

## **5.5. Limitations**

This study and using MarshMorpho2D model have limitations that is mentioned in the following context:

- 1- Predictive models Simplify complex ecological processes, introducing uncertainties into the results and interpretations.
- 2- This study primarily focuses on internal factors such as TR, SSC, and SLR in predicting Siwash Island evolution, and factors such as extreme weather events, anthropogenic activities, and other factors that impact Siwash Island dynamic and resilience.
- 3- The accuracy of MarshMorpho2D output and the projected evolution of Siwash Island highly depend on the input values. The future condition of Siwash Island affects all input parameters outlined in Table 1, leading to uncertainties.
- 4- This study may be limited by its spatial and temporal scale, and it cannot extrapolate and accurately represent other wetlands dynamics.
- 5- The uncertainty surrounding SLR condition is another issue. While a linear rate of SLR is considered in this model, researchers have second thoughts about the possibility of nonlinearity of SLR due to factors such as extreme weather events and melting large tract of ice sheets.

## **5.6. Recommendation**

In accordance with the results and limitations of the MarshMorpho2D model simulation, here are recommendations for future studies and management of Siwash Island.

- 1- the first recommendation is to prioritize incorporating a clear understanding of local characteristics such as wave dynamics, because as mentioned above in method section, Wave dynamics are uncertain at Siwash Island, and clear understanding of these characteristics may bring about more concise results in MarshMorho2D model simulations.
- 2- The second one is to develop a roughly 5–10-year recurring monitoring plan to evaluate relative to model projections.

- 3- Siwash Island may be protected using thin-layer placement technique and vegetation planting to help preserve marsh areas under different SLR scenarios. Thin-layer placement techniques is the way that dredged material is deposited on the marsh surface.

## **5.7. Conclusion**

This research demonstrates that how MarshMorrpho2D model can simulate long-term marsh evolution in a numerically efficient way on Siwash Island. MarshMorho2D provides a powerful framework for the development of tidal marshes that basically focuses on characteristics like TR, SSC, and SLR. Model projections in this study illustrate that in different scenarios TR and SLR are the crucial factor in the future condition of Siwash Island.

While MarshMorpho2D model simplifies complex ecological processes and introduces uncertainties, its capacity to model various scenarios offers crucial insights into the dynamics of tidal wetlands. This allows for the development of adaptive strategies to address the impact of SLR on Siwash Island and to strengthen the resilience of tidal marshes in the face of changing environmental conditions. Although Hutchins in 2021 has stated that his study can provide a great insight into other marshes within the Fraser River, his results were not compatible with this study in terms of SSC.

Overall, as shown in figures above, Siwash Island is projected to submerge within the next 80 years, resulting in detrimental effect on ecological function such as habitat loss for flora and fauna, carbon sequestration, and vulnerability to storm surge. Since there is no specific study on Siwash Island prior to this study, this information can provide great insight to researchers and policy makers to identify vulnerable areas and prioritize conservation efforts effectively.

## References

- Alizad, K., Hagen, S. C., Morris, J. T., Medeiros, S. C., Bilskie, M. V. and Weishampel, J. F. (2016). Coastal wetland response to sea-level rise in a fluvial estuarine system. *Earth's Future*, 4(11), 483–497. <https://doi.org/10.1002/2016EF000385>.
- Anderson, E. (2022). Modelling tidal channel restoration in Marshes facing sea level rise. Master's thesis. Simon Fraser University.
- Ashley, G.W. (1977). Sedimentology of a freshwater tidal system, Pitt River-Pitt Lake, British Columbia. PhD Dissertation, The University of British Columbia.
- Barbier, E.B., Hacker, S.D., Kennedy, C., Koch, E.W., Stier, A.C., and Silliman, B.R. (2011). The value of estuarine and coastal ecosystem services. *Ecological Monographs*, 81: 169-193.
- B. Raposa, K., Wasson, K., Smith, E., A. Crooks, J., Delgado, P., H. Fernald, S., C. Ferner, M., Helms, A., A. Hice, L., W. Mora, J., Puckett, B., Sanger, D., Shull, S., Spurrier, L., Stevens, R., Lerberg, S. (2016). Assessing tidal marsh resilience to sea-level rise at broad geographic scales with multi-metric indices. *Biological Conservation*, 204, 263-275. <https://doi.org/10.1016/j.biocon.2016.10.015>.
- Cahoon, D.R., P.F. Hensel, T. Spencer, D.J. Reed, K.L. McKee, and N. Saintilan. (2006). Coastal wetland vulnerability to relative sea-level rise: Wetland elevation trends and process controls. *Wetlands and Natural Resource Management* 190: 271-292.
- Cahoon, D.R., and G.R. Guntenspergen. (2010). Climate change, sea-level rise, and coastal wetlands. *National Wetlands Newsletter*, 32, 8–12.
- Cahoon, D.R., Lynch, J.C., Roman, C.T., Schemit, J.P., Skidds, D.E. (2019). Evaluating the relationship among wetland vertical development, elevation capital, sea-level rise, and tidal marsh sustainability. *Estuaries and Coasts*, 42, 1-15. <https://doi.org/10.1007/s12237-018-0448-x>
- Callaway, J.C., Borgnis, E.L., Turner, R.E., Milan, C.S. (2012). Carbon sequestration and sediment accretion in San Francisco Bay tidal wetlands. *Estuaries and Coasts*, 35, 1163-1181.
- Chen, H., Li, D., Chen, Y., Zhao, ZH. (2023). Spatial-temporal evolution monitoring and ecological risk assessment of coastal wetlands on Hainan Island, China. *Remote Sensing*, 15(4), 1035. <https://doi.org/10.3390/rs15041035>.
- Chmura, G.L., Hung, G.A. (2004). Controls on salt marsh accretion: A test in salt marshes of eastern Canada. *Estuaries*, 27, 70-81. Doi:10.1007/BF02803561

- Christiansen, T, Wiberg, PL, Milligan, TG (2000). Flow and Sediment Transport on a Tidal Salt Marsh Surface. *Estuarine, Coastal, and Shelf Science*, 50, 315-331.
- Conner, W., Krauss, K., Baldwin, A., Hutchinson, S. (2014). Wetlands: Tidal, National Wetland Research Centre. [10.1081/E-ENRL-120047505](https://doi.org/10.1081/E-ENRL-120047505)
- Costanza, R., d'Arge, R., deGroot, S., Farber, M., Grasso, B., Hannon, K., Limburg, S., Naeem, R.V., O'Neill, J., Paruelo, R.G., Raskin, P., Sutton, and M. vandenBelt. (1997). The value of the world's ecosystem services and natural capital. *Nature* 387: 253-260.
- Craft, C., J. Clough, J.Ehman, S.Joye, R.park, S.pennings, H.Guo, and M. Machmuller. (2008). Forecasting the effects of accelerated sea level rise on tidal marsh ecosystem services. *Frontiers in Ecology and the environment*, 7, 73-78.
- D. Philips, J. (2018). Coastal wetlands, sea level, and the dimensions of geomorphic resilience. *Geomorphology*, 305, 173-184. <https://doi.org/10.1016/j.geomorph.2017.03.022>.
- Enwright, N.M., Griffith, K.T., Osland, M.J. (2016). Barriers to and opportunities for landward migration of coastal wetlands with sea level rise. *Frontiers in Ecology and the Environment*, 14(6), 307-316
- Evely, A. (2016). Widgeon marsh regional park reserve. MetroVancouver. [widgeon-biophysical-report-2016.pdf \(metrovancover.org\)](https://www.metrovancouver.org/files/media/pdf/widgeon-biophysical-report-2016.pdf)
- Fagherazzi, S, Kirwan, ML, Mudd, SM, Guntenspergen, G., Temmerman, S., D'Alpaos, A., van de Koppel, J., Rybczyk, J.M., Reyes, E., Craft, C., Clough, J. (2012). Numerical Models of Salt Marsh Evolution: Ecological, Geomorphic, and Climatic Factors. *Reviews of Geophysics*, 50(1).
- Fagherazzi, J., Mariotti, G., Leonardi, N, Canestrelli, A., Nardin, W., and Kearney, W.S. (2020). Salt marsh dynamics in a period of accelerated sea level rise. *Journal of Geographical Research: Earth Surface*, 125(8), 1-31. <https://doi.org/10.1029/2019JF005200>
- Friedrichs, C.T., Perry, J.E. (2001). Tidal salt marsh morphodynamics:A synthesis. *Journal of Coastal Research*. 27, 7-37.
- Hay, C. C., Morrow, E., Kopp, R.E. and Mitrovica, J. X. (2015). Probabilistic reanalysis of twentieth-century sea level rise. *Nature*, 517(7535), 481-484. DOI: 10.1.38/nature14093
- Horton, B., S. Khan, N., Cahill, N., S.H. Lee, J., A. Shaw, T., J. Garner, A., C. Kemp, A., E. Engelhart, S., Rahmstorf, S. (2020). Estimating global mean sea-level rise and its uncertainties by 2100 and 2300 from an expert survey. *npj Climate and Atmospheric Science*, 3(1), 1-8.

- Hutchins, K. (2021). Modeling potential impacts of sea level rise on fish habitat offsets. Master's Thesis. Simon Fraser University.
- Kirwan, M.L., Guntenpergen, G.R. (2012). Feedback between inundation, root production and shoot growth in a rapidly submerging brackish marsh. *Journal of Ecology*, 100, 764-770.
- Kirwan, M.L., Walters, D.C., Reay, W.G., Carr, J.A. (2016). Sea level driven marsh expansion in a coupled model of marsh erosion and migration. *Geophysical Research Letter*, 43,4366-4373.
- Mariotti, G., Finotello, A. (2023). A flow-curvature-based model for channel meandering in tidal marshes. *Coastal Sediments*, 837-841.  
[https://doi.org/10.1142/9789811275135\\_0077](https://doi.org/10.1142/9789811275135_0077)
- Mariotti, G. (2020). Beyond marsh drowning: the many faces of marsh loss (and gain). *Advances in Water Resources*, 144,103710.  
<https://doi.org/10.1016/j.advwatres.2020.103710>
- Mariotti, G., and Fagherazzi, S. (2010). A numerical model for the coupled long-term evolution of salt marshes and tidal flats. *Journal of Geophysical Research: Earth Surface*, 115(1), 1-15. <https://doi.org/10.1029/2009JF001326>.
- Mazor, T., K. Runting, R., I. Saunders, M., Huang, D., A. Friess, D., T.H. Nguyen, N., J. Lowe, R., P. Gilmour, J., A. Todd, P. (2021). Future-proofing conservation priorities for sea level rise in coastal urban ecosystems. *Biological Conservation*, 260, 109-190. <https://doi.org/10.1016/j.biocon.2021.109190>.
- Mcleod, E., G.L. Chmura, S. Bouillon, R.Salm, M. Bjork, C.M. Duarte, C.E. Lovelock, W.H. Schlesinger, and B.R. Silliman. (2011). A blueprint for blue carbon: toward an improved understanding of the role of vegetated coastal habitats in sequestering CO<sub>2</sub>. *Frontiers in Ecology and the Environment*, 9:552-560.
- Mackenzie, W.H., Moran, J.R. (2004). *Wetlands of British Columbia: A Guide to Identification*. British Columbia Ministry of Forests
- Mitsch, W.J., Gosselink, J.G. (2015). *Wetlands*.
- Morris, J. T., P. V. Sundareshwar, C. T. Nietch, B. Kjerfve, and D. R. Cahoon (2002), Responses of coastal wetlands to rising sea level, *Ecology*, 83(10), 2869-2877.
- National Research Council. (2012). *Sea-Level Rise for the Coasts of California, Oregon, and Washington: Past, Present, and Future*. Washington, DC: The National Academies Press. <https://doi.org/10.17226/13389>.
- Pang, B., Xie, T., Cui, B., Wang, Q., Ning, ZH., Liu, Z., Chen, C., Lu, Y., Zhao, X. (2023). Adaptability of common coastal wetland plant population to future sea level rise. *Ecosystem Health and Sustainability*, 9 (0005). DOI:[10.34133/ehs.0005](https://doi.org/10.34133/ehs.0005)

- Parris, A., Bromirski, P., Burkett, V., Cayan, D., Culver, M., Hall, J., Horton, R., Knuuti, K., Moss, R., Obeysekera, J., Sallenger, A. and Weiss, J. (2012). Global Sea Level Rise Scenarios for the US National Climate Assessment. NOAA Tech Memo OARCPO,1–37. Retrieved from [http://cpo.noaa.gov/sites/cpo/Reports/2012/NOAA\\_SLR\\_r3.pdf](http://cpo.noaa.gov/sites/cpo/Reports/2012/NOAA_SLR_r3.pdf)
- Pacific Birds Habitat Joint Venture (2021) Wildlife and People Depend on Healthy Estuaries Coastal Wetlands. <https://pacificbirds.org/2021/02/an-updated-ranking-of-british-columbias-estuaries/%0A>
- Ray, G.C. (2005). Connectivities of estuarine fishes to the coastal realm. *Estuarine Coastal and Shelf Science* 64: 18-32.
- Saintilan, N., Kovalenko, K., Guntenspergen, G., Rogers, K., C. Lynch, J., R. Cahoon, D., E. Lovelock, C., A. Friess, J., Ashe, E., W. Krauss, K., Cormier, N., Spencer, T., Adams, J., Raw, J., Ibanez, C., Scarton, F., Temmerman, S., Meire, P., Maris, T., Throne, K., Brazner, J., L. Chmura, G., Bowron, T., P. Gamage, V., Cressman, K., Endris, C., Marconi, C., Marcum, P., St. Laurent, K., Reay, W., B. Raposa, K., A. Garwood, J., Khan, N. (2022). Constraints on the adjustment of tidal marshes to accelerating sea level rise. *Science*, 377(6605), 523-527.
- Sweet, W., Kopp, R., weaver, Ch., Obeyesekera, J., Horton, R., Thieler, R., Zervas, Ch. (2017). Global and regional sea level rise scenarios for the United States. (NOS CO-OPS 083), 75.
- Tabak, N. M., Laba, M. and Spector, S. (2016). Simulating the effects of Sea Level Rise on the resilience and migration of tidal wetlands along the Hudson River. *PLoS ONE*, 11(4), 1–25. <https://doi.org/10.1371/journal.pone.0152437>.
- Thorne, K., J. Buffington, K., L. Elliott-Fisk, D., Y. Takekawa, J. (2015). Tidal marsh susceptibility to sea-level rise: importance of local scale models. *Journal of Fish and Wildlife Management*, 6(2), 290-304. <https://doi.org/10.3996/062014-jfwm-048>
- Thorne, K., MacDonald, G., Guntenspergen, G., Ambrose, R., Buffington, K., Dugger, B., Freeman, C., Janousek, C., Brown, L., Rosencranz, J., Holmquist, J. (2018) U.S. Pacific coastal wetland resilience and vulnerability to sea-level rise. *Science Advances*, 4(2), 1-11.
- Triana, K., Wahyudi, A. (2020). Sea level rise in Indonesia: the drivers and combined impacts from land subsidence. *Asean Journal on Science and Technology for Development*. 37(3),115-121. DOI: 10.29037/ajstd.627
- Turner, R.E. (2009). Doubt and the values of an ignorance-based world view for restoration: Coastal Louisiana wetlands. *Estuaries and Coasts*, 32: 1054-1068.
- United States Environmental Protection Agency. (2018). Classification and Types of Wetlands. Retrieved from: <https://www.epa.gov/wetlands/classification-andtypes-wetlands#marshes>.

W. Day, J., R. Christian, R., M. boesch, D., Yáñez-Arancibia, A., Morris, J., R. Twilley, R., Naylor, L., Schaffner, L., Stevenson, C. (2008). The consequence of climate change on the ecomorphology of coastal wetlands. *Estuaries and Coasts*, 31, 477-491.

Wiberg, P.L., Fagherazzi, S., Kirwan, M.L. (2020). Improving predictions of salt marsh evolution through better integration of data and models. *Annual Review of Marine Science*, 12, 389-413.